CHRNS -MACS

2021 VIRTUAL SCHOOL

JOSE A RODRIGUEZ-RIVERA YIMING QIU

MACS ITINERARY

Monday Experimental Sessions

2:15-3:30

-Introduction to Neutron Spectroscopy (MACS). (J. A. Rodriguez-Rivera)

4:20-5:30

-Experiment: 1D antiferromagnet S=1/2 CuPZN system (J. A Rodriguez-Rivera)

Wednesday Experimental sessions:

2:05-3:00

-Informal talk by Prof. Chris Stock from University of Edinburgh

3:00-3:30

-CuPZN MACS Experimental Setup

4:20-5:20

-Informal talk by Prof. Kemp Plumb from Brown University

MACS ITINERARY

Friday Experimental Sessions
- 2:05-3:30
  - -Data analysis (Yiming Qiu)
- 4:20-5:30
  - -Data analysis (Yiming Qiu)

SCATTERING PROCCESS

$$A(\Delta\vec{k}) \sim \sum_j b_j\, e^{i\frac{2\pi}{\lambda}(\vec{k}_i-\vec{k}_f)\vec{r}_j}$$

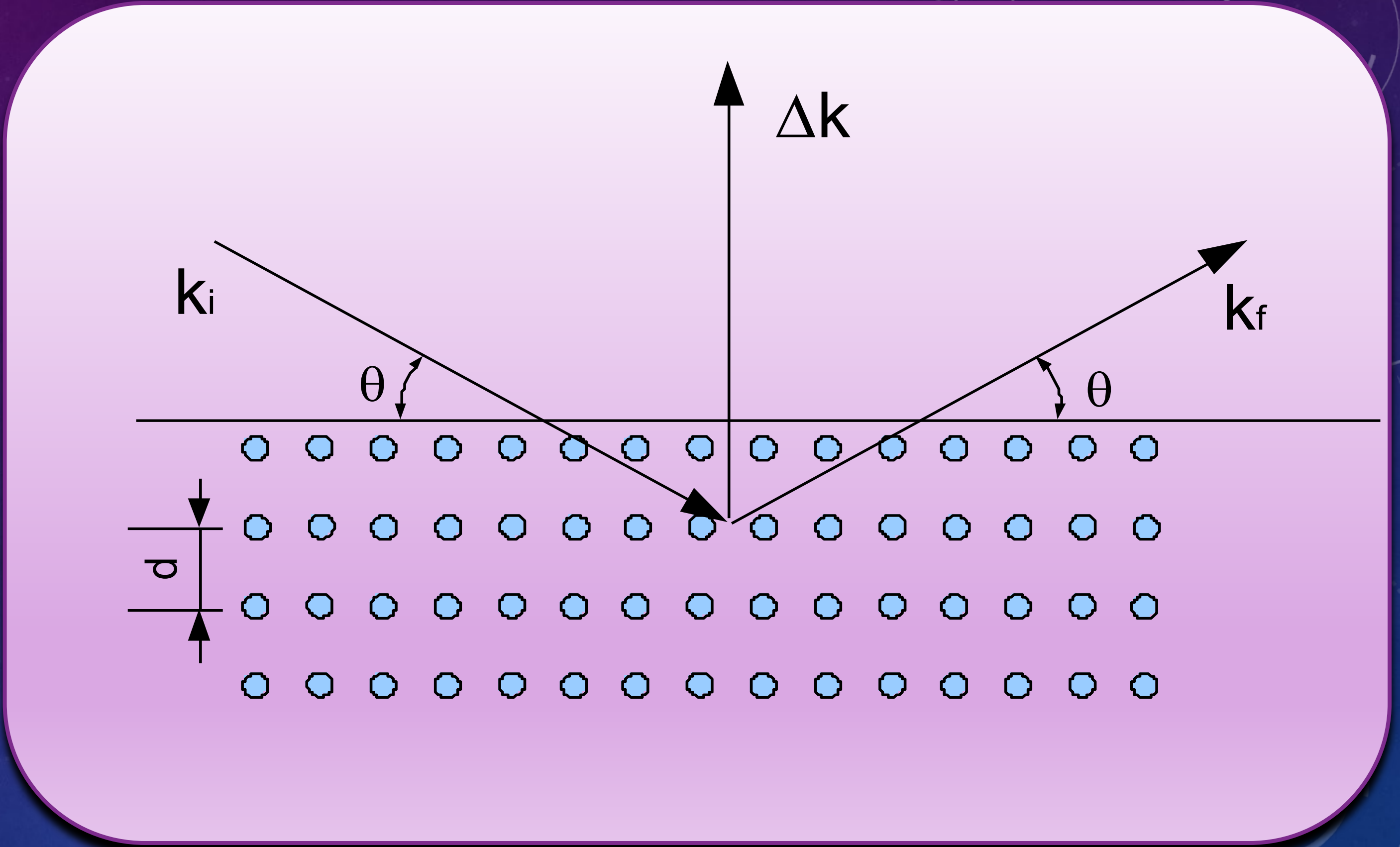

We cannot access the amplitude experimentally but we can acces the Intensity

$$I(\overrightarrow{\Delta k}) = A^*(\overrightarrow{\Delta k})A(\overrightarrow{\Delta k}) \sim \sum_{ij} b_i b_j\, e^{i\frac{2\pi}{\lambda}(\vec{k}_i-\vec{k}_f)\vec{r}_{ij}}$$

$$I(\overrightarrow{\Delta k}) = A^*(\overrightarrow{\Delta k})A(\overrightarrow{\Delta k}) \sim \sum_{ij} b_i b_j\, e^{i\frac{2\pi}{\lambda}(\vec{k}_i - \vec{k}_f)\vec{r}_{ij}}$$

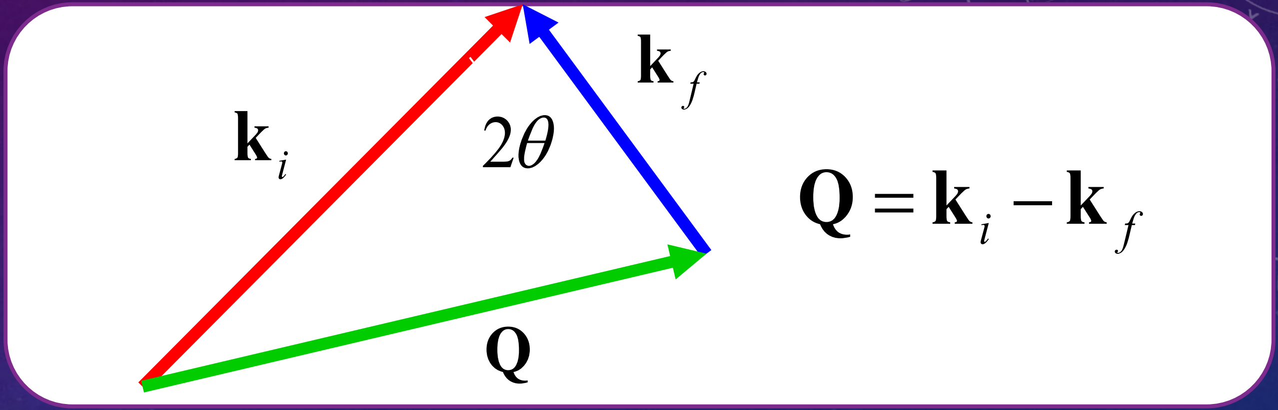

$$I(\vec{Q}) \sim \sum_{ij} b_i b_j\, e^{i\vec{Q}\cdot\vec{r}_{ij}}$$

The intensity is the Fourier transform of the interatomic array.

The scattering experiments measure the correlations between atoms.

FOURIER WEBCAM

HTTPS://NCNR.NIST.GOV/INSTRUMENTS/MAGIK/CALCULATORS/FOURIER_WEBCAM/
(TAKING FROM RYAN MURPHY 2021 NCNR VIRTUAL SCHOOL TALK)

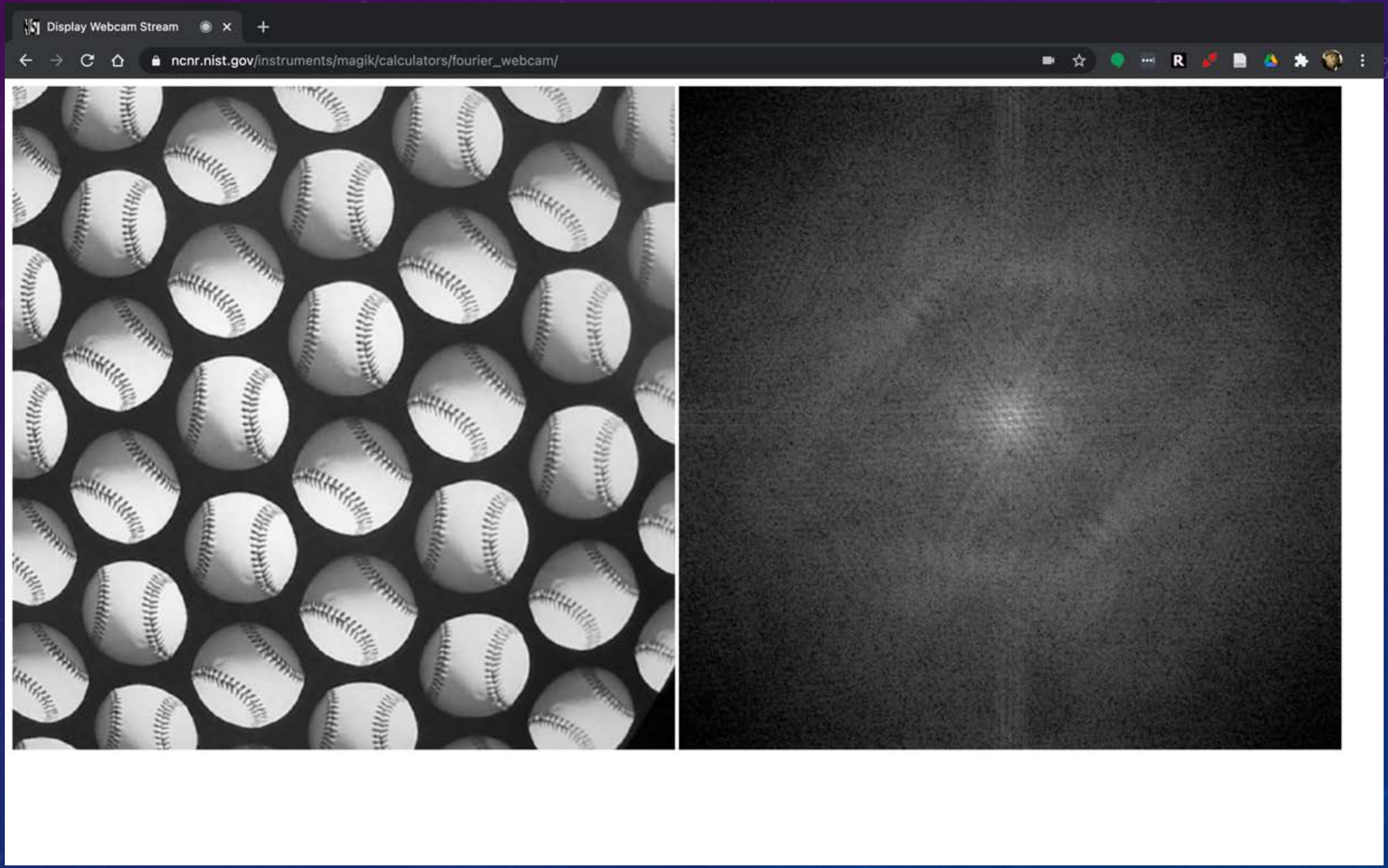

A simple experiment

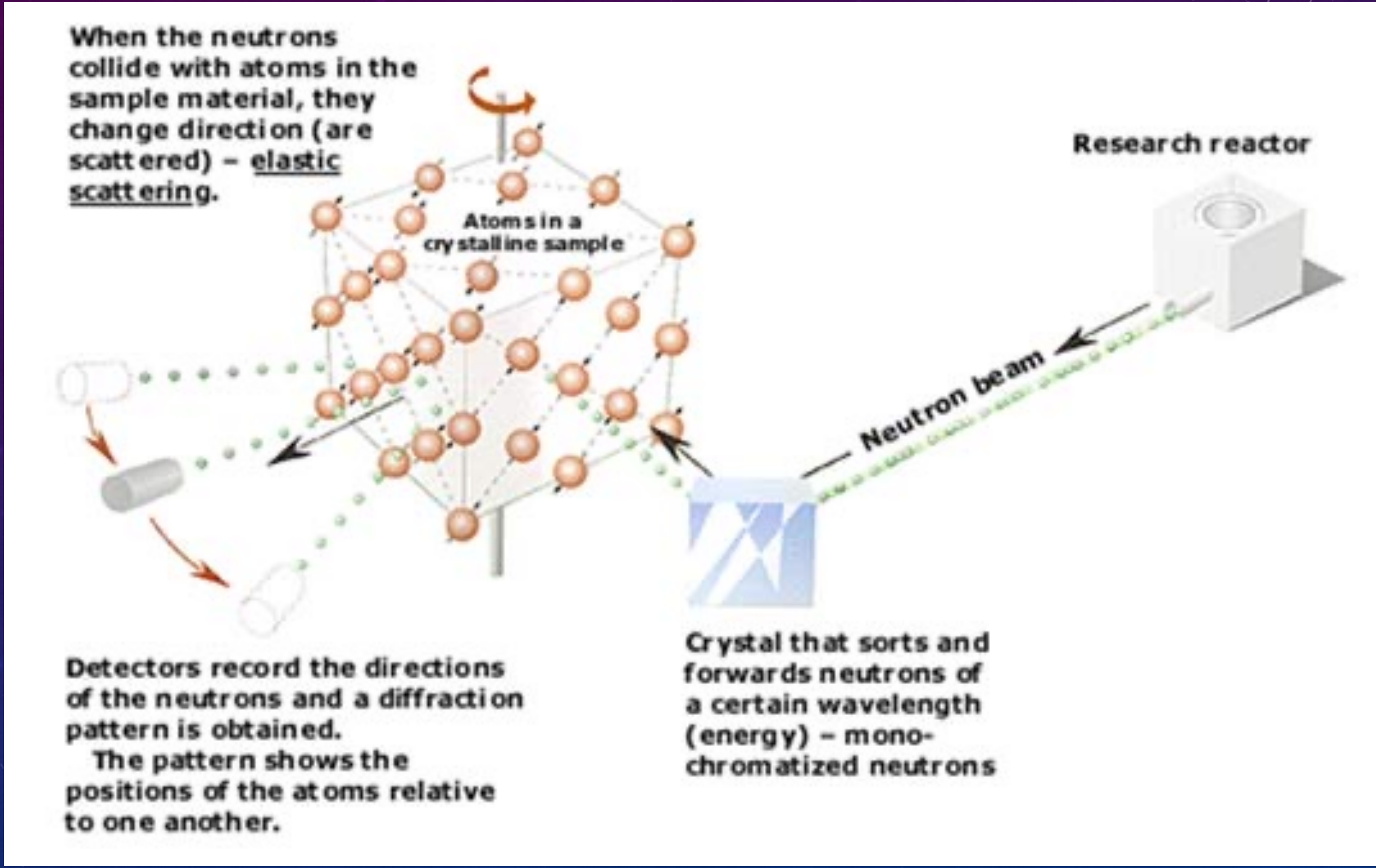

X-rays and Neutron scattering cross sections.

Neutron scattering lengths for isotopes of the same element can have very different neutron scattering properties

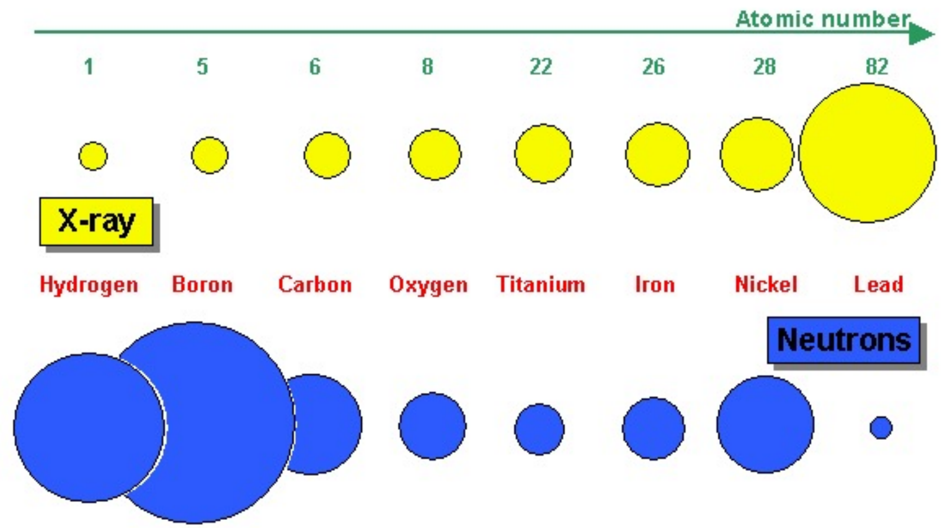

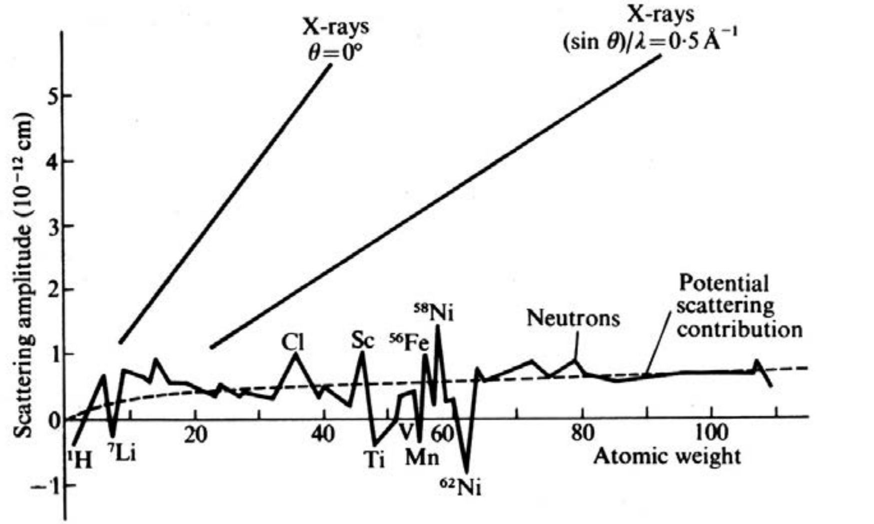

FIG. 22. Irregular variation of neutron scattering amplitude with atomic weight due to superposition of 'resonance scattering' on the slowly increasing 'potential scattering'; for comparison the regular increase for X-rays is shown. (From *Research* (*London*) 7, 257 (1954).)

Why neutron scattering is important?

The Wavelengths of neutrons are similar to atomic spacing!

- Sensitive to structure
- Gathers information from 10^{-10} to 10^{-7} m
- Crystal structures and atomic spacing

Neutrons probe Nuclei!

- Light atom sensitive
- Sensitive to isotopic substitution

Neutrons have a Magnetic Moment!

- Magnetic structure
- Fluctuations
- Magnetic materials

Neutrons have No Charge!

- Highly penetrating
- Nondestructive

The Energies of neutrons are similar to the energies of elementary excitations!

- Molecular Vibrations and Lattice modes
- Magnetic excitations

Neutrons have Spin!

- Polarized beams
- Atomic orientation

NEUTRON SOURCES: NUCLEAR REACTORS

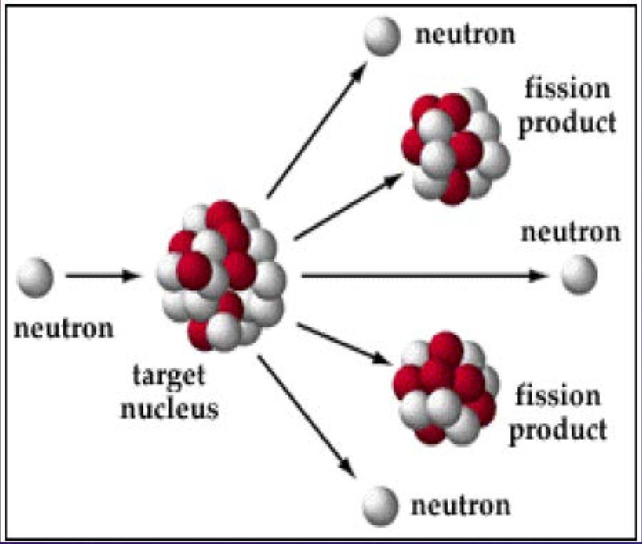

Pynn, *Neutron Scattering: A Primer* (1989)

- Nuclear fision
- Continuos neutron source

NEUTRON SOURCES: SPALLATION

HOT VS COLD VS THERMAL INSTRUMENTS

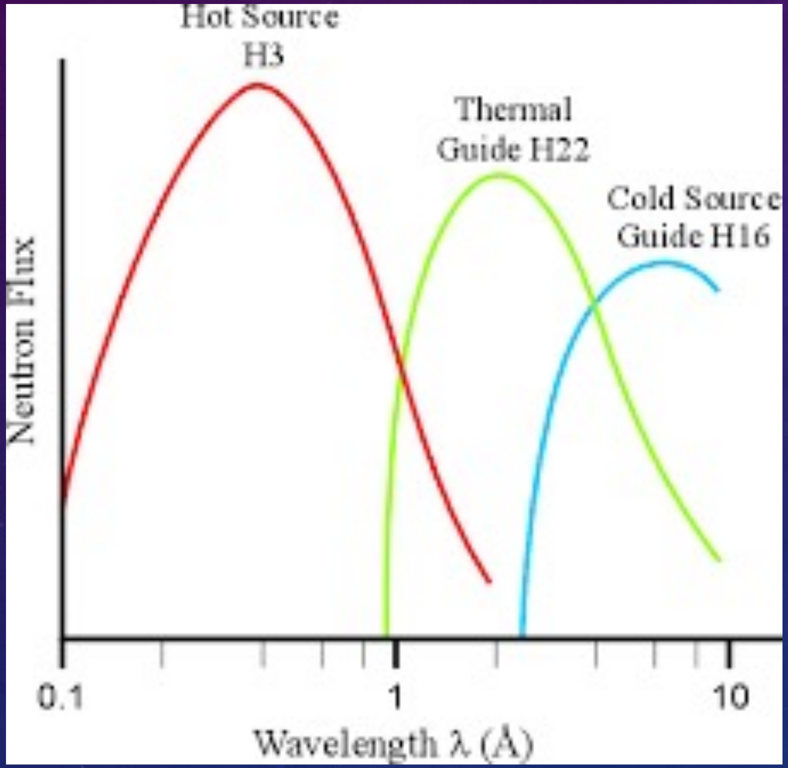

- Thermal neutrons are produced by the reactor D2O moderator (300K)
- Cold neutrons are produced by cooling down the neutrons. NCNR uses liquid hydrogen (33K)
- Hot neutrons are produced with a large piece of graphite (2500 C).

At the NCNR we have only thermal and cold neutrons

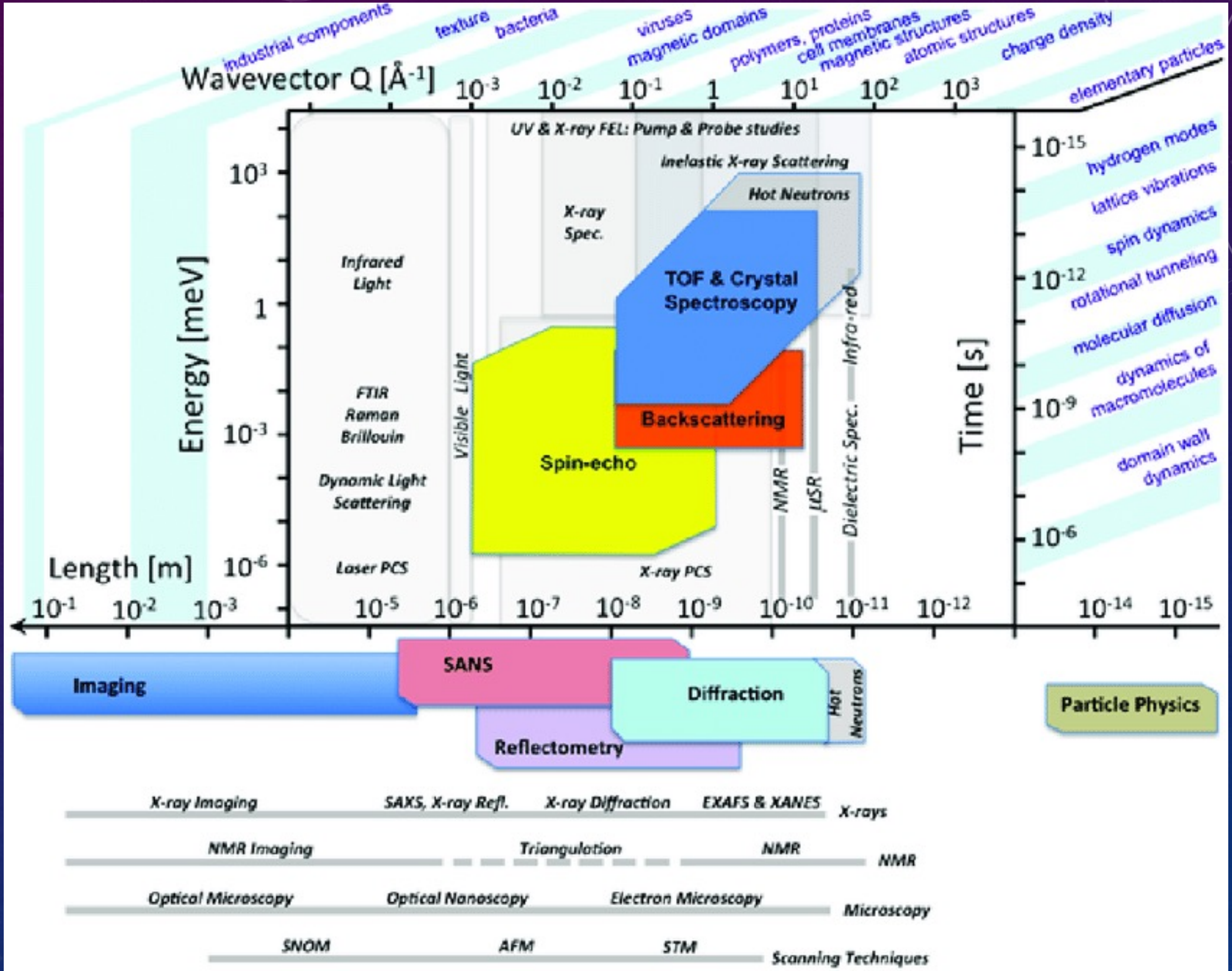

industrial components
texture
bacteria
viruses
magnetic domains
polymers, proteins
cell membranes
magnetic structures
atomic structures
charge density
elementary particles
Wavevector Q [Å-1]
10-3 10-2 10-1 1 101 102 103
UV & X-ray FEL: Pump & Probe studies
Inelastic X-ray Scattering
Hot Neutrons
X-ray Spec.
Infrared Light
TOF & Crystal Spectroscopy
FTIR Raman Brillouin
Visible Light
Backscattering
Spin-echo
Dynamic Light Scattering
Laser PCS
X-ray PCS
NMR
μSR
Dielectric Spec.
Infra-red
Energy [meV]
10³ 1 10-3 10-6
Time [s]
10-15 10-12 10-9 10-6
hydrogen modes
lattice vibrations
spin dynamics
rotational tunneling
molecular diffusion
dynamics of macromolecules
domain wall dynamics
Length [m]
10-1 10-2 10-3 10-5 10-6 10-7 10-8 10-9 10-10 10-11 10-12 10-14 10-15
Imaging
SANS
Diffraction
Hot Neutrons
Reflectometry
Particle Physics
X-ray Imaging
SAXS, X-ray Refl.
X-ray Diffraction
EXAFS & XANES
X-rays
NMR Imaging
Triangulation
NMR
NMR
Optical Microscopy
Optical Nanoscopy
Electron Microscopy
Microscopy
SNOM
AFM
STM
Scanning Techniques

BRAGG LAW

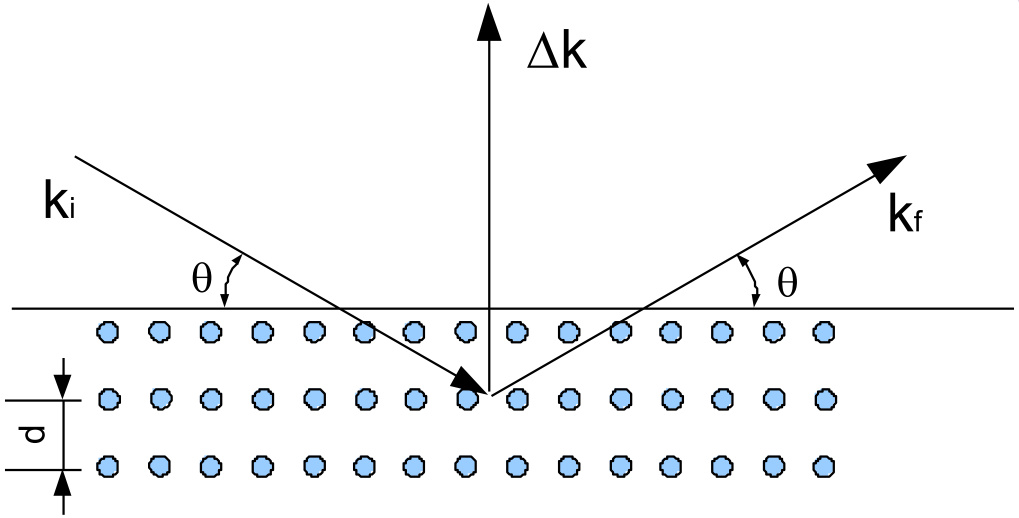

Bragg condition:

$$\lambda = 2d\sin(\theta)$$

For highly oriented pyrolytic graphite(002)

$$d = 3.35\,\mathring{A}$$

$$\theta_{mon} = \arcsin\left(\frac{\lambda}{2d}\right)$$

$$E = \frac{81.81}{\lambda^2}$$

E in meV

λ in $\mathring{A}$

TRIPLE AXIS SPECTROMETER

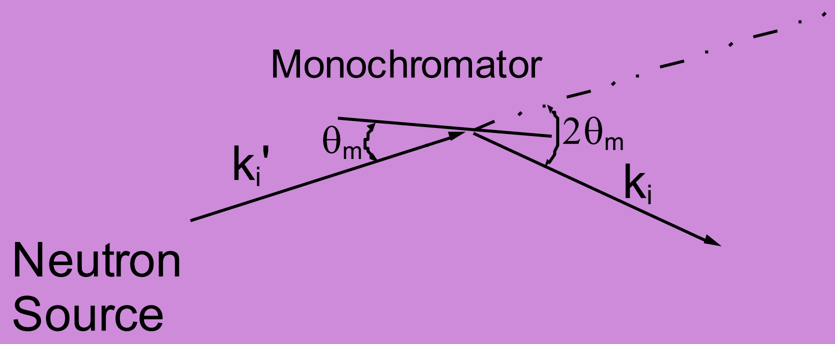

$$\lambda_{mon} = 2d\sin(\theta_{mon})$$

$$E_i = \frac{81.81}{\lambda_{mon}^2}$$

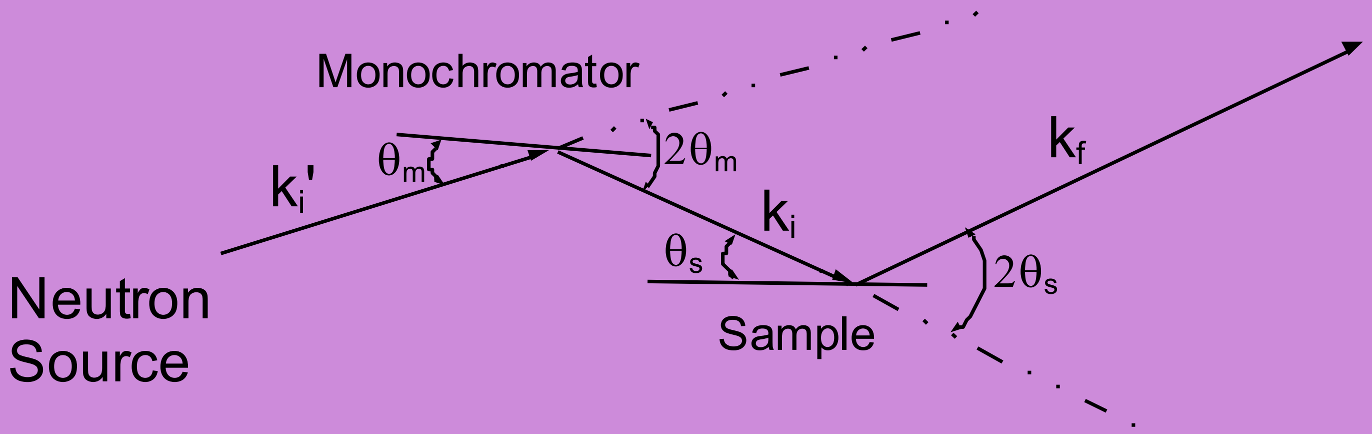

TRIPLE AXIS SPECTROMETER

Bertram Brockhouse
1994 Novel Prize in physics

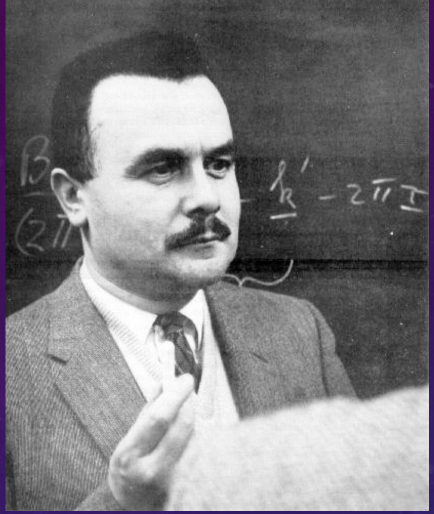

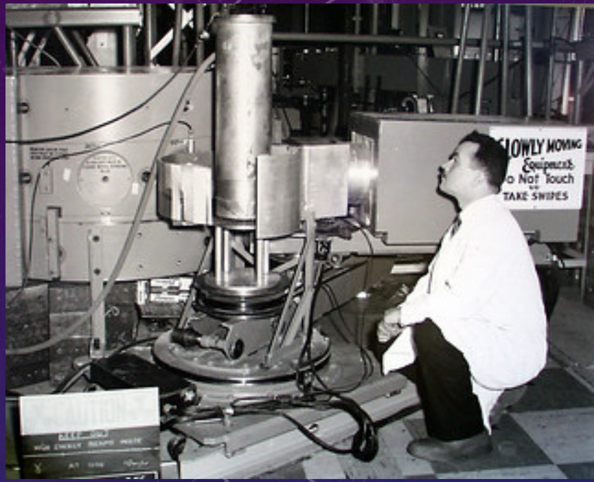

θ_{mon}	A_1
$2\theta_{mon}$	A_2
θ_{sample}	A_3
$2\theta_{sample}$	A_4
$\theta_{Analyzer}$	A_5
$2\theta_{Analyzer}$	A_6

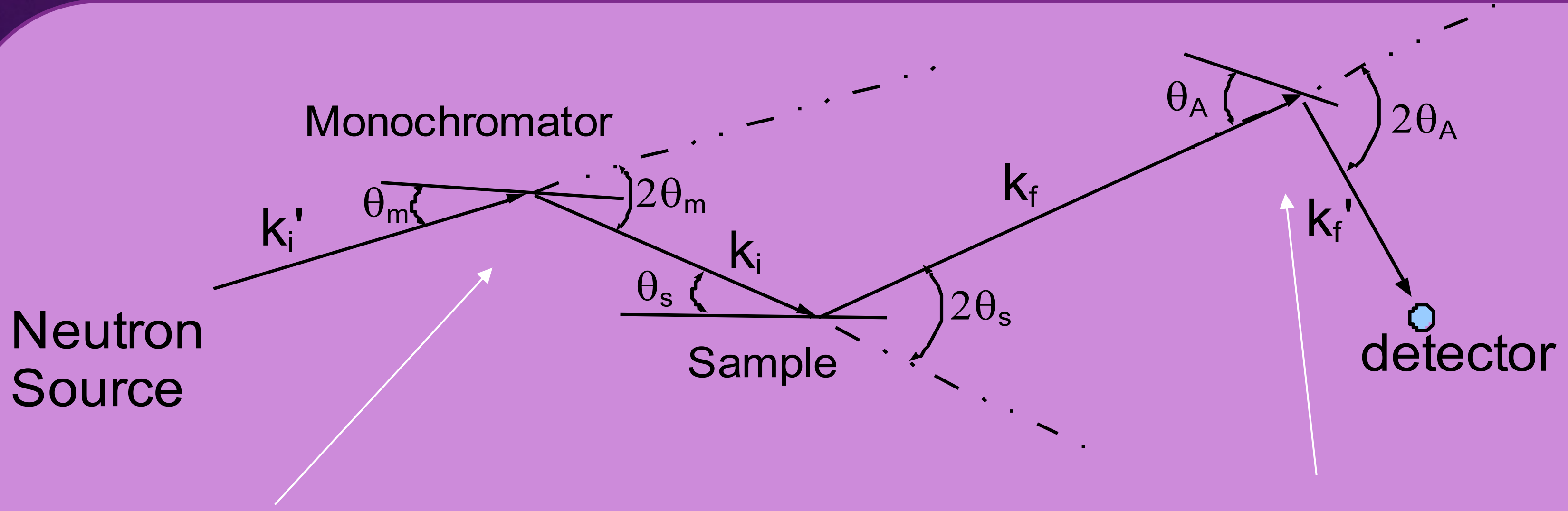

$$\lambda_{mon} = 2d_{mon}\sin(\theta_{mon})$$

$$\lambda_{analyzer} = 2d_{analyzer}\sin(\theta_{analyzer})$$

$$E_i = \frac{81.81}{\lambda_{mon}^2}$$

$$E_f = \frac{81.81}{\lambda_{analyzer}^2}$$

COLD TRIPLE AXIS SPINS-NCNR

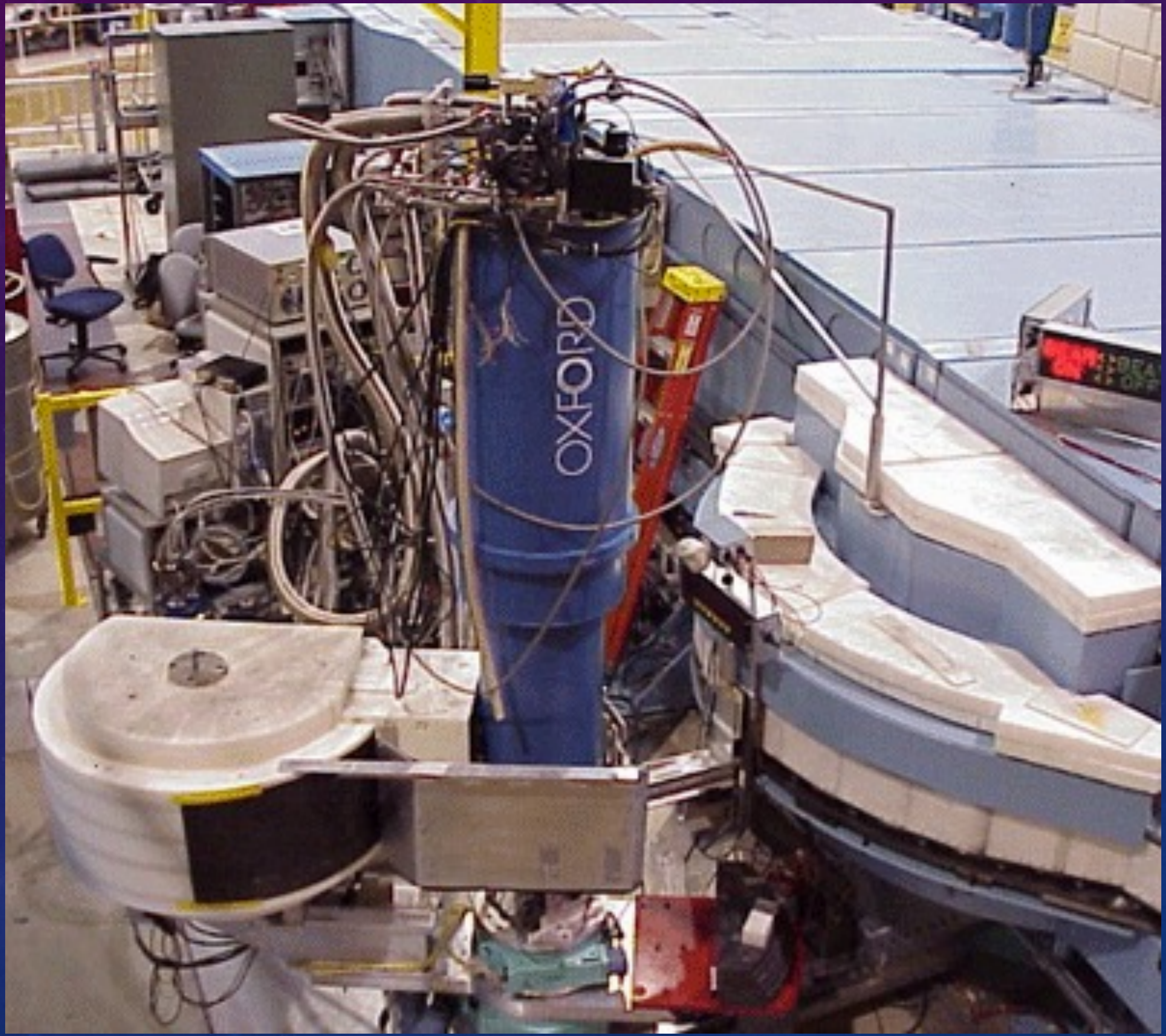

THERMAL TRIPLE AXIS BT7 AT NCNR

TIME OF FLIGHT SPECTROMETER DCS AT NCNR

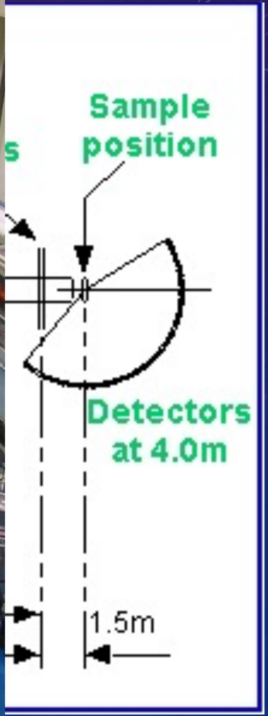

Neutrons disadvantages

- Neutron sources are limited and very expensive.
- Neutron sources have low flux compared to x-ray sources.
- Long scanning times.
- Large samples (1-20 g).
- Difficult to perform experiments with highly neutron absorbent materials.

Smaller Samples for new materials:

$NiGa_2S_4$ single crystals

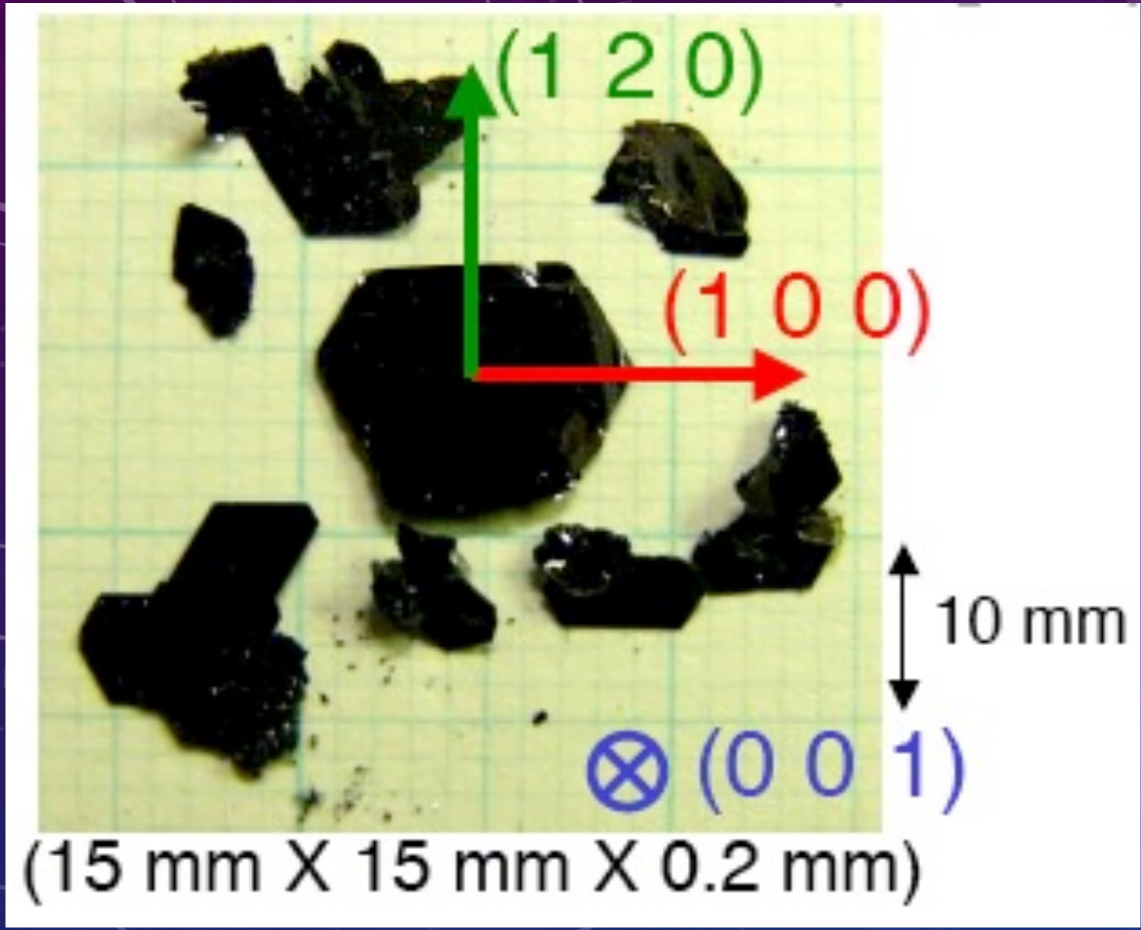

Symmetry: P3m1

7 crystals

coaligned (HHL)

~ 300 mg

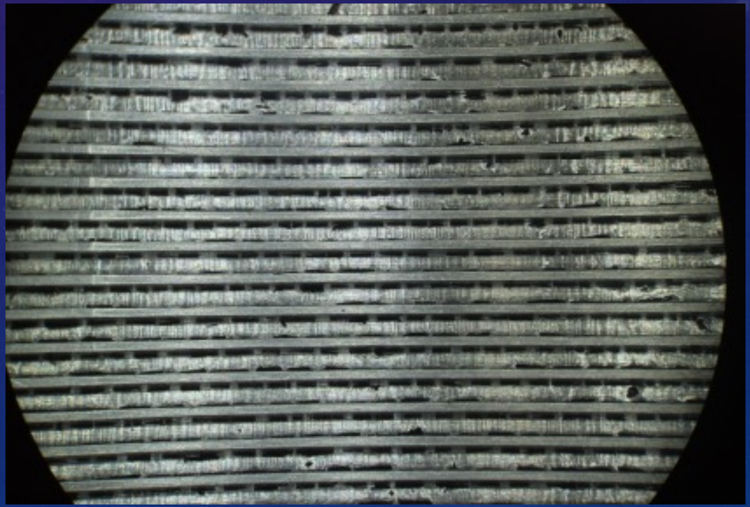

~ 3000-5000 crystals ~ 1 g

Photon flux at various sources.

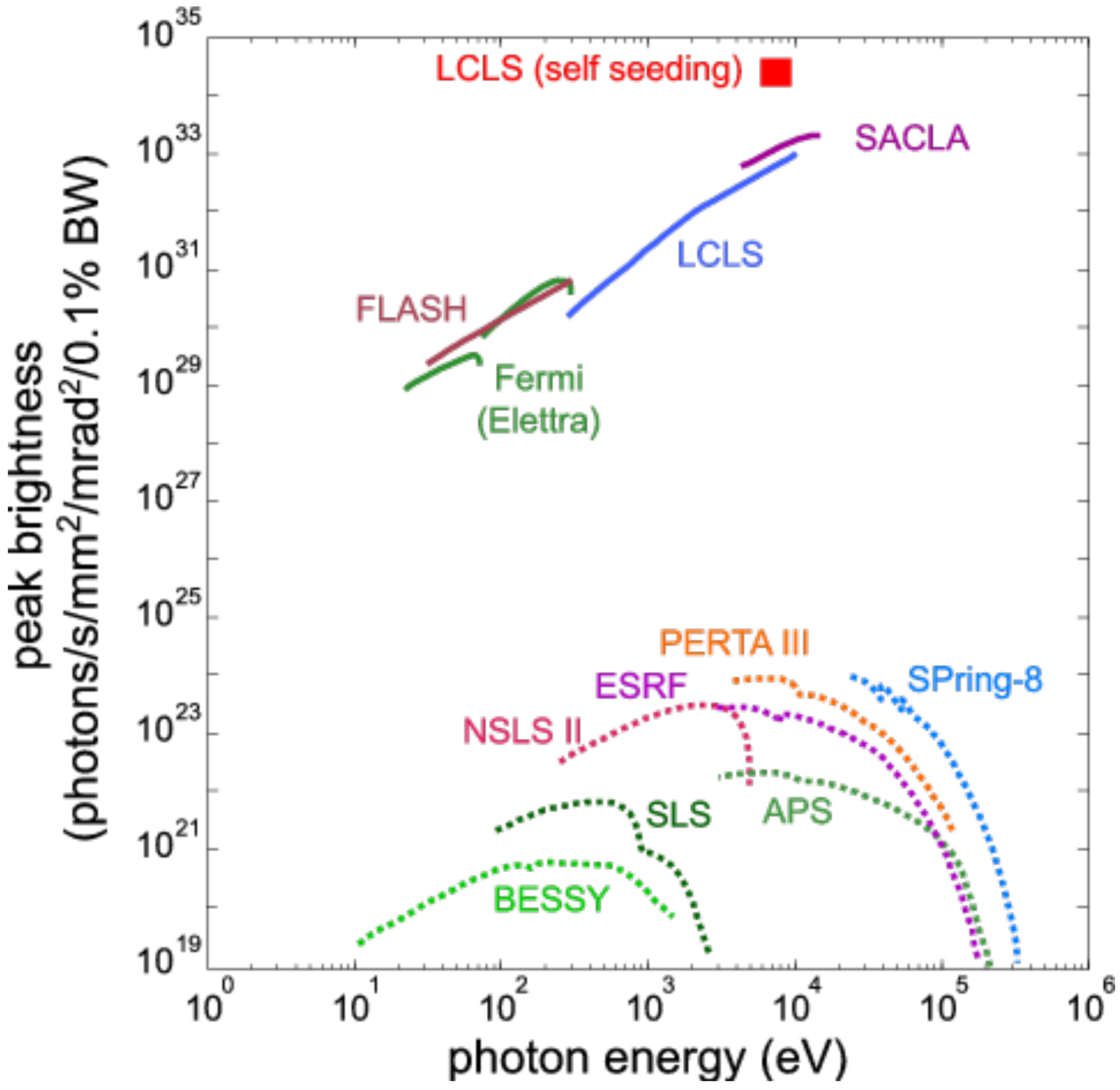

Neutron flux at various sources.

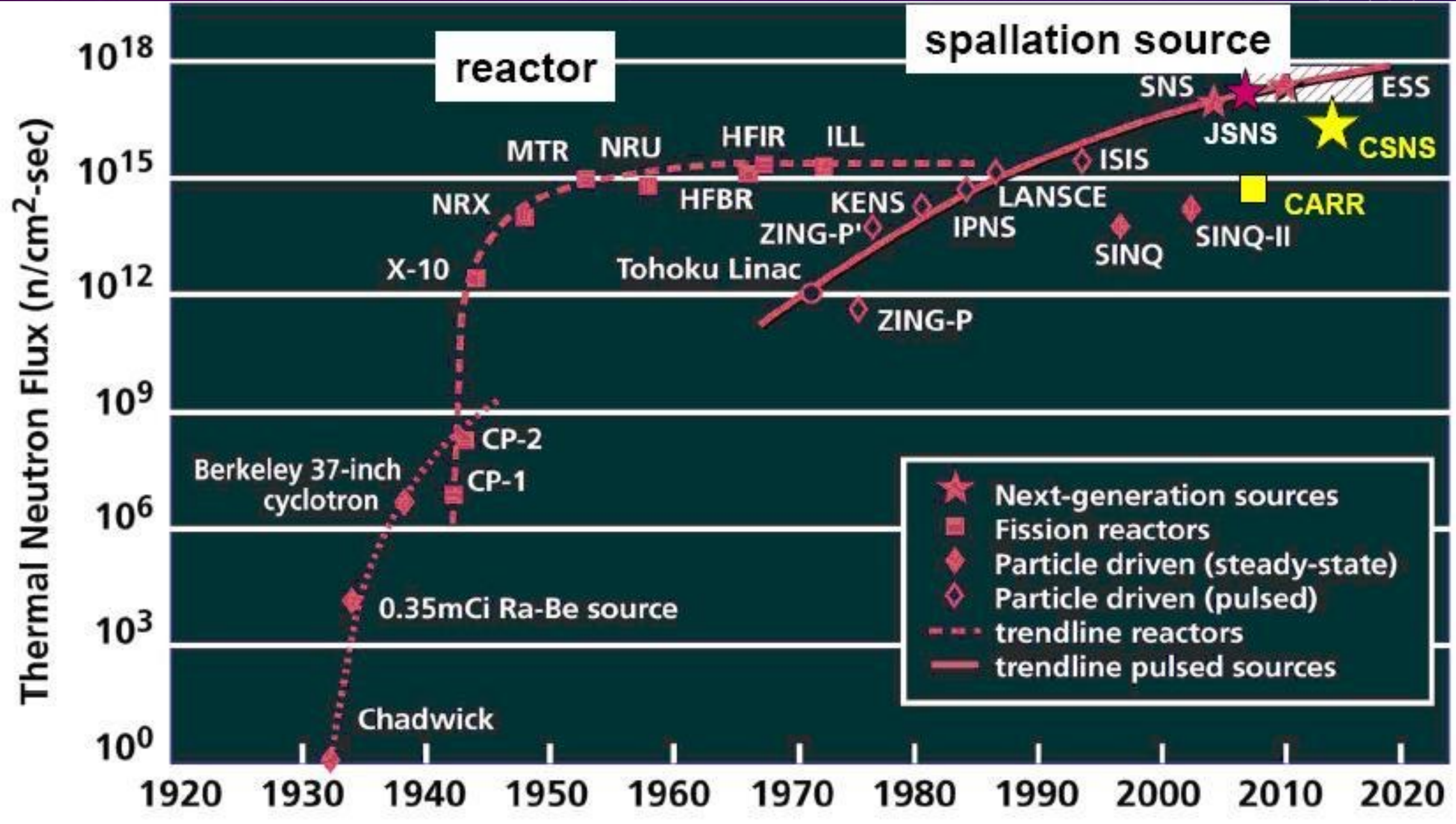

Optimizing the neutron flux and neutron detection

Increase the neutron flux

- ~~Development of a new neutron sources.~~
- Install the spectrometer near a neutron source and/or use ballistic guides
- Focusing monochromator

Increase the number of neutrons detected.

- Focusing analyzers
- Increase the number of detectors.
- Continuous motion/Time stamping

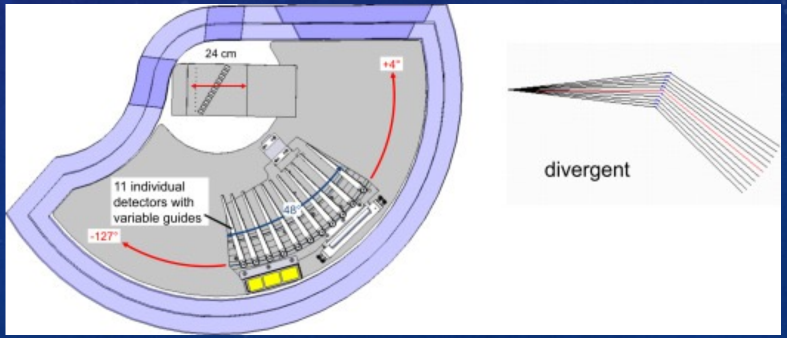

MACS project

- 1995 Collin Broholm (JHU) instrument proposal
  - Propose to build an instrument near the NCNR cold source (NG0 beam tube) with a low background doubly focusing monochromator.

N·H
ELSEVIER

Nuclear Instruments and Methods in Physics Research A 369 (1996) 169–179

NUCLEAR INSTRUMENTS & METHODS IN PHYSICS RESEARCH
Section A

Proposal for a doubly focusing cold neutron spectrometer at NIST

Collin Broholm[a,b,*]

[a]Department of Physics and Astronomy, The Johns Hopkins University, Baltimore, MD 21218, USA
[b]National Institute of Standards and Technology, Gaithersburg, MD 20899, USA

Received 21 March 1995; revised form received 7 August 1995

Abstract

I propose to build a cold neutron spectrometer with a doubly focusing monochromator viewing the liquid hydrogen moderator at the NBSR reactor at NIST. First I describe a practical formalism for calculating the monochromatic neutron flux at the sample position for various monochromating systems. Then I show that the large solid angle by which a doubly focusing crystal monochromator could view the cold neutron source at the NBSR would allow the construction of an instrument surpassing any current instrument for neutron spectroscopy with $0.1 < \Delta E < 0.5$ meV and $\Delta Q \approx 0.1$ Å^{-1}. I contrast the merits of this instrument to those of other neutron spectrometers at NIST and elsewhere and discuss the scientific opportunities that the instrument would provide.

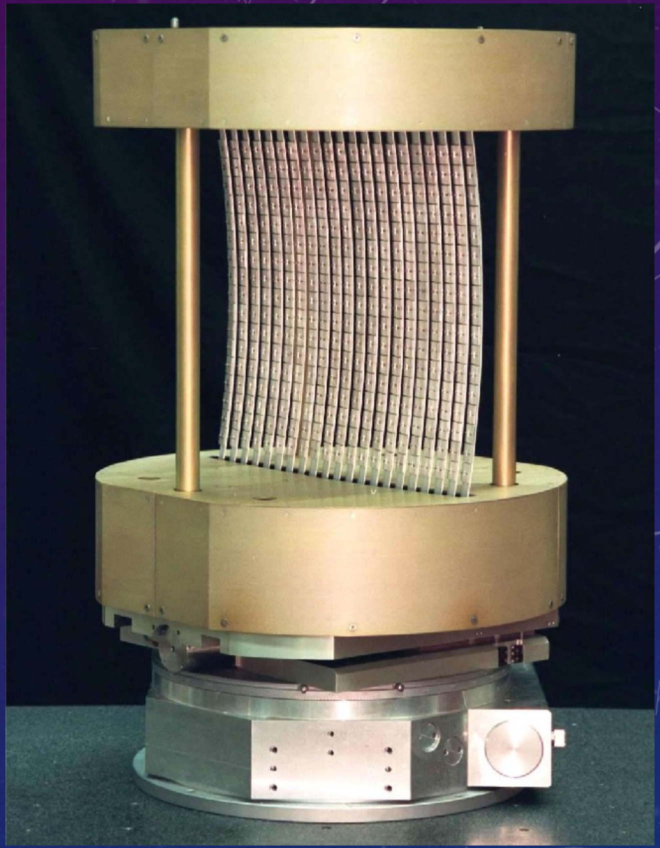

On November 2006 the front end was installed. (First beam)

- Neutron flux optimization.
- Neutron flux measurements.

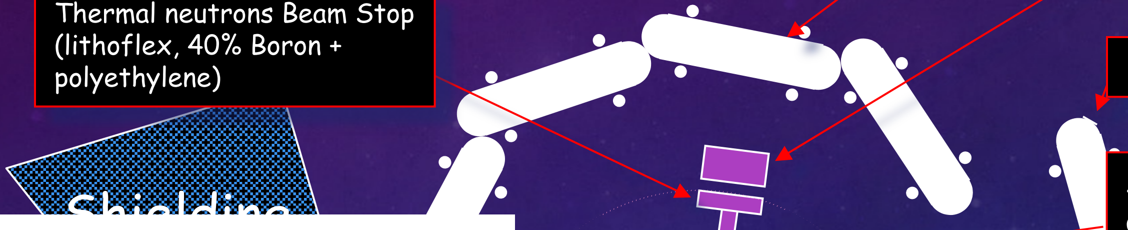

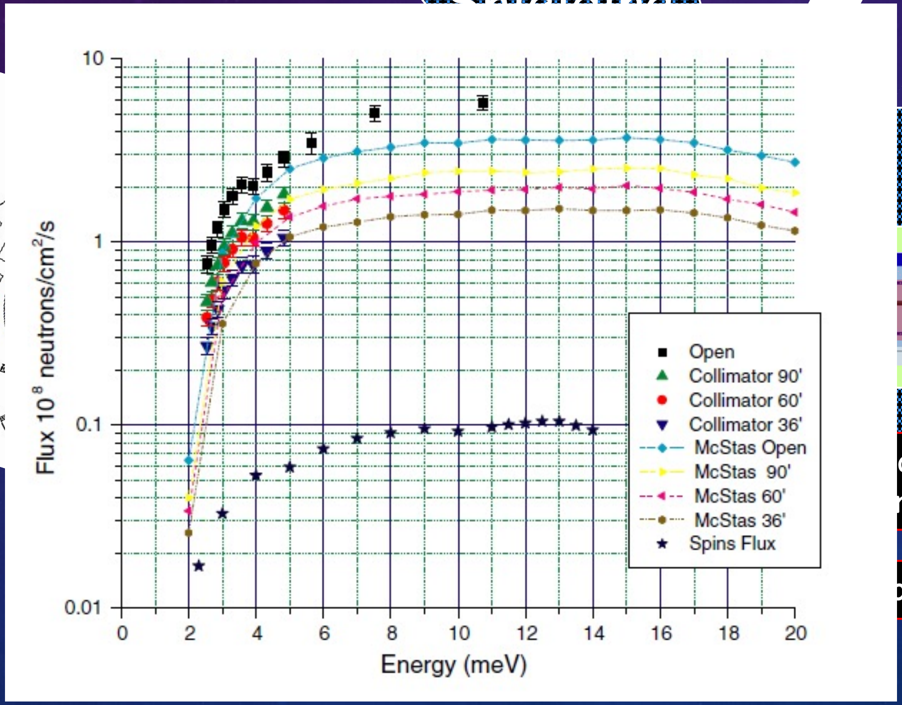

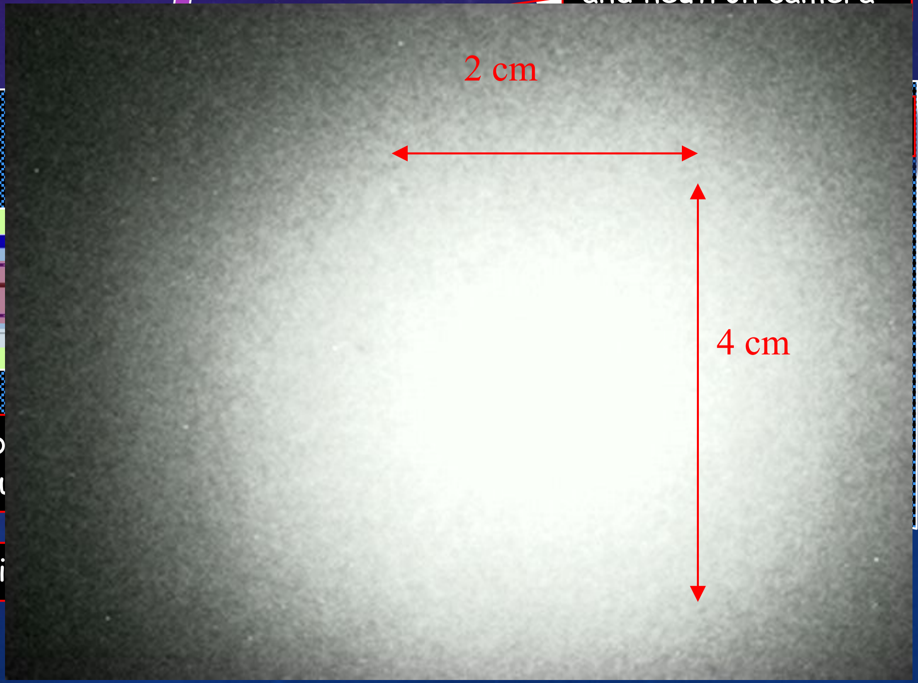

MULTI AXIS CRYSTAL SPECTROMETER (MACS)

- 10 X more neutron flux compared to IN14 and spins

- 20 X more detectors

Two orders of magnitude more efficient than IN14 and spins

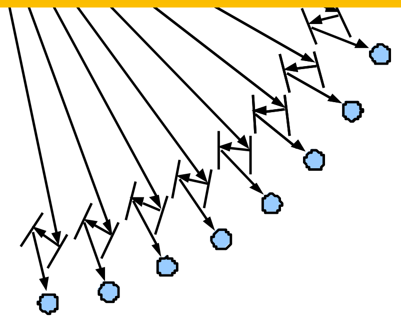

20 $2\theta_{Sample}$

20 k_f

20 $\theta_{Analyzer}$

MACS PROYECT. FIRST EXPERIMENT 07/2009

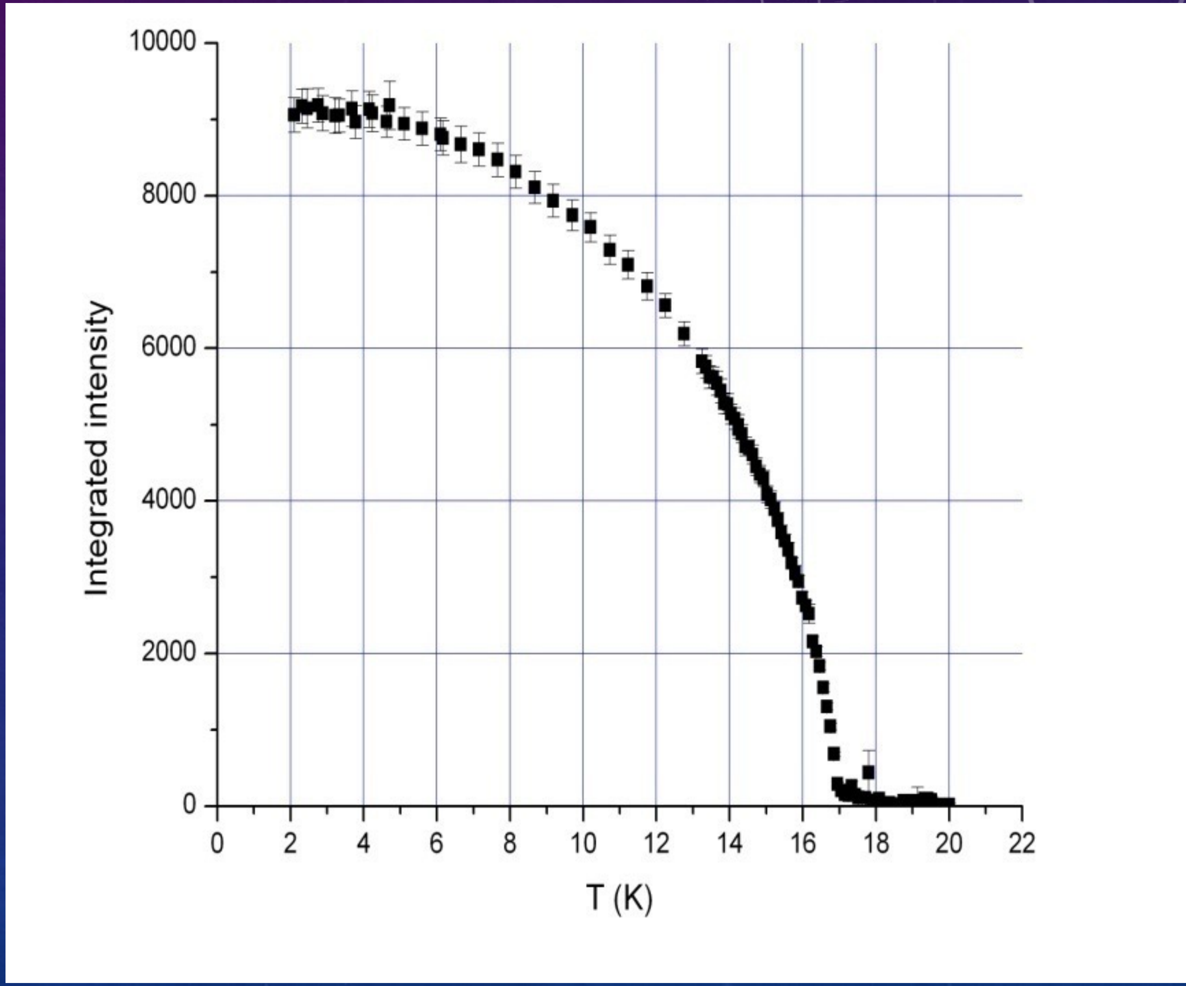

CHARACTERISTICS OF MACS AT NCNR

- Q-resolution with “full” cold beam:

$$\Delta Q \approx k_i \Delta\alpha_{source} \approx 0.05\text{A}^{-1}$$

- Energy Resolution:

$$\Delta E \approx 2E\sqrt{\left(\tfrac{2k_i}{\tau}\right)^2 - 1}\,\Delta\alpha_{sample} \approx 0.2\,\text{meV}$$

- Flux on sample:

$$\phi \approx \phi_0 \cdot \Delta\Omega_{source} \cdot \Delta E \geq 10^8\ \text{n/cm}^2\text{/s}$$

- Incident Energy Range 2.35-16 meV. (Dinamical range from 0 to 13.65 meV)

→ Ideal for slow quasi-particles in hard matter

Multi Axis Crystal Spectrometer (MACS)

MACS NEUTRON FLUX AND ENERGY RESOLUTION.

MACS at NG0 Neutron flux

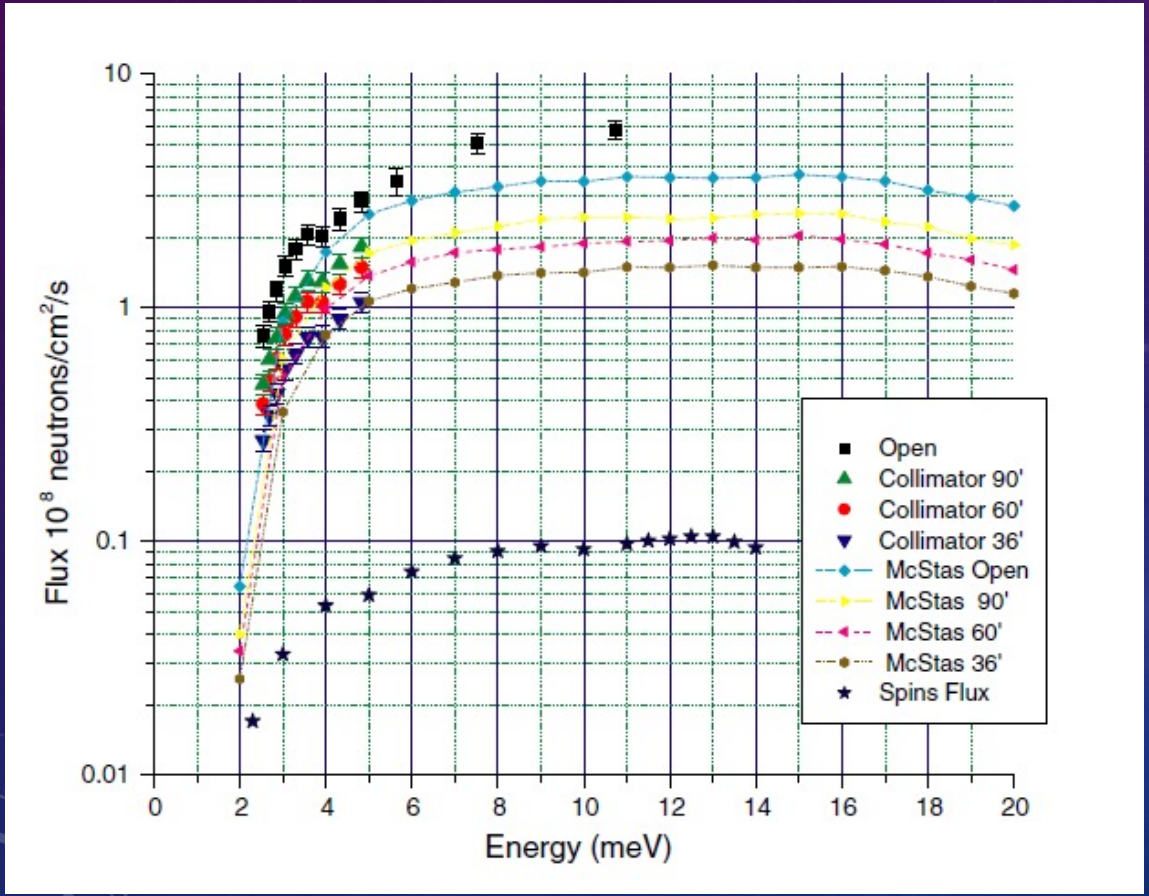

MACS Resolution measured with a V standard.

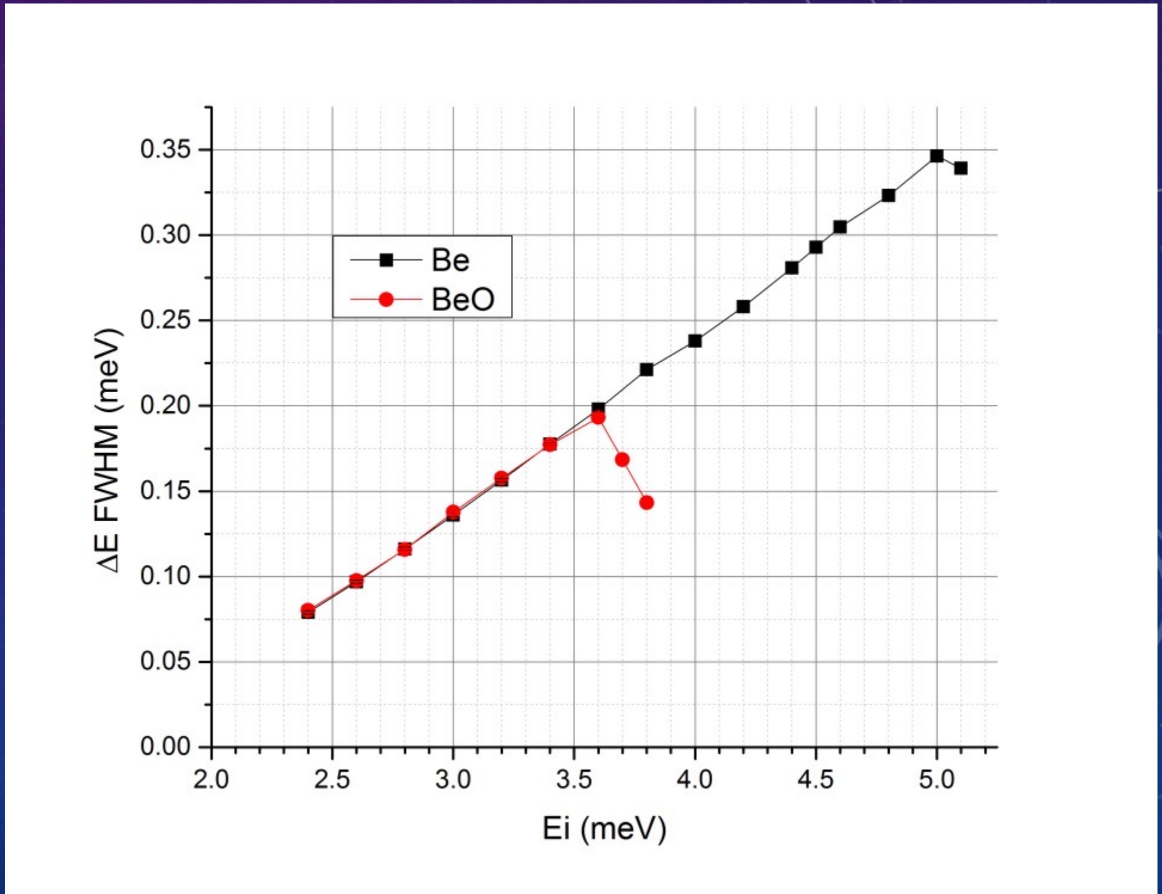

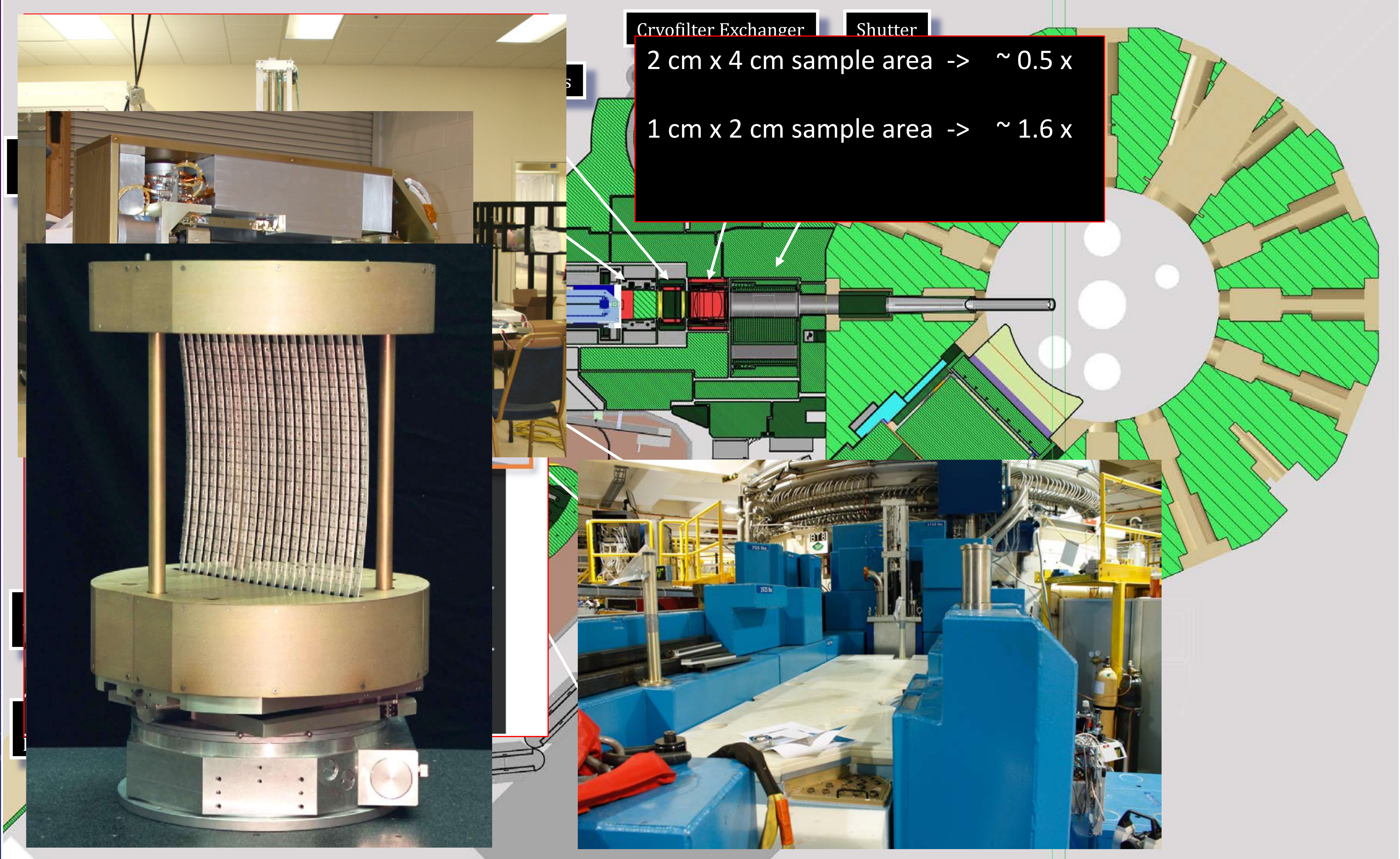
Cryofilter Exchanger
Shutter
2 cm x 4 cm sample area -> ~ 0.5 x
1 cm x 2 cm sample area -> ~ 1.6 x

Cooled filters Be, BeO and HOPG (MCFX)

Vertically focusing analyzers

Diffraction detectors

Sample stage

90' Collimators

Spectroscopic detectors

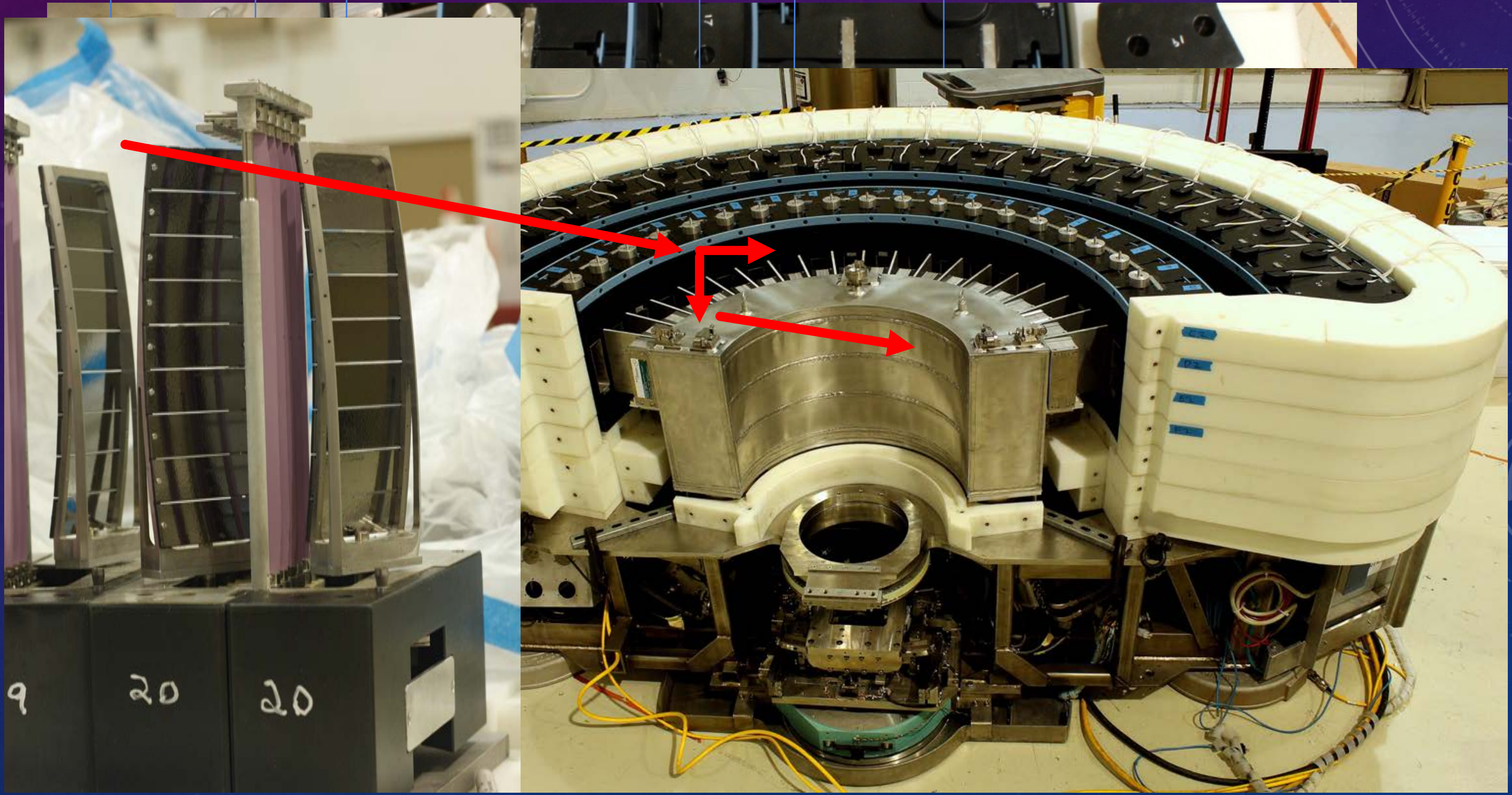

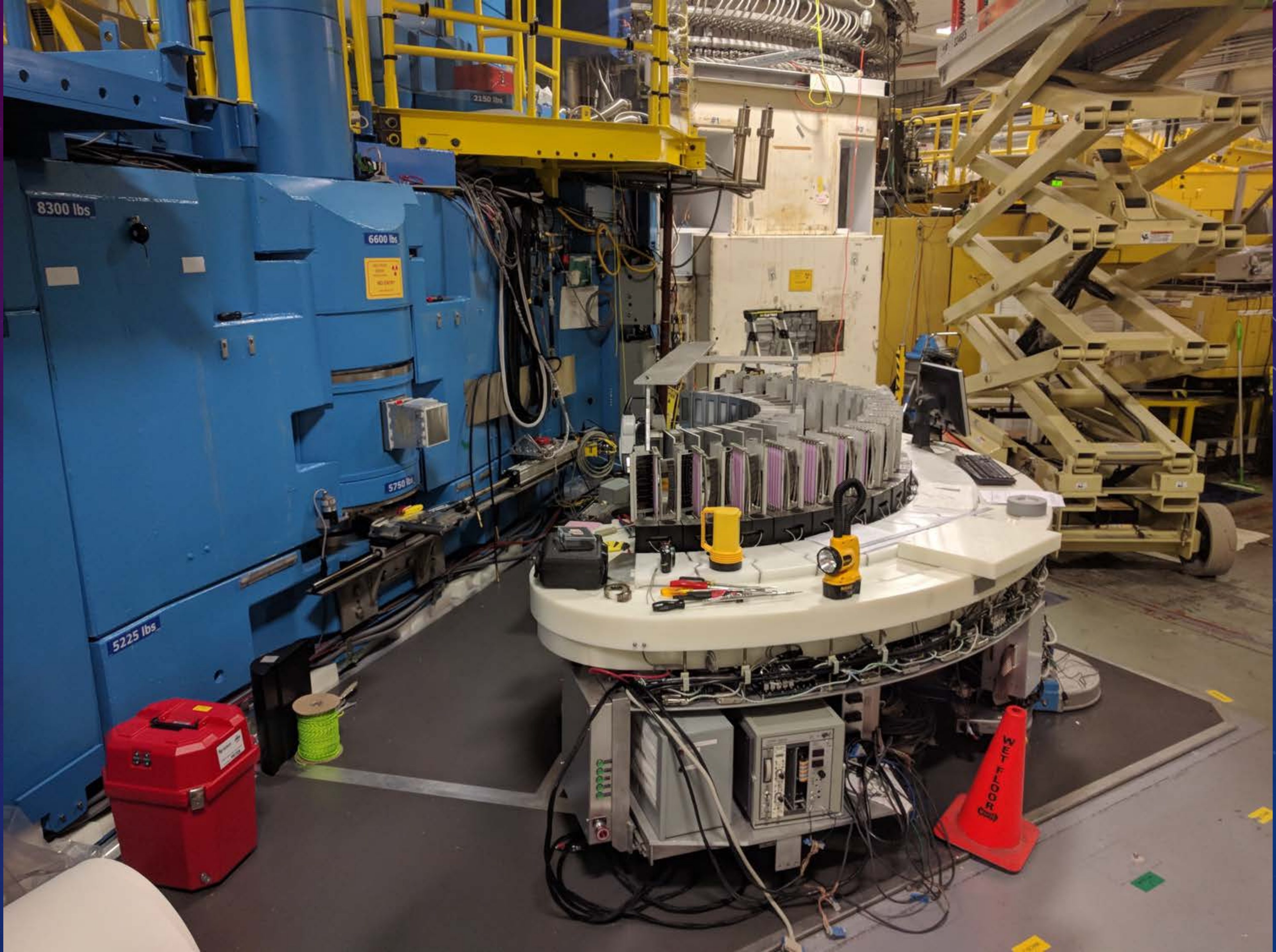
8300 lbs
6600 lbs
2150 lbs
5750 lbs
5225 lbs
WET FLOOR


EVACUATION ROUTES and PROCEDURES
WHAT TO DO
LIFTING SLINGS
HEAVY-DUTY ROTARY HAMMER
15 TON

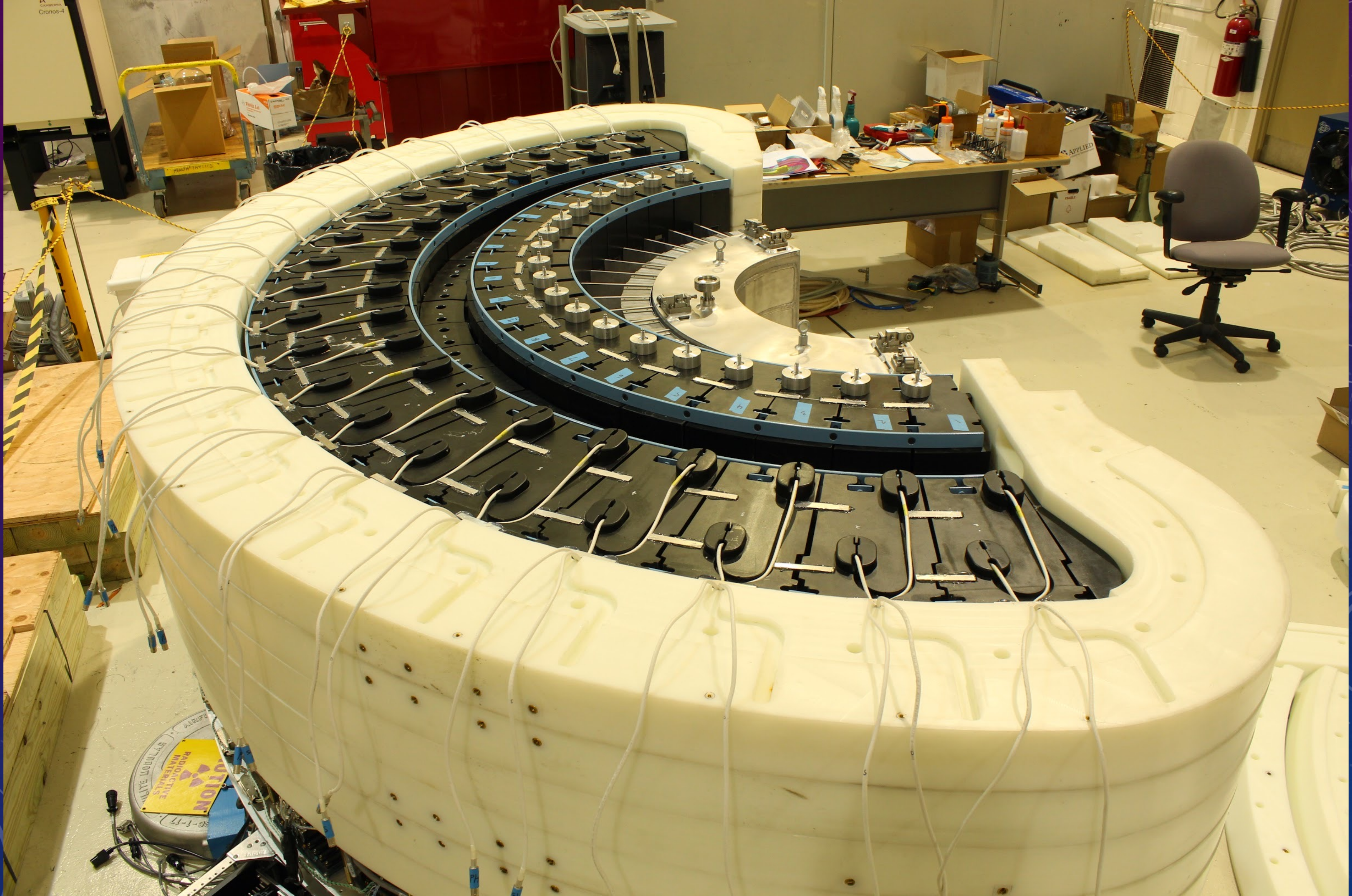
Cronos-4
APPLIED


6600
NO ENTRY

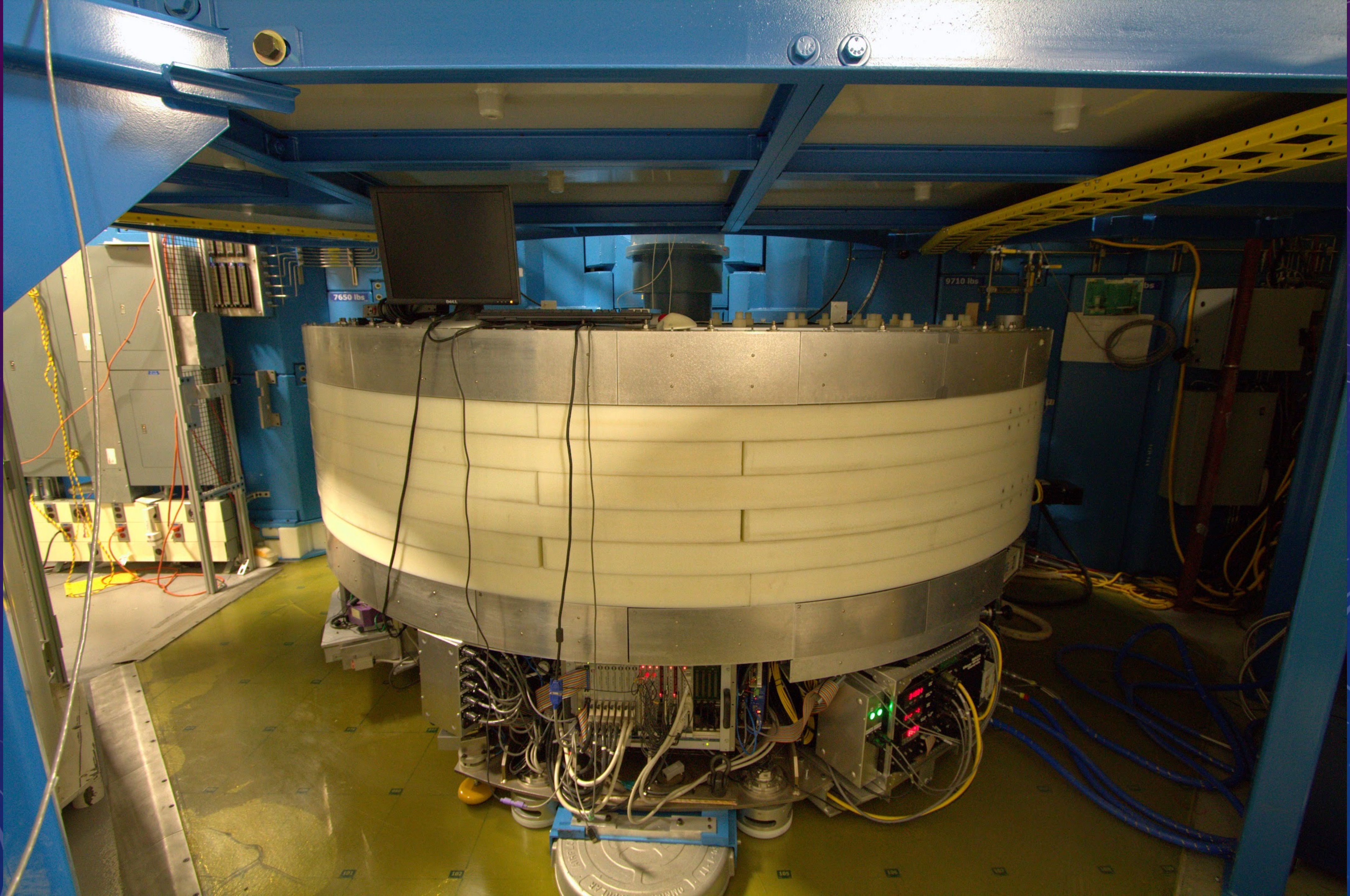
7650 lbs
9710 lbs


CAUTION
TRIPPING
HAZARD
3100 lbs

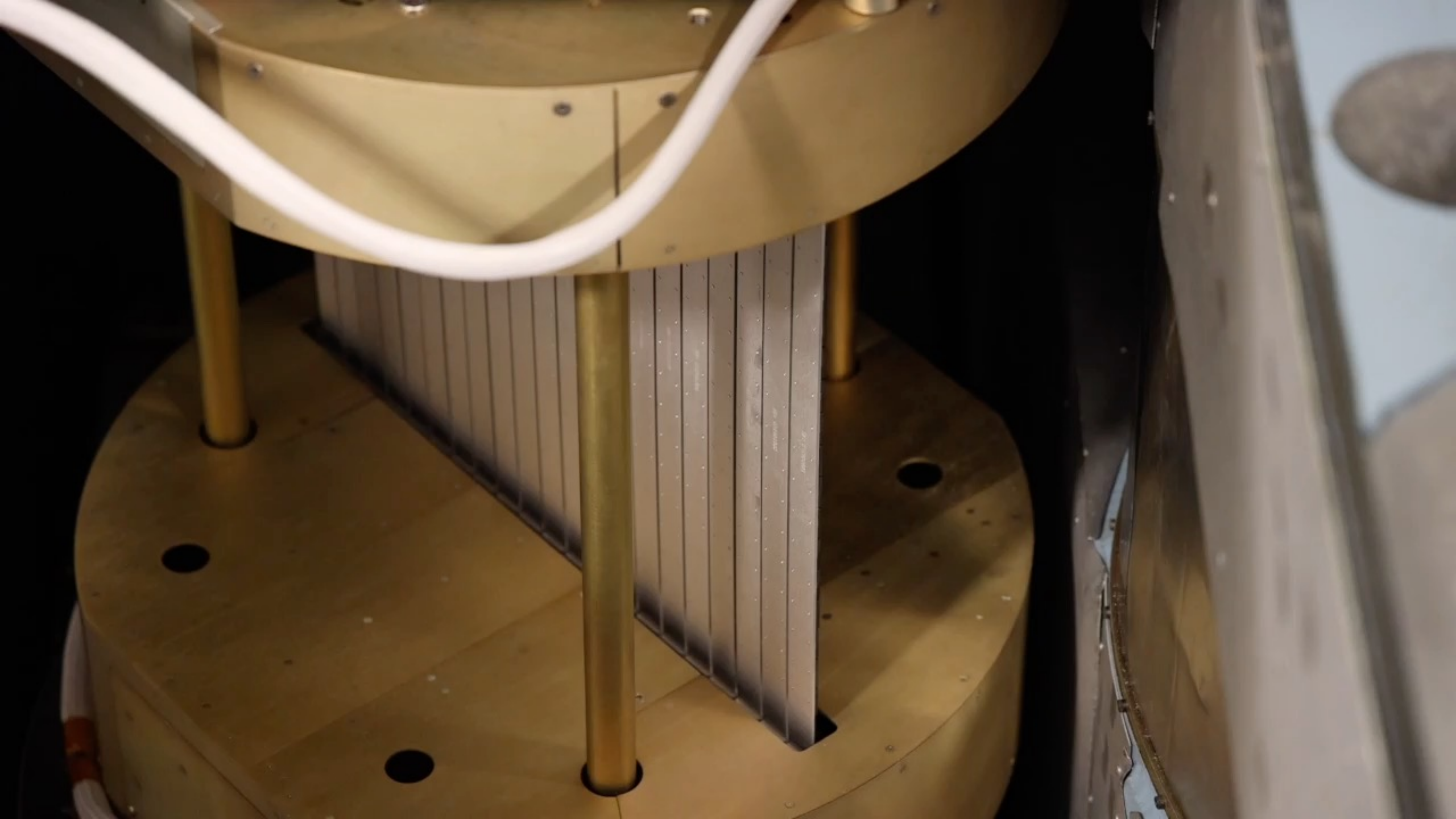


Kranco
HOUSTON, TEXAS
CAPACITY 15 TONS
CAUTION LOW HEADROOM
BEAM OFF
2850 lbs
3950 lbs
8300 lbs
7650 lbs
6600 lbs
5295 lbs
4135 lbs
2150 lbs
3045 lbs
3905 lbs


ENTRY
BEAM ON
BEAM OFF
OXFORD
8300 lbs.
6600 lbs.

Questions about MACS?

Experimental examples with the Multi-Axis Crystal Spectrometer

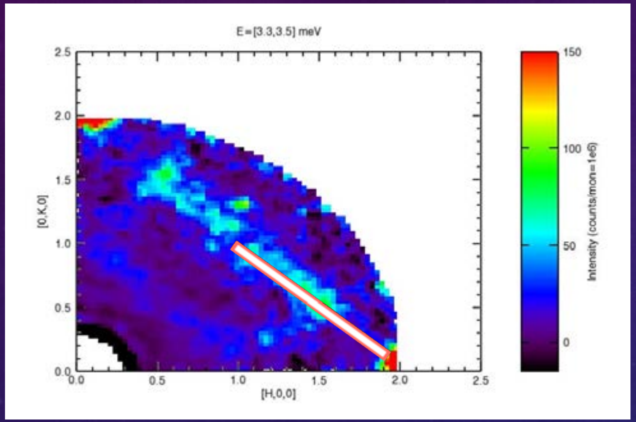

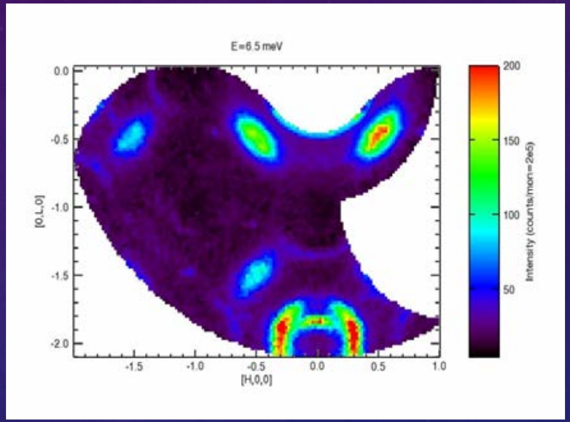

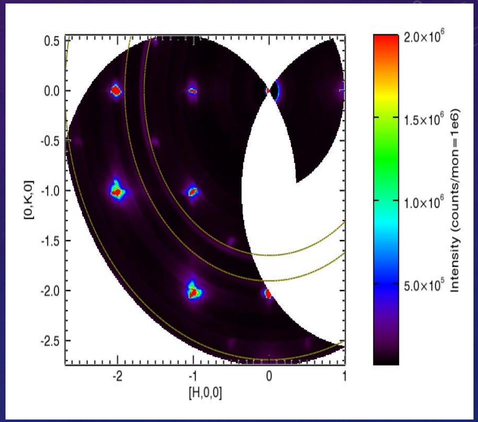

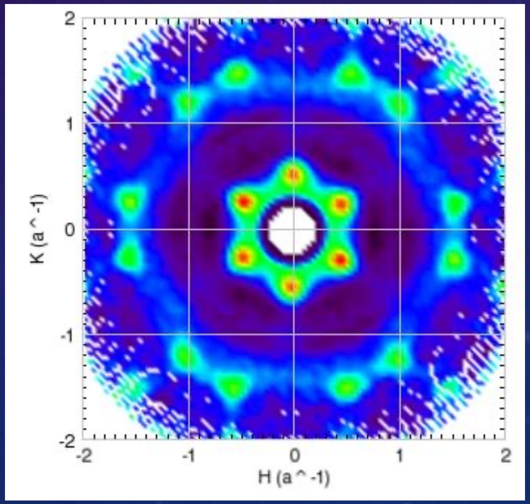

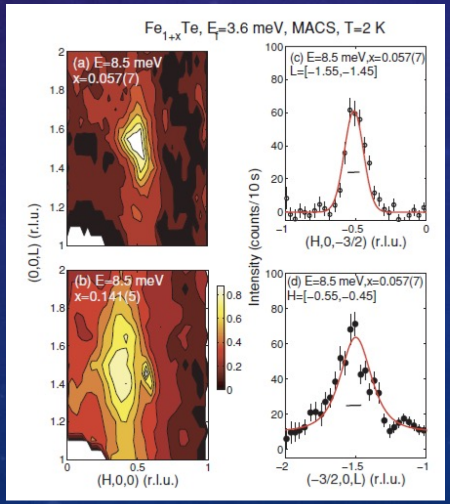

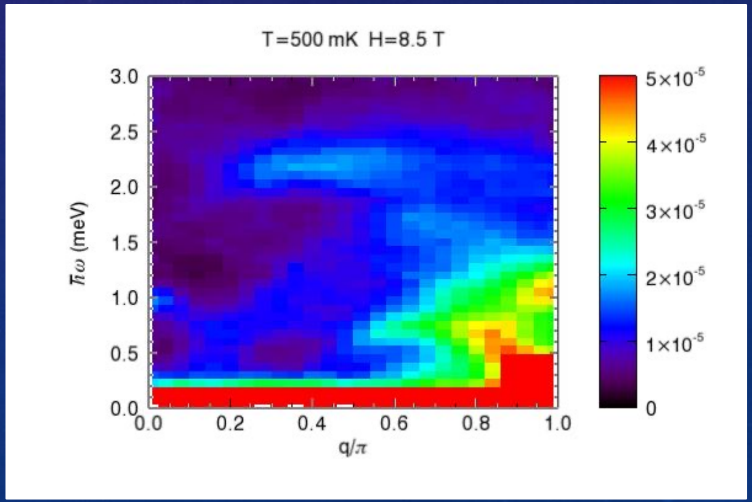

2D spin ½ antierromagnet $TeVO_4$

- Monoclinic (P 21/c, β ~ 105.8)
- Quasi 2D spin lattice

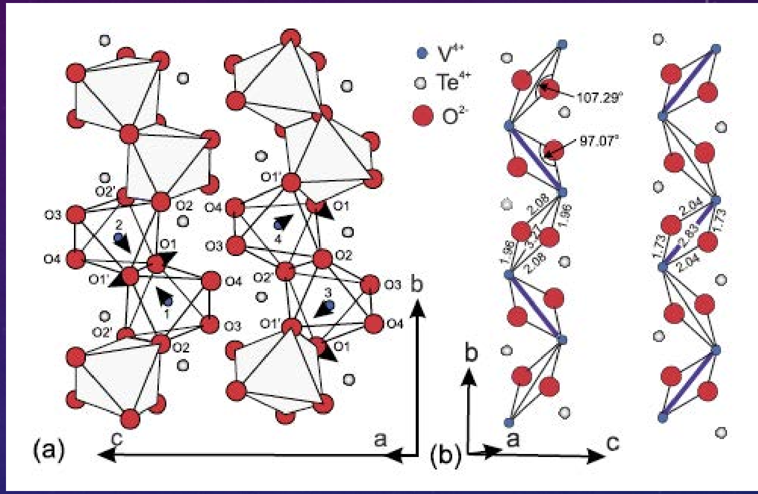

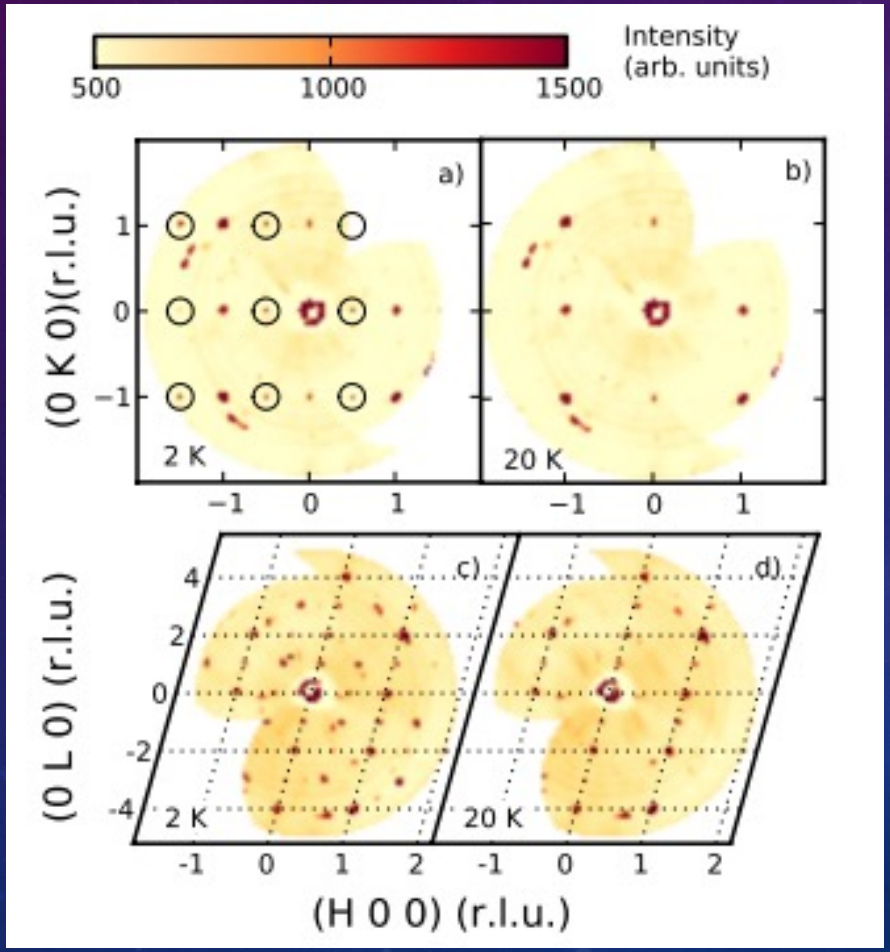

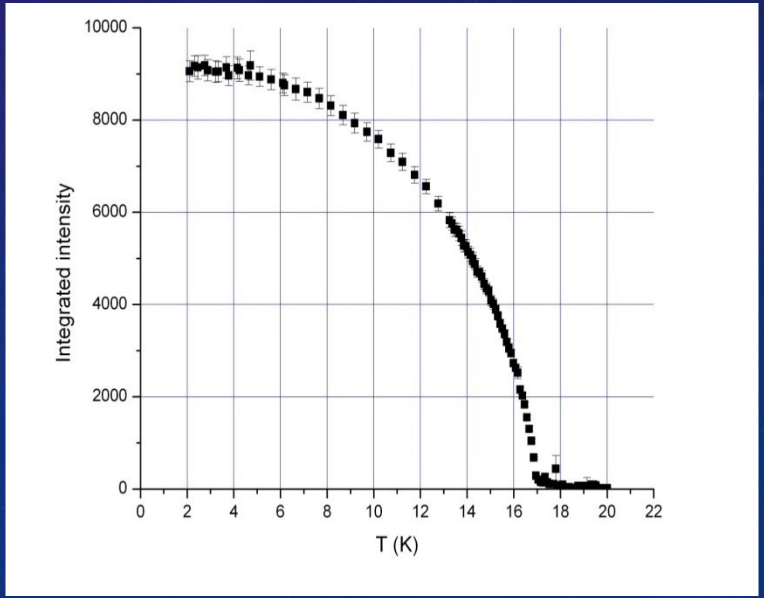

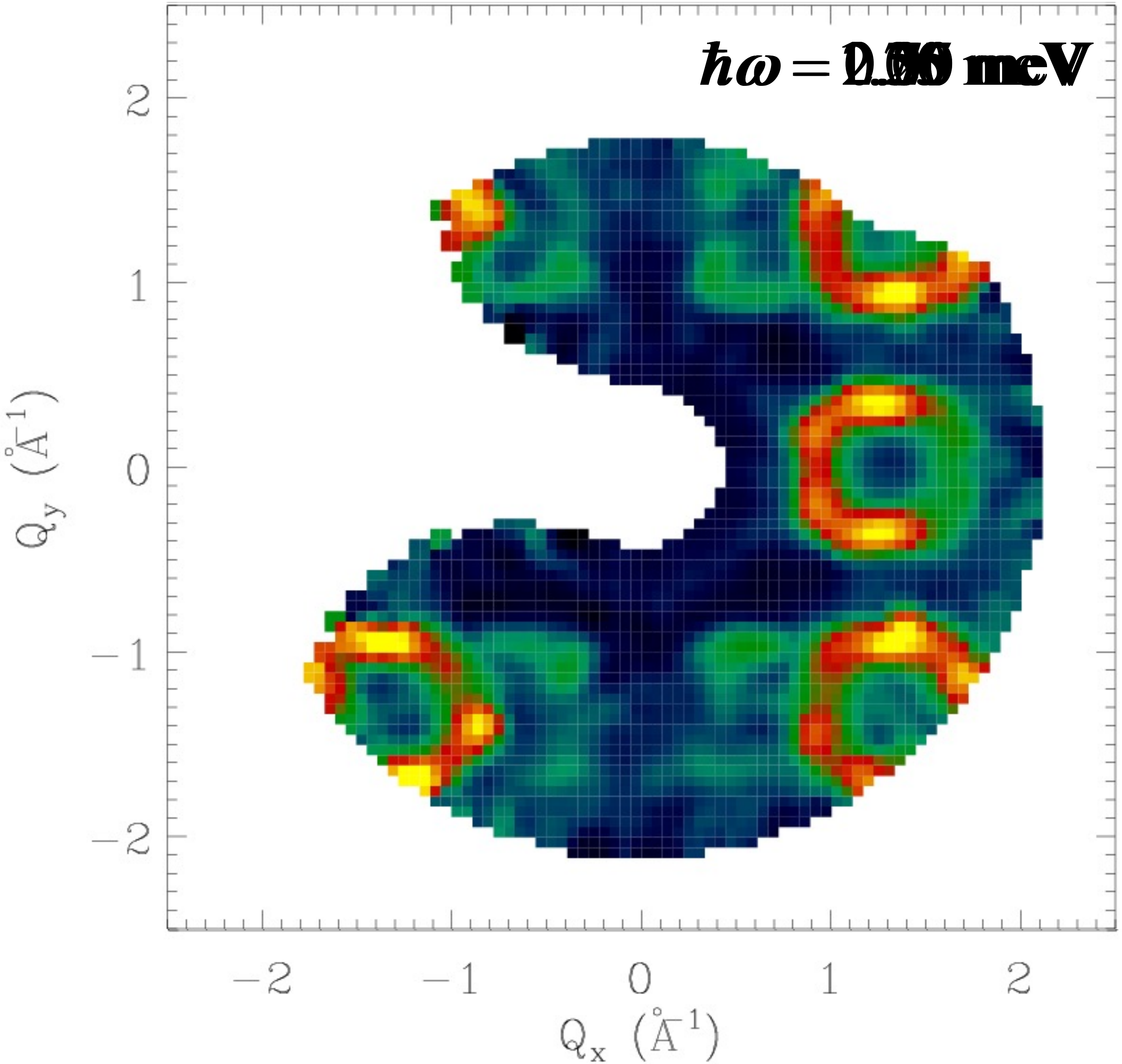

Q_y (Å^{-1})
Q_x (Å^{-1})
2
1
0
−1
−2

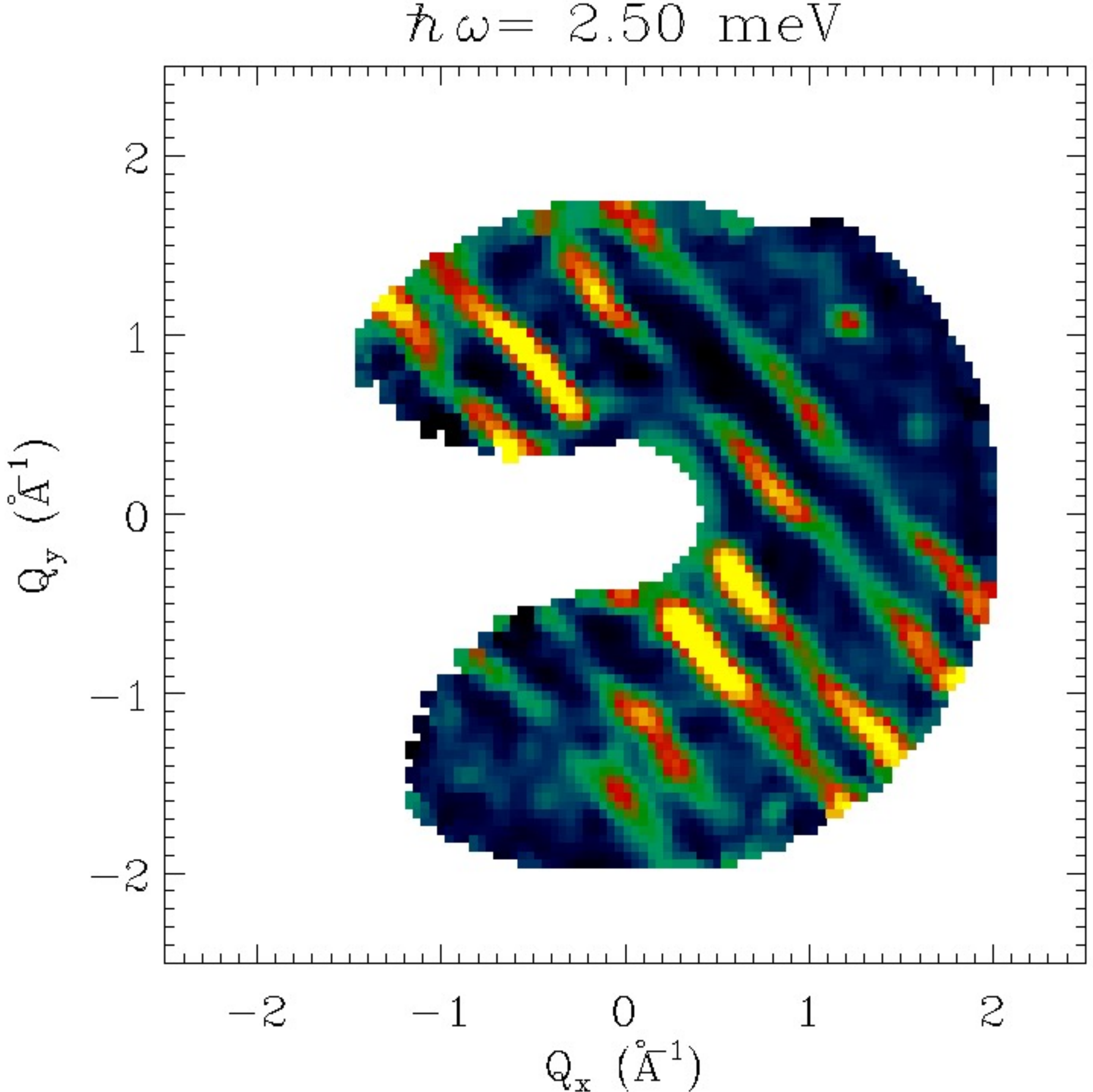

$\hbar\omega = 2.50$ meV
Q_y (Å^{-1})
Q_x (Å^{-1})
2
1
0
−1
−2
−2
−1
0
1
2

DISPERSION: SLICES THROUGH A **Q**-E

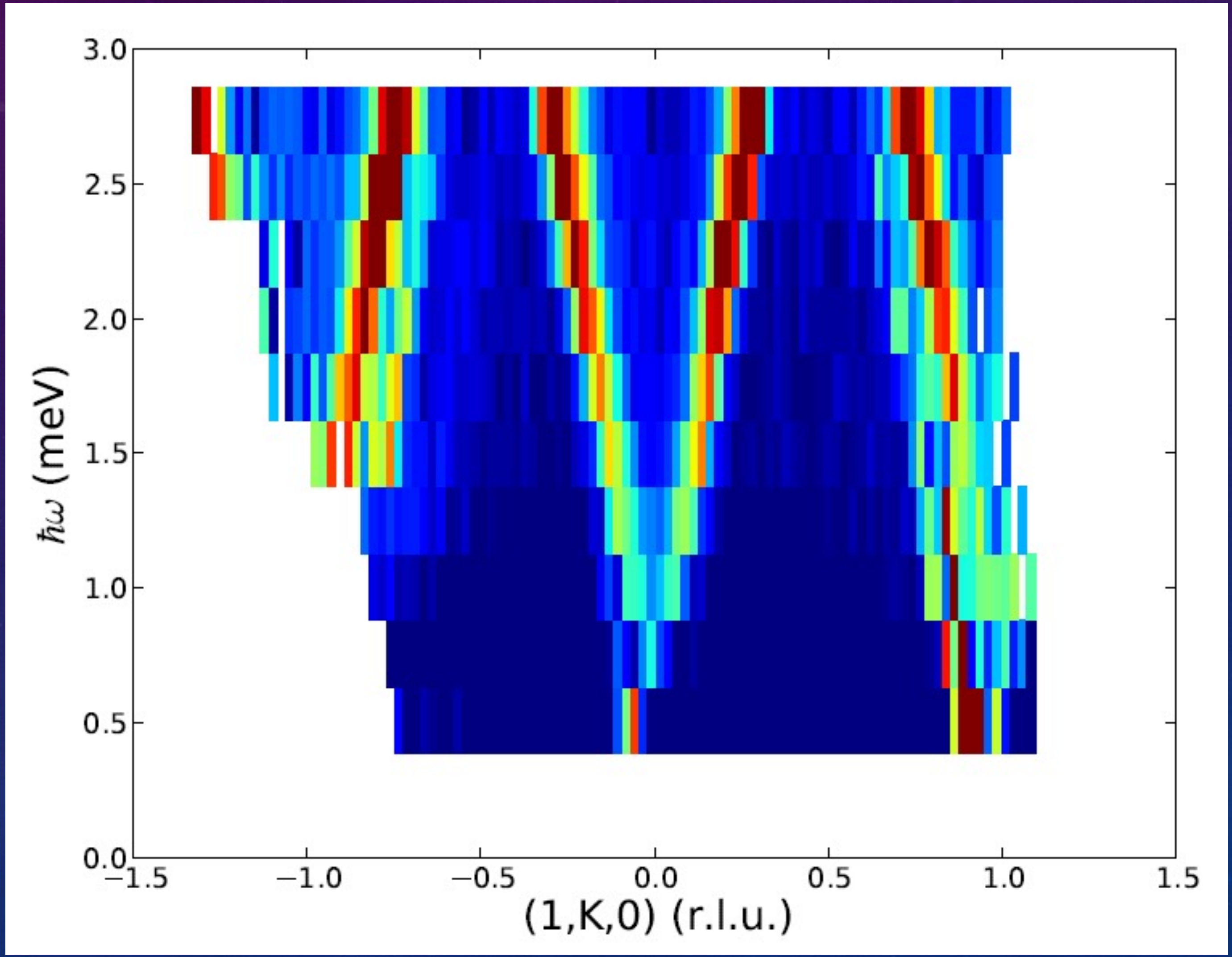

MAGNETIC FRUSTRATION

- All the interactions compete.
- The spins do not satify all the interactions.
  Eg: Antiferromagnetic triangular crystal.

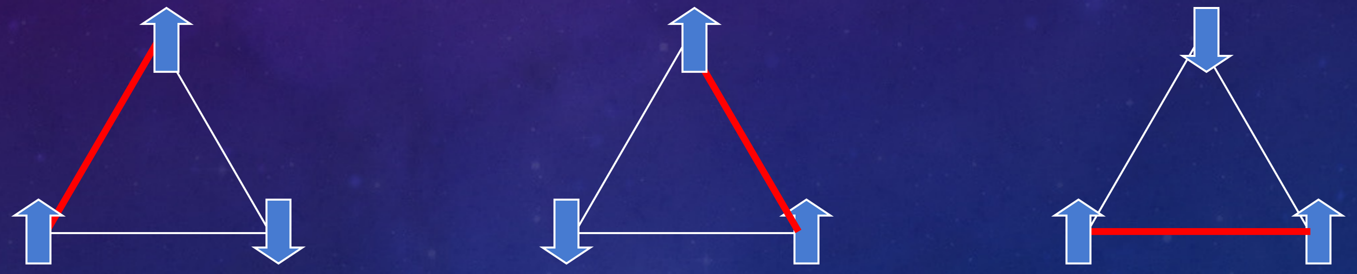

There is not an optimal spin “ordering”.

Geometrically Frustrated Lattices

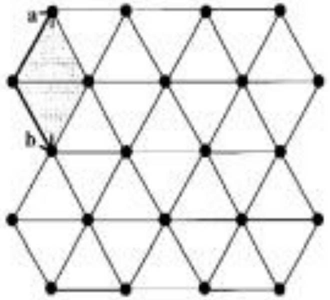

Triangular lattice

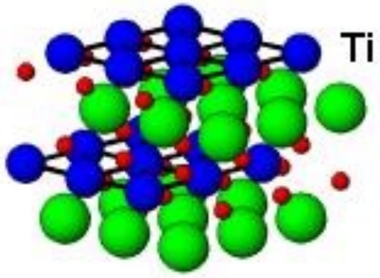

$NaTiO_2$, $LiVO_2$, ...

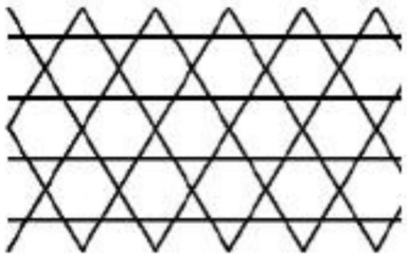

Kagome lattice

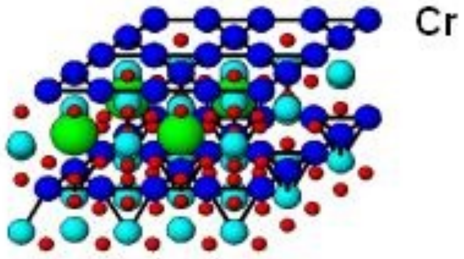

$SrCr_9Ga_3O_{19}$

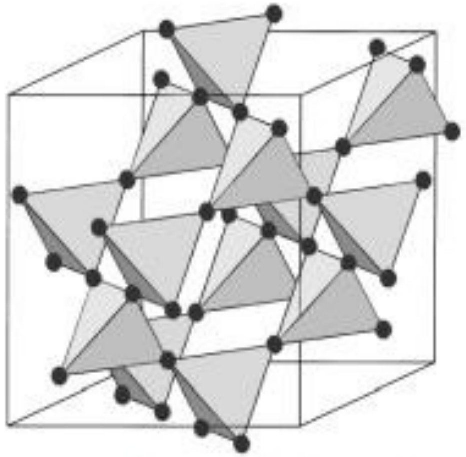

Pyrochlore lattice

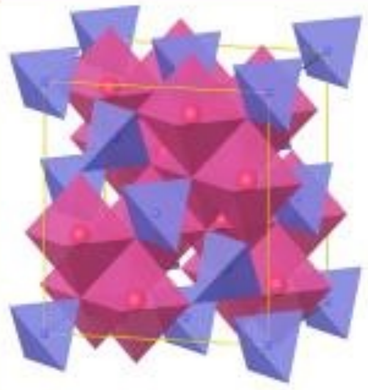

Spinel (AB_2O_4)

$Fe_3O_4 = FeFe_2O_4$

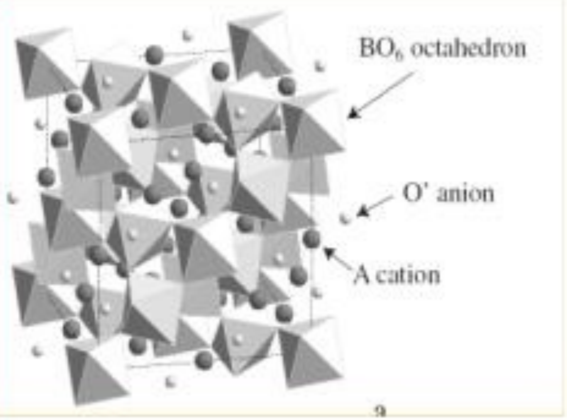

Pyrochlore($A_2B_2O_7$)

$Y_2Mo_2O_7$

Quantum Spin Liquid Candidate Herbersmithite ($ZnCu_3(OD)_6Cl_2$)

In a spin liquid the magnetic moment are highly correlated. The spins do not order neither freeze.

$$\mathbf{H} = \sum_{ll'} J_{ll'} \mathbf{S}_l \cdot \mathbf{S}_{l'} - \mu_B \mathbf{H} \cdot \sum_l g_l \mathbf{S}_l$$

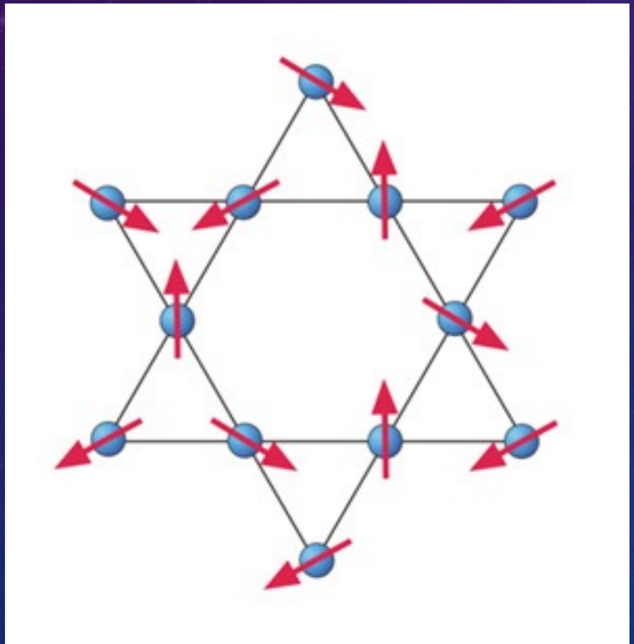

Kagome crystal

T=1.6K

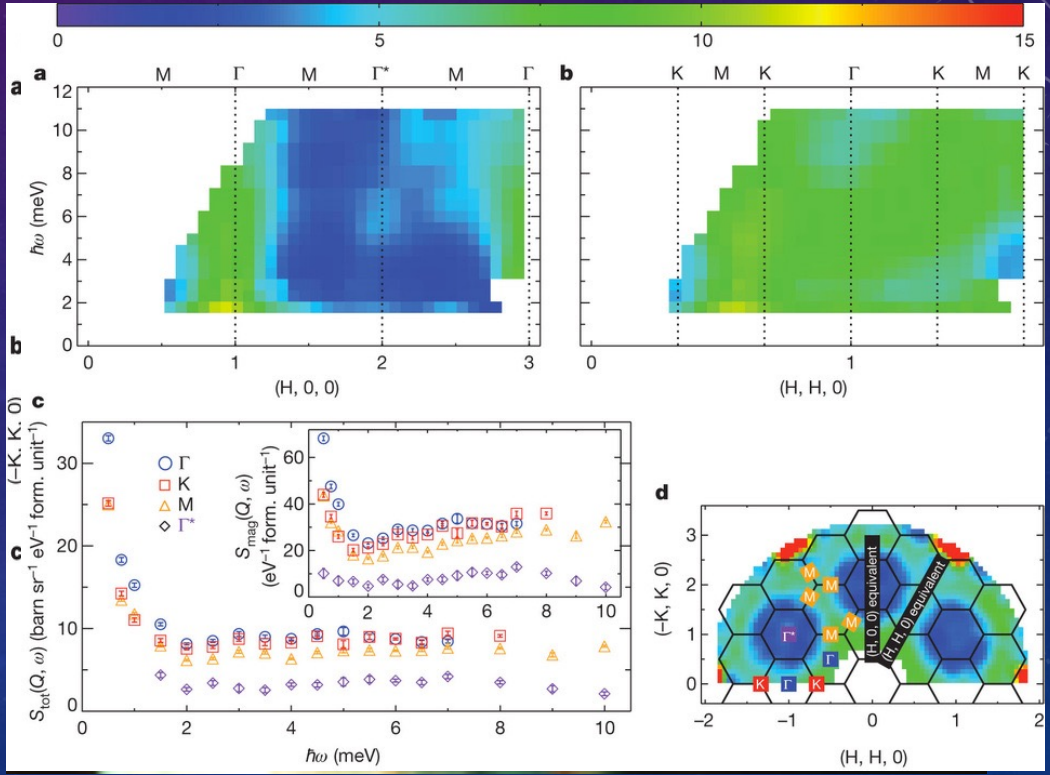

T-H Han et al. Nature, 492, Dec. 20, 2012,

Quantum Spin liquid candidate $Ca_{10}Cr_7O_{28}$. Complex frustration mechanism.

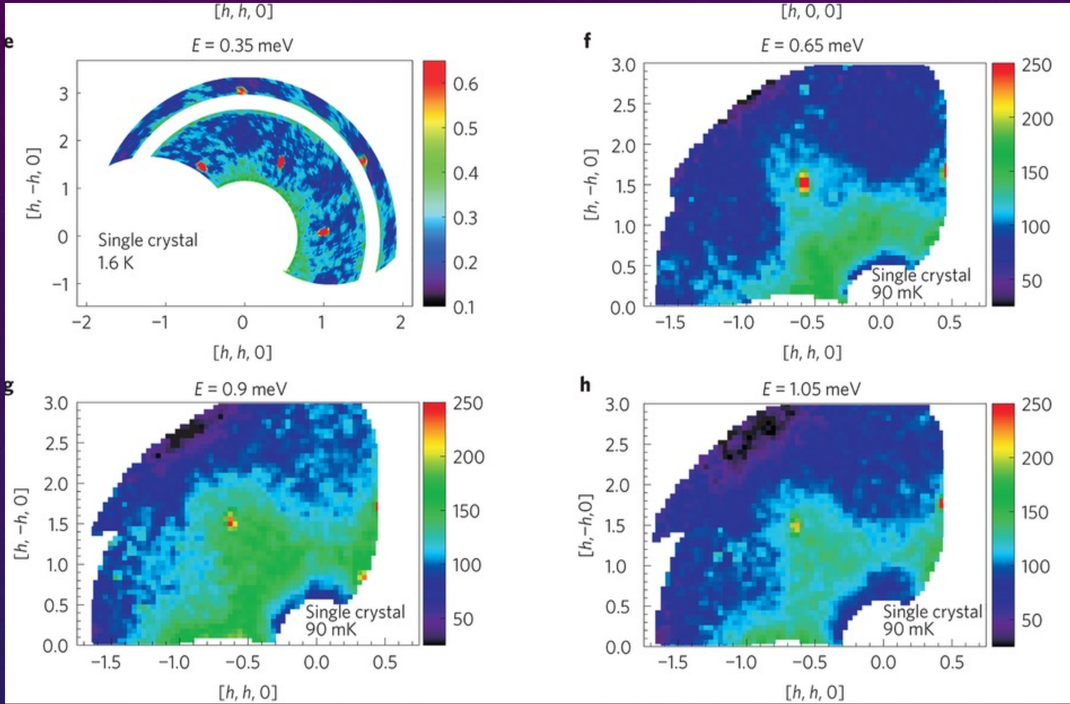

"Here investigate the novel, unexplored magnet $Ca_{10}Cr_7O_{28}$ which has a complex Hamiltonian consisting of several different isotropic interactions and where the ferromagnetic couples are stronger than the antiferromagnetic.

C. Baltz et al. Nature Physics **12**, 942–949 (2016).

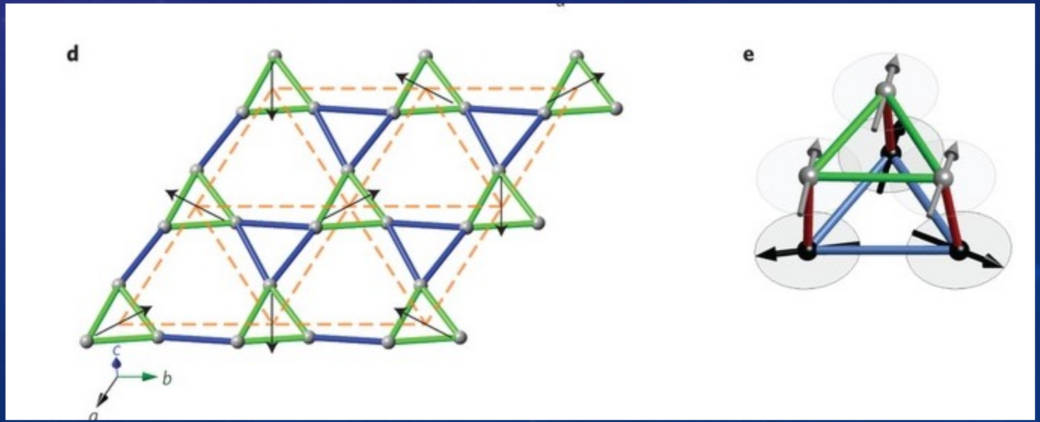

Pyrochlore $NaCa_2CoF_7$

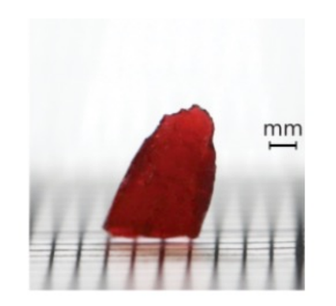

Second XY pyrochlore reported.

Magnetic interaction:

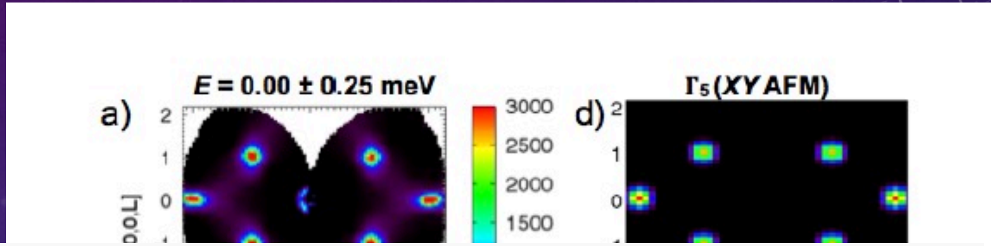

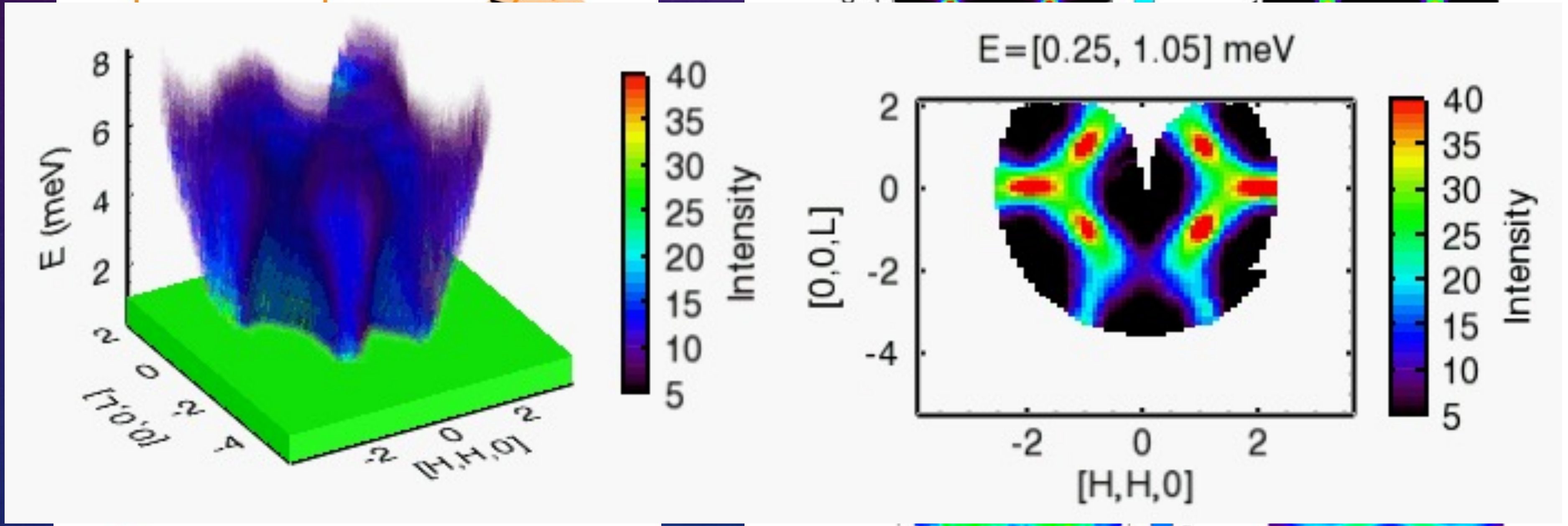

K. A. Ross et al.

Polarized beam capabilities
$Ho_2Ti_2O_7$ pyrlochlore spin ice

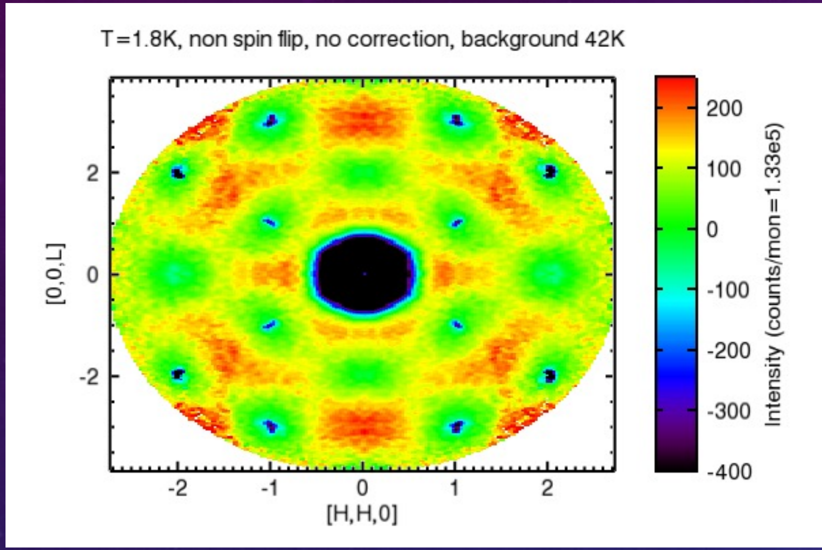

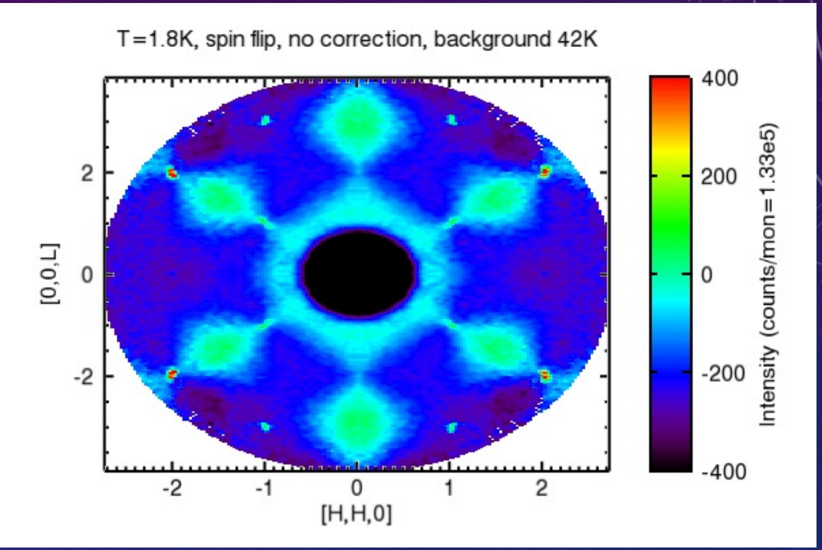

J. Gaudet et al.

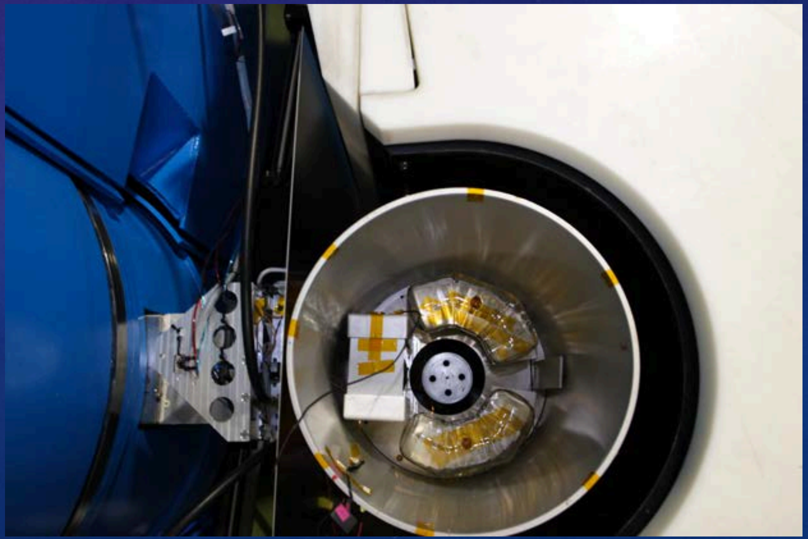

$CeCu_2Si_2$ Heavy fermion superconductor

Magnetic exitations arise from quasiparticles associated with is heavy electron band, which are also resposible for sueprconductivity

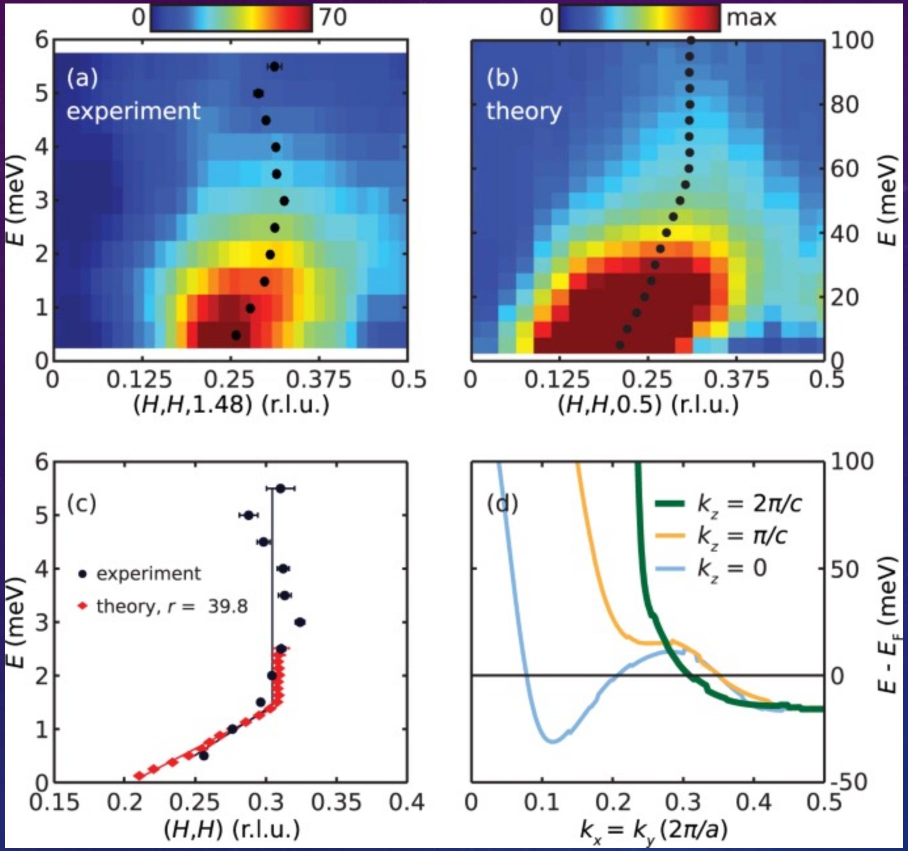

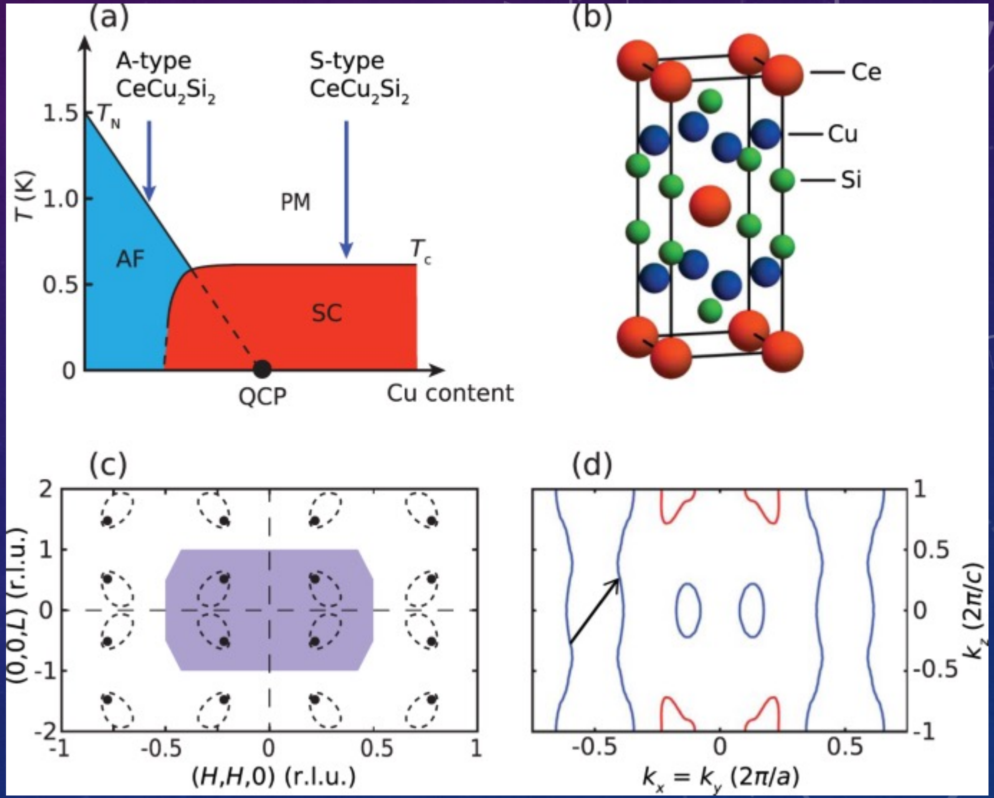

Song, Y., Wang, W., Cao, C. *et al.* High-energy magnetic excitations from heavy quasiparticles in $CeCu_2Si_2$. *npj Quantum Mater.* **6,** 60 (2021). https://doi.org/10.1038/s41535-021-00358-x

Weyl fermions in NdAlSi

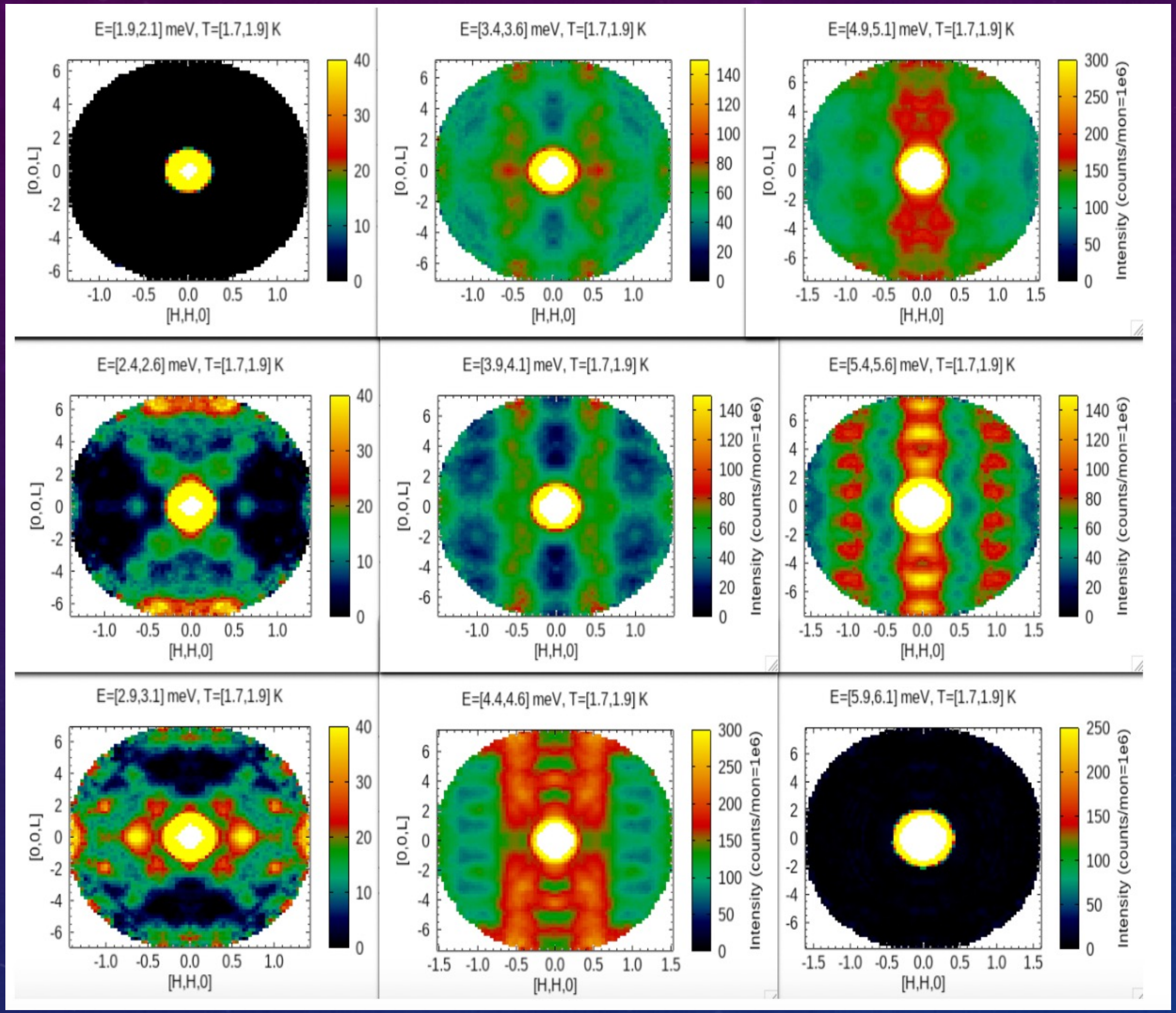

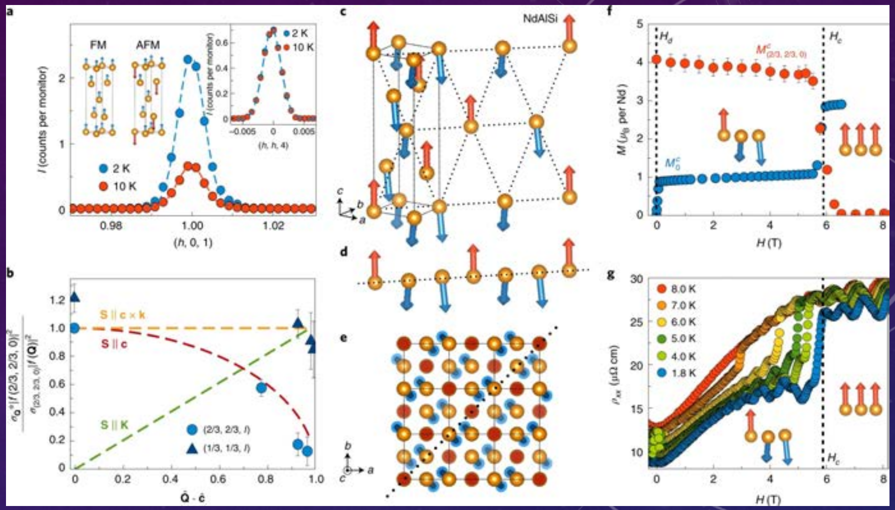

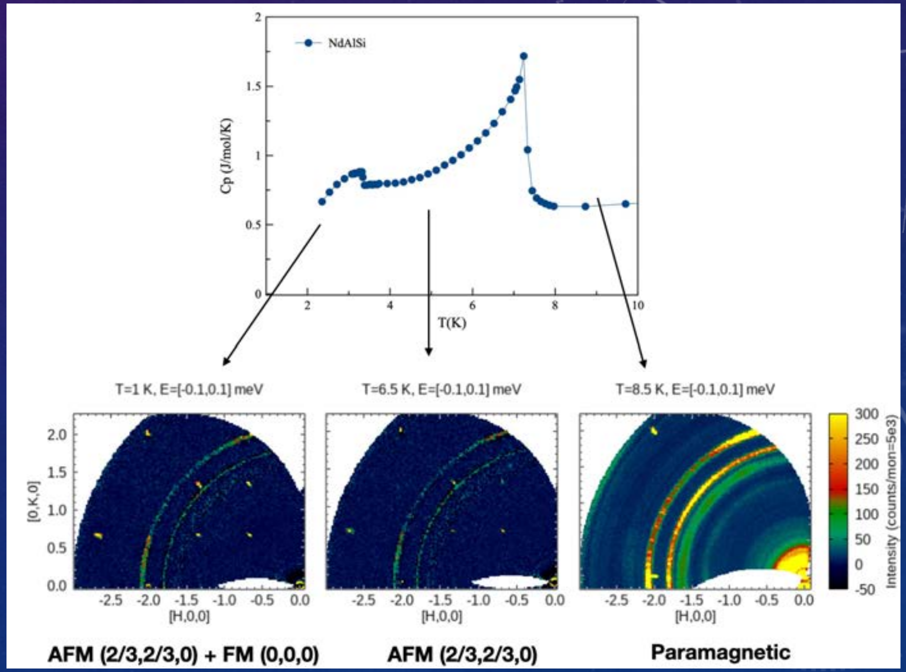

Gaudet, J., Yang, HY., Baidya, S. *et al.* Weyl-mediated helical magnetism in NdAlSi. *Nat. Mater.* **20,** 1650–1656 (2021). https://doi.org/10.1038/s41563-021-01062-8

SRO AND SE IN A NULL-MATRIX NIPT (DONE IN DCS)

$$I = I_{Bragg} + I_{SRO} + I_{SE} + I_{HDS+1st\ order\ TDS}$$

$$I_{Bragg}, I_{HDS}, I_{TDS} \sim (c_A b_A + c_A b_A)^2$$

$$I_{SRO} \sim c_A c_B (b_B - b_A)^2$$

$$I_{SE} \sim b_A(b_B - b_A),\ b_B(b_B - b_A)$$

$$I_{null-matrix} = I_{SRO} + I_{SE}$$

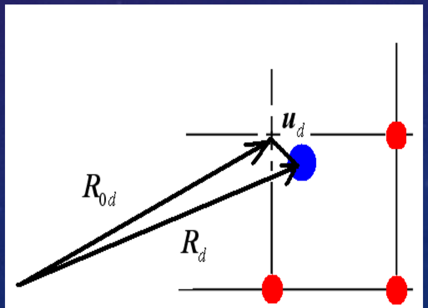

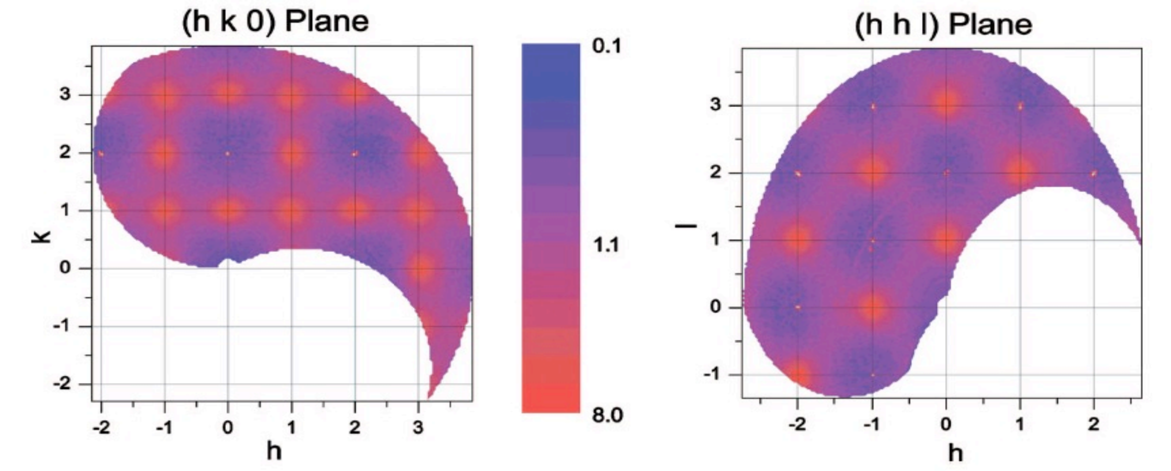

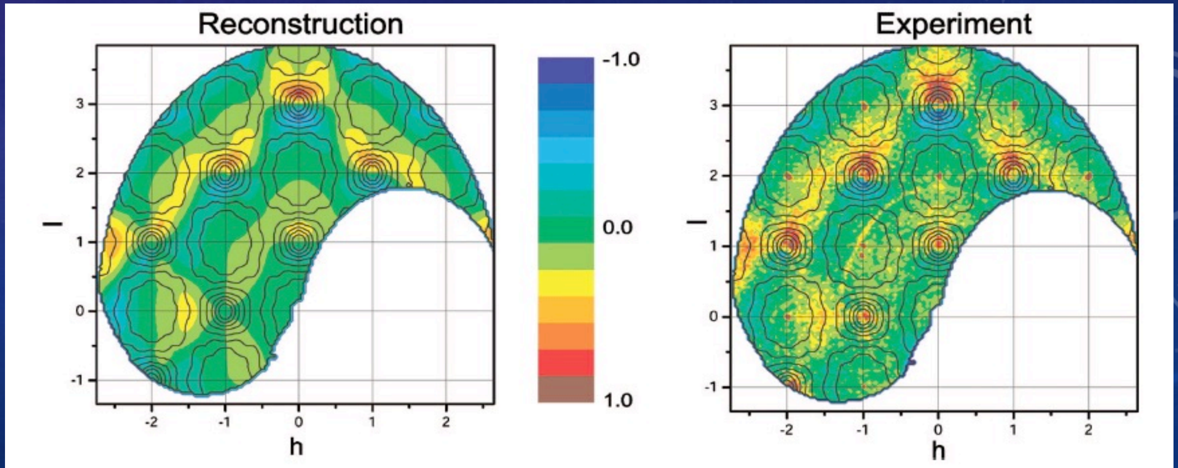

LEAD FREE RELAXOR $NA_{1/2}BI_{1/2}TIO_3$

$$I = I_{Bragg} + I_{SRO} + I_{SE} + I_{HDS+1st\ order\ TDS}$$

Relaxor have a large dielectric permitivity.

Relaxor based ferroelectric single crystals are considered as the next generation transducer materials.

The structure of PMN, NBT and many other relaxors is based on the cubic perovskite structure

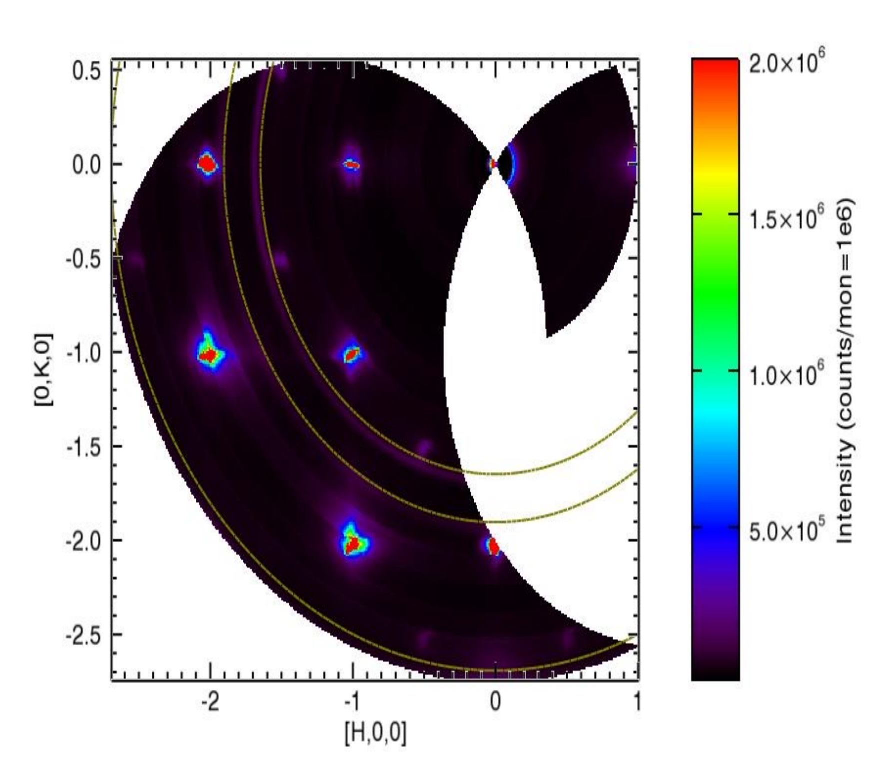

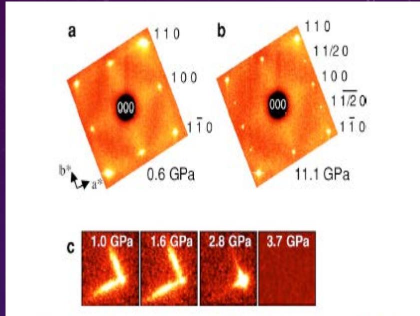

FIG. 4. (Color online) Pressure-dependent evolution of the diffuse scattering in NBT. (a), (b) Illustration of the pressure-independence of the diffuse scattering named type B in the text. Note, that the 11.1 GPa pattern is characterized by, first, the appearance of distortion-related superstructure reflections and second, a sharpening of the Bragg spots. The reduction of the asymmetric diffuse scattering around the $\bar{3}20$ reflection in (c) gives evidence for fundamental structural changes on a local scale. Pattern c is obtained from small 0.5° oscillations around the Bragg angle of the $\bar{3}20$ reflection to emphasize the diffuse scattering.

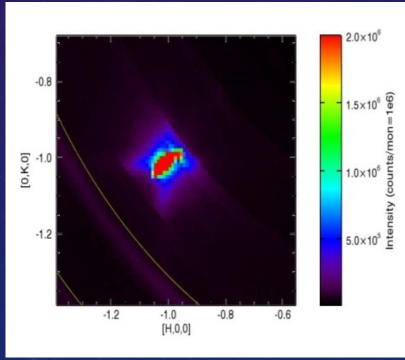

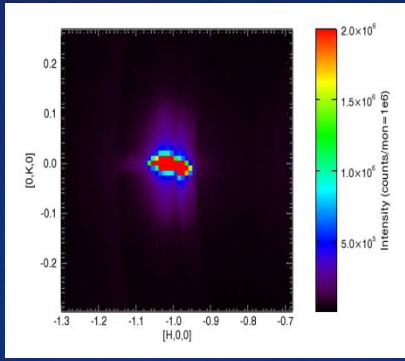

P. Gehring et al. (unpublished)

$$I_{HDS} = cN\left|c_A b_A + c_B b_B\right|^2 \left|\mathbf{Q} \cdot \tilde{\mathbf{t}}(\mathbf{q})\right|^2$$

POLARIZED ACUSTIC MODE IN PZT
PB $(ZR_{0.5}TI_{0.5})O_3$

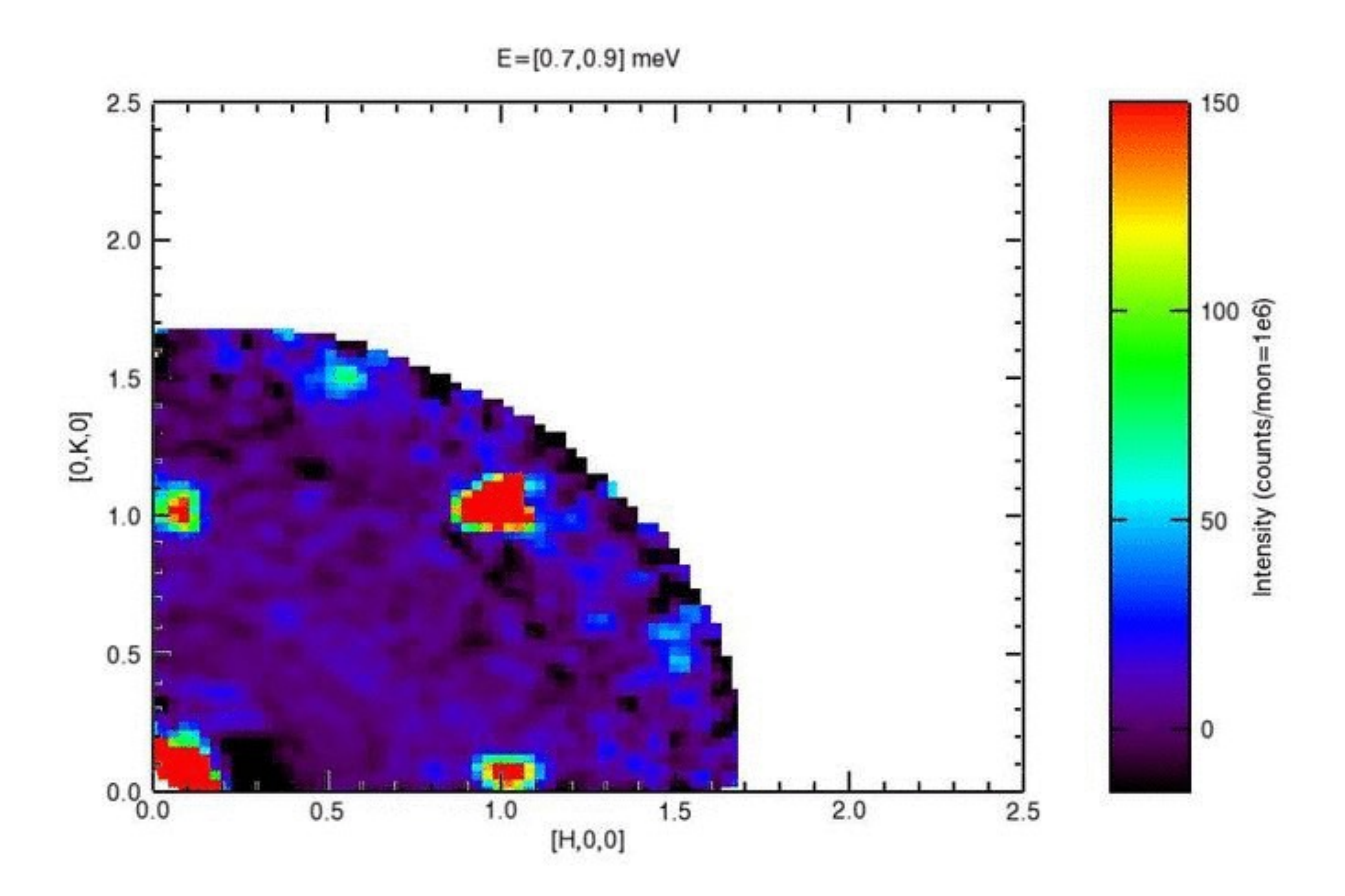

Why the donut shape in reciprocal space?

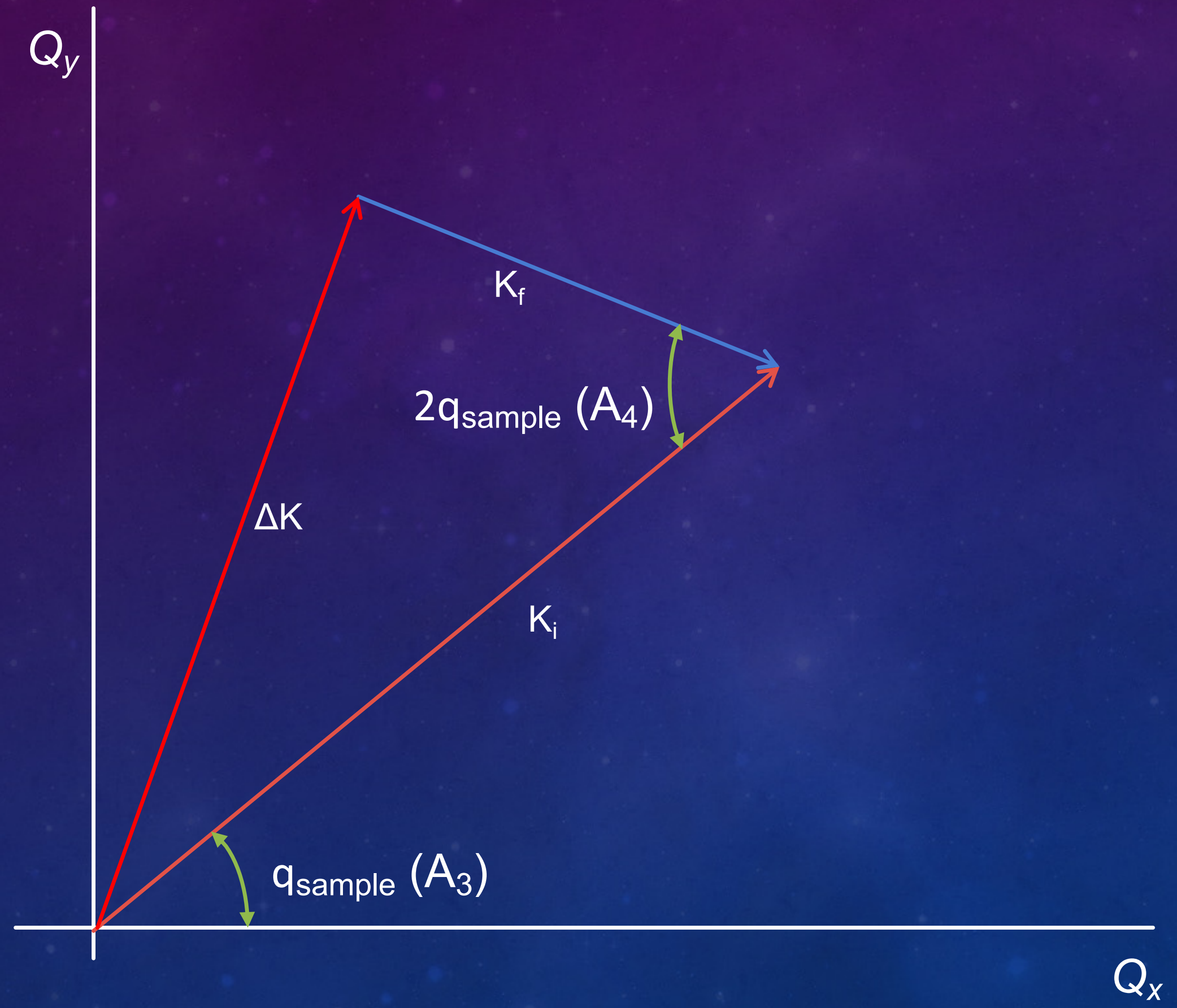

Why the donut shape in reciprocal space?

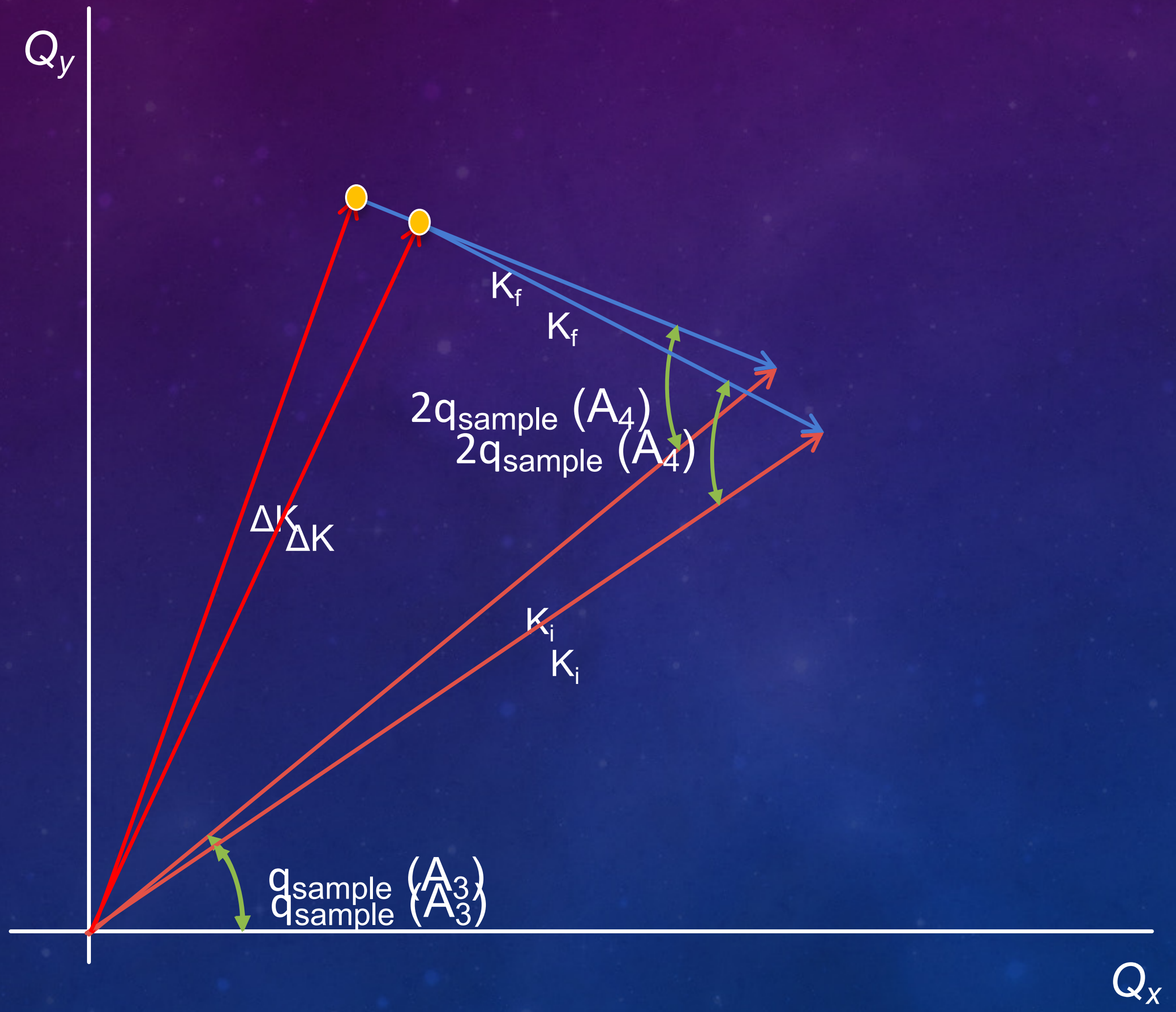

Why the donut shape in reciprocal space?

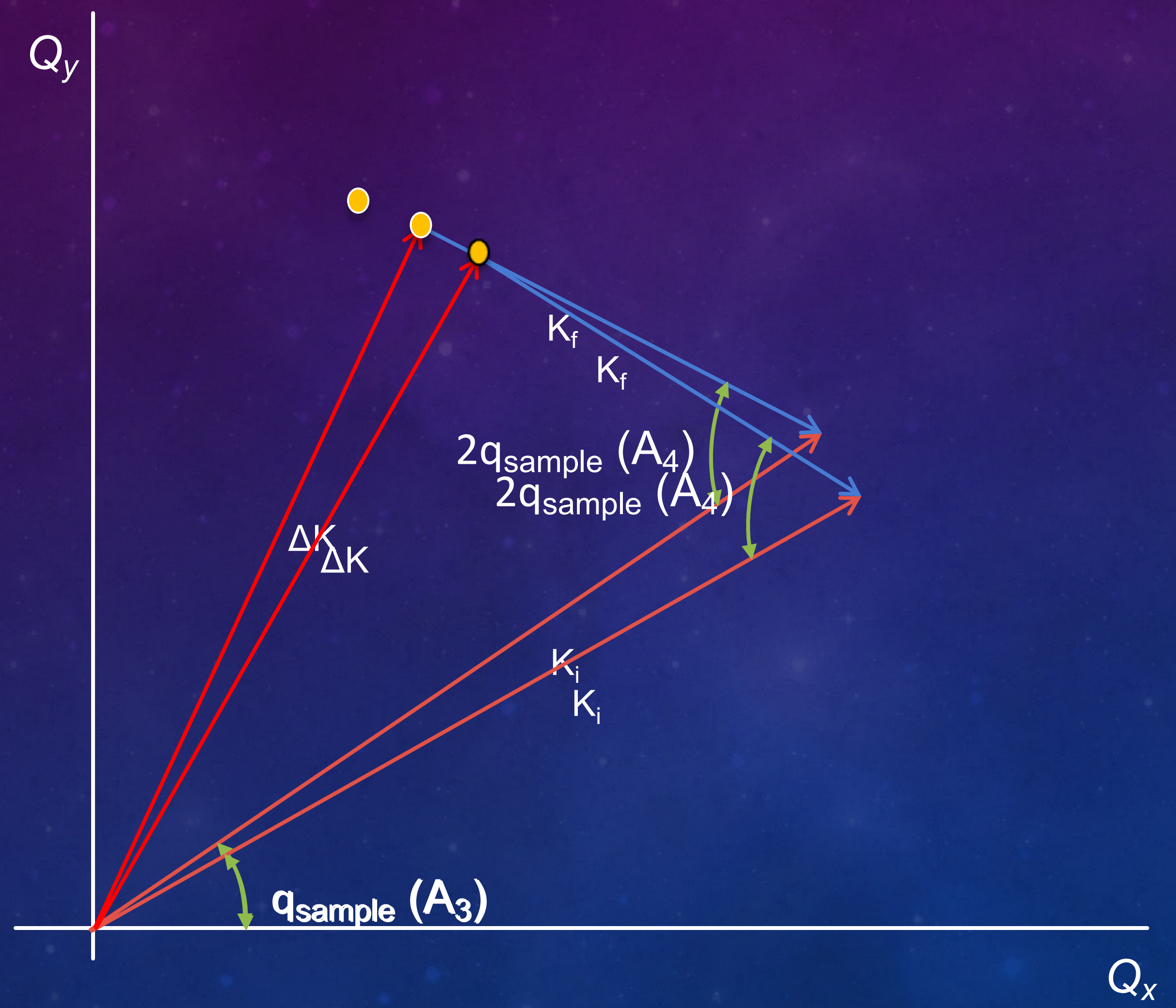

Why the donut shape in reciprocal space?

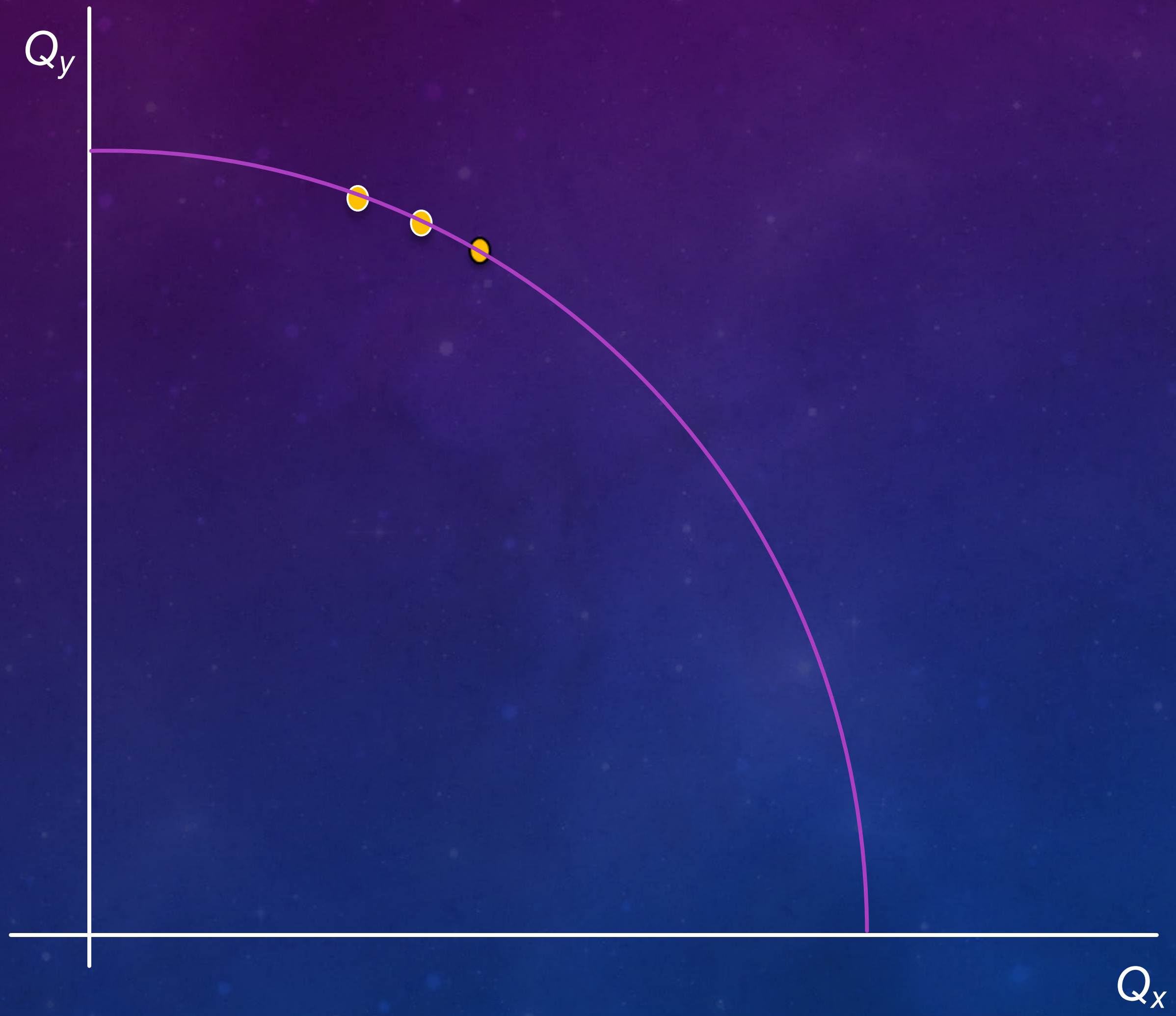

Why the donut shape in reciprocal space?

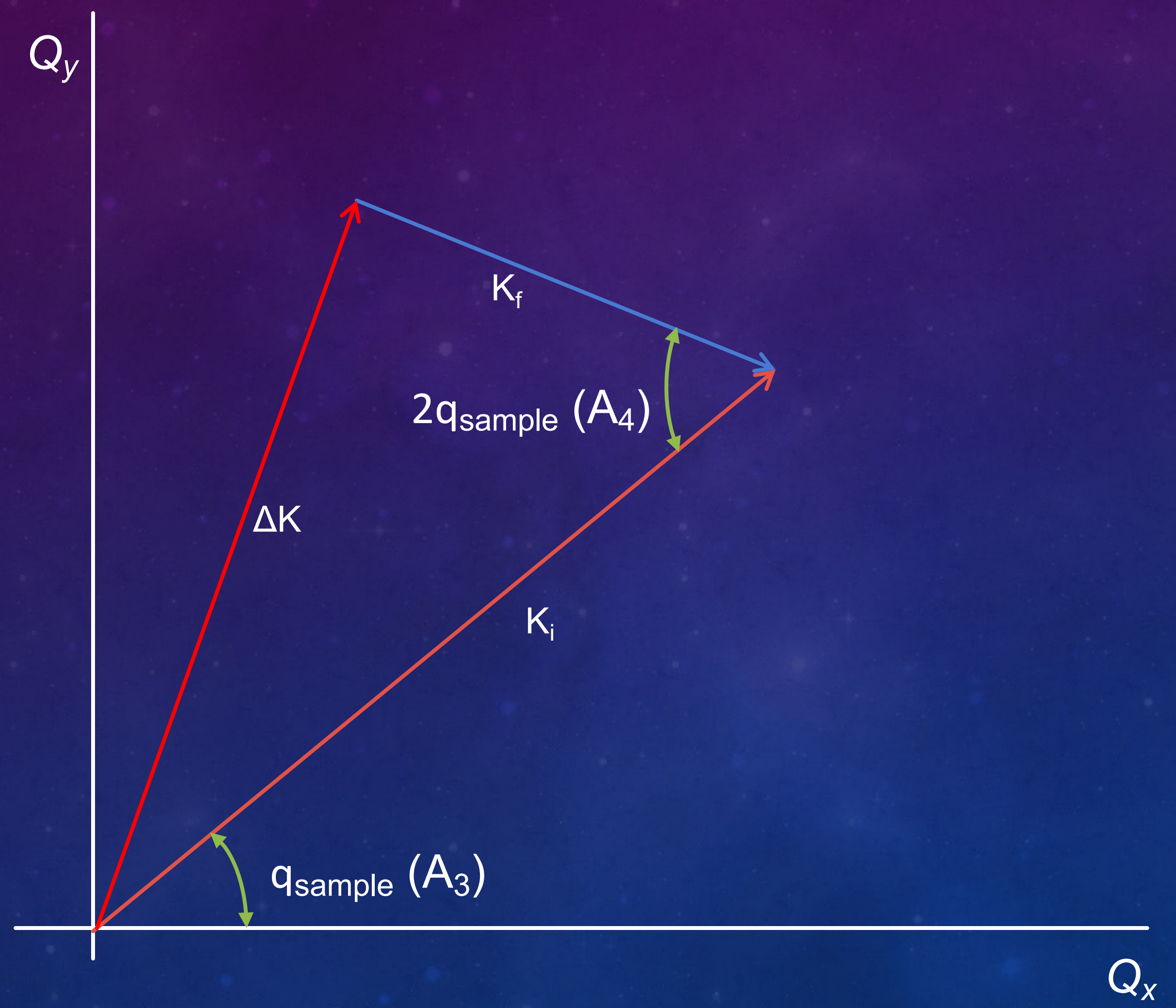

Why the donut shape in reciprocal space?

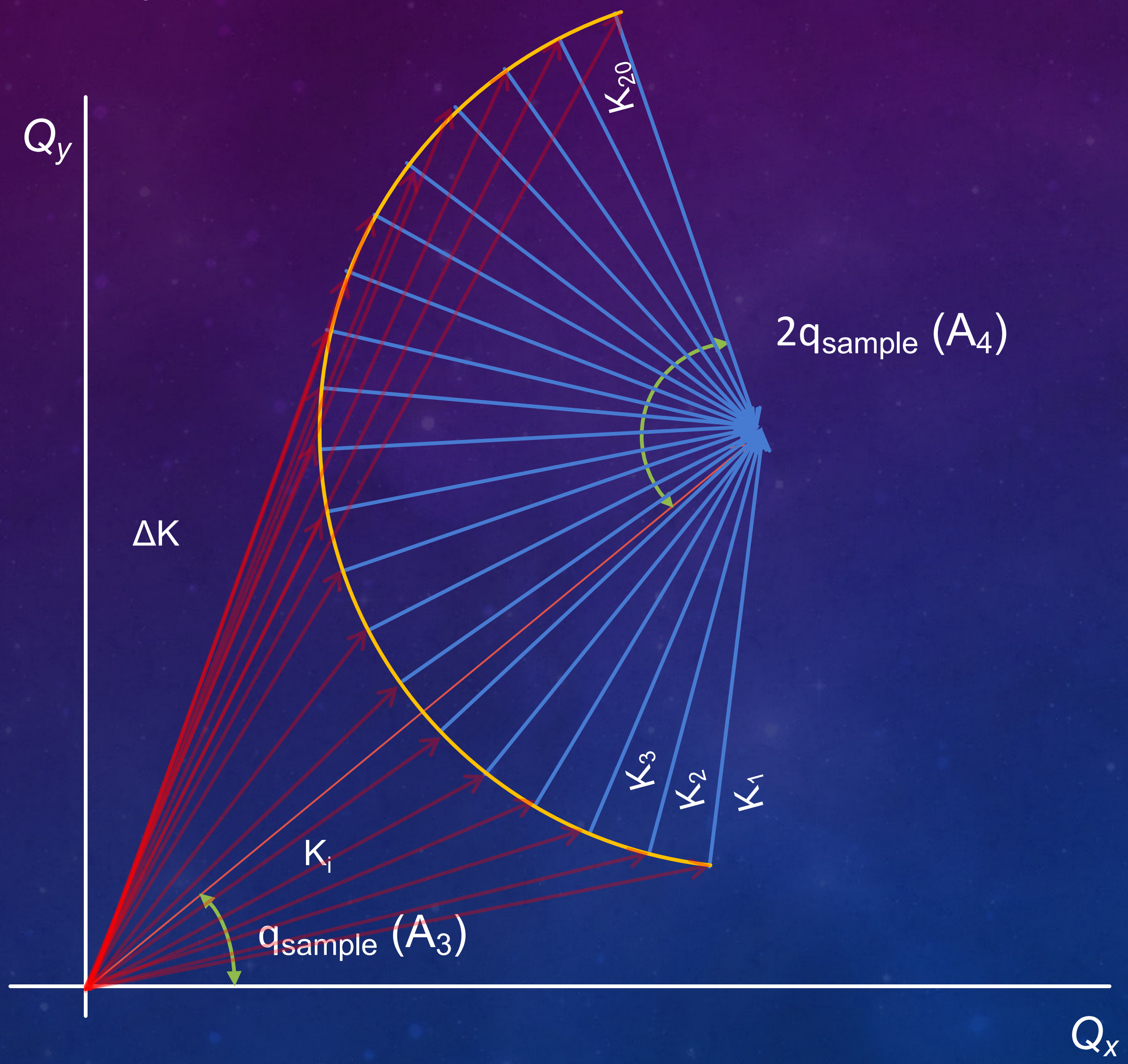

Why the donut shape in reciprocal space?

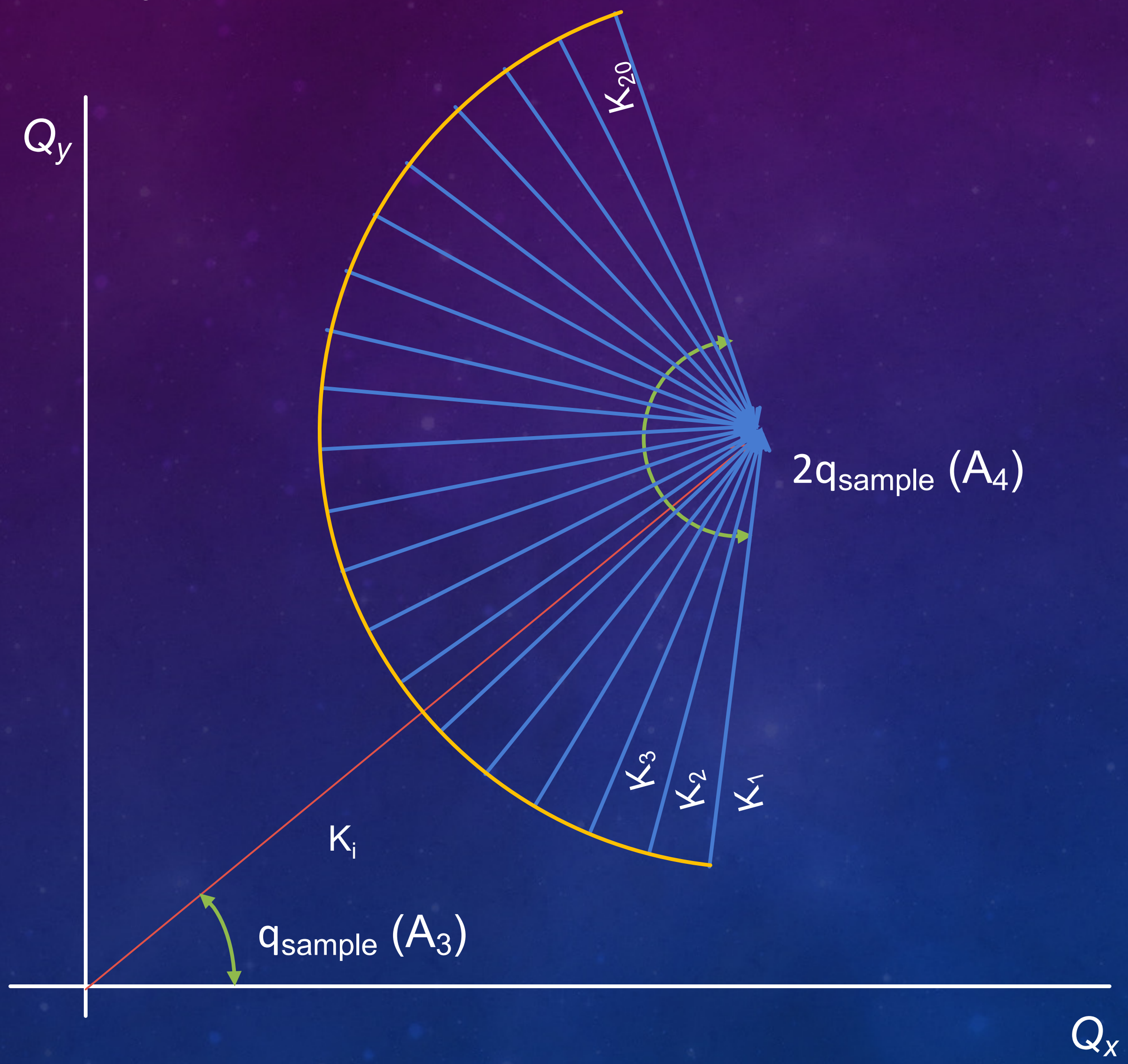

Why the donut shape in reciprocal space?

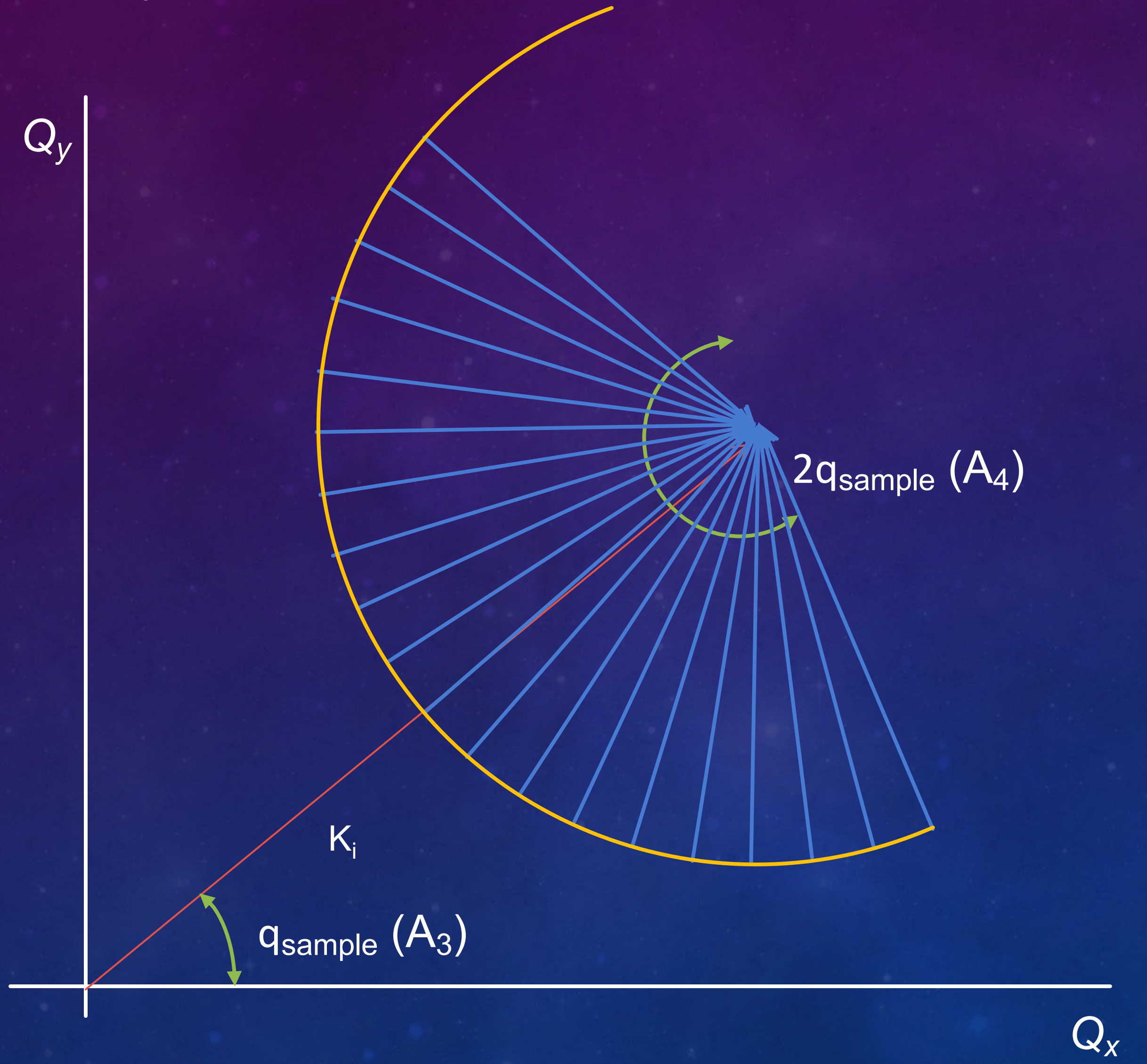

Why the donut shape in reciprocal space?

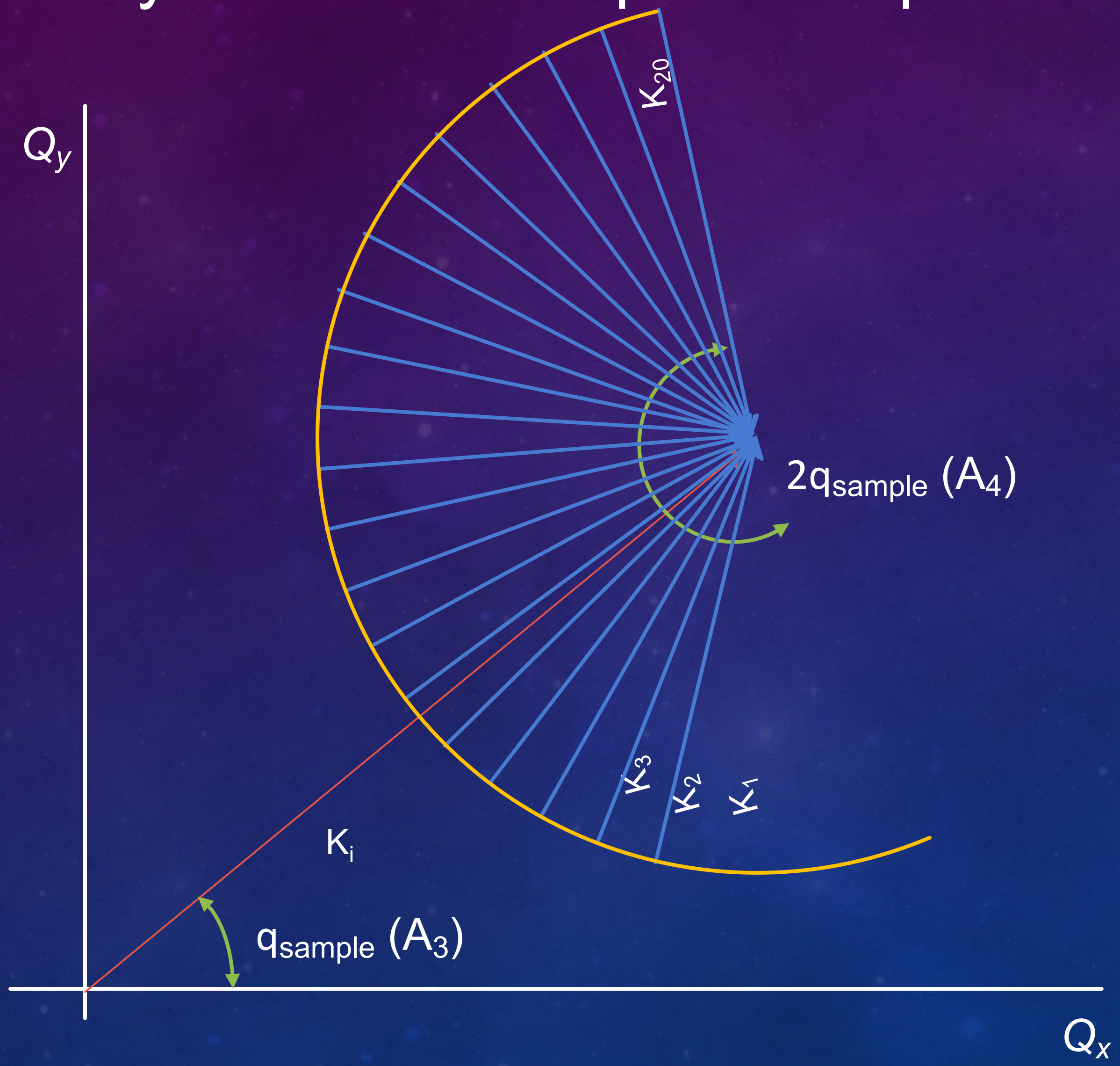

Why the donut shape in reciprocal space?

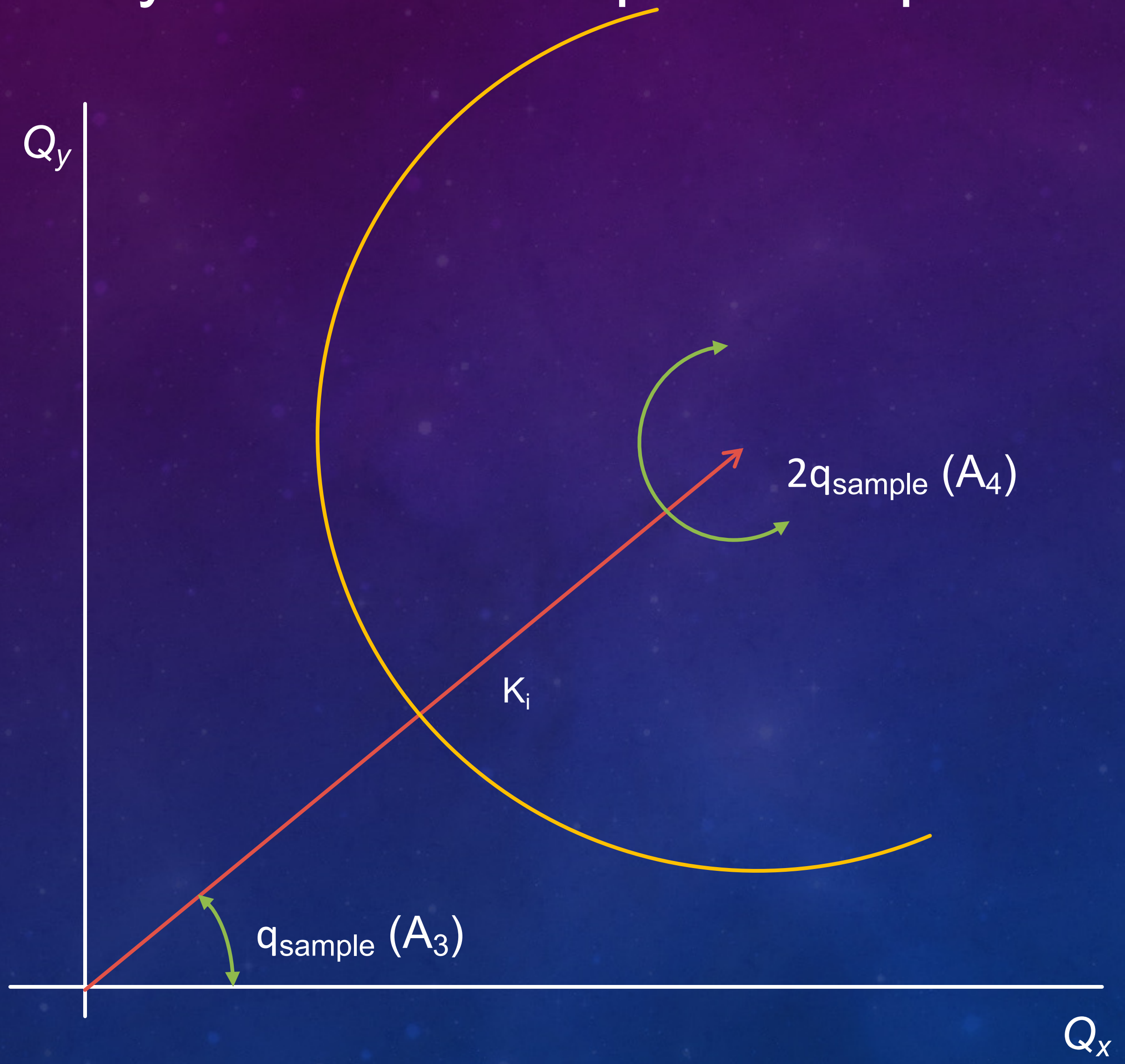

Why the donut shape in reciprocal space?

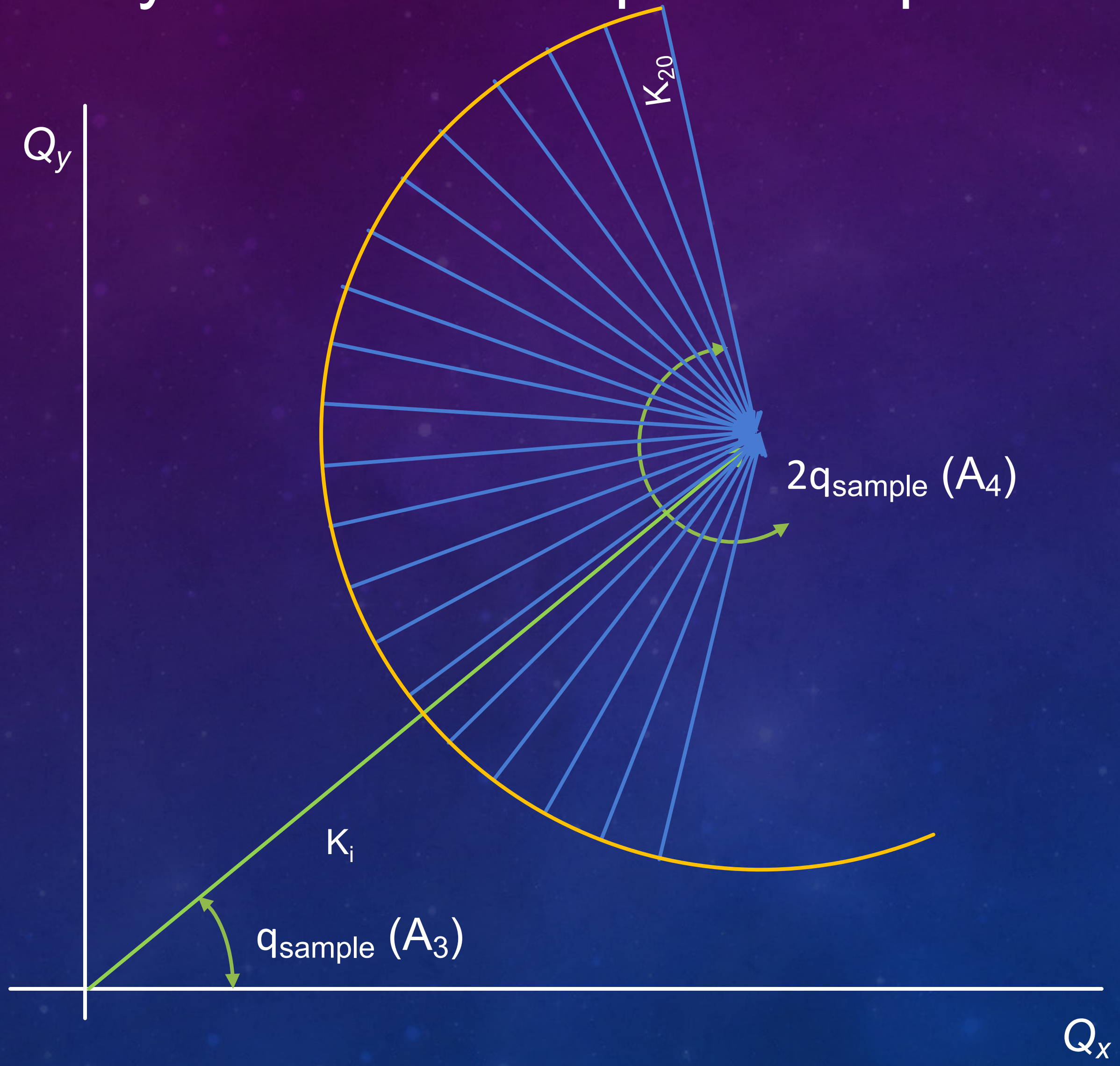

Why the donut shape in reciprocal space?

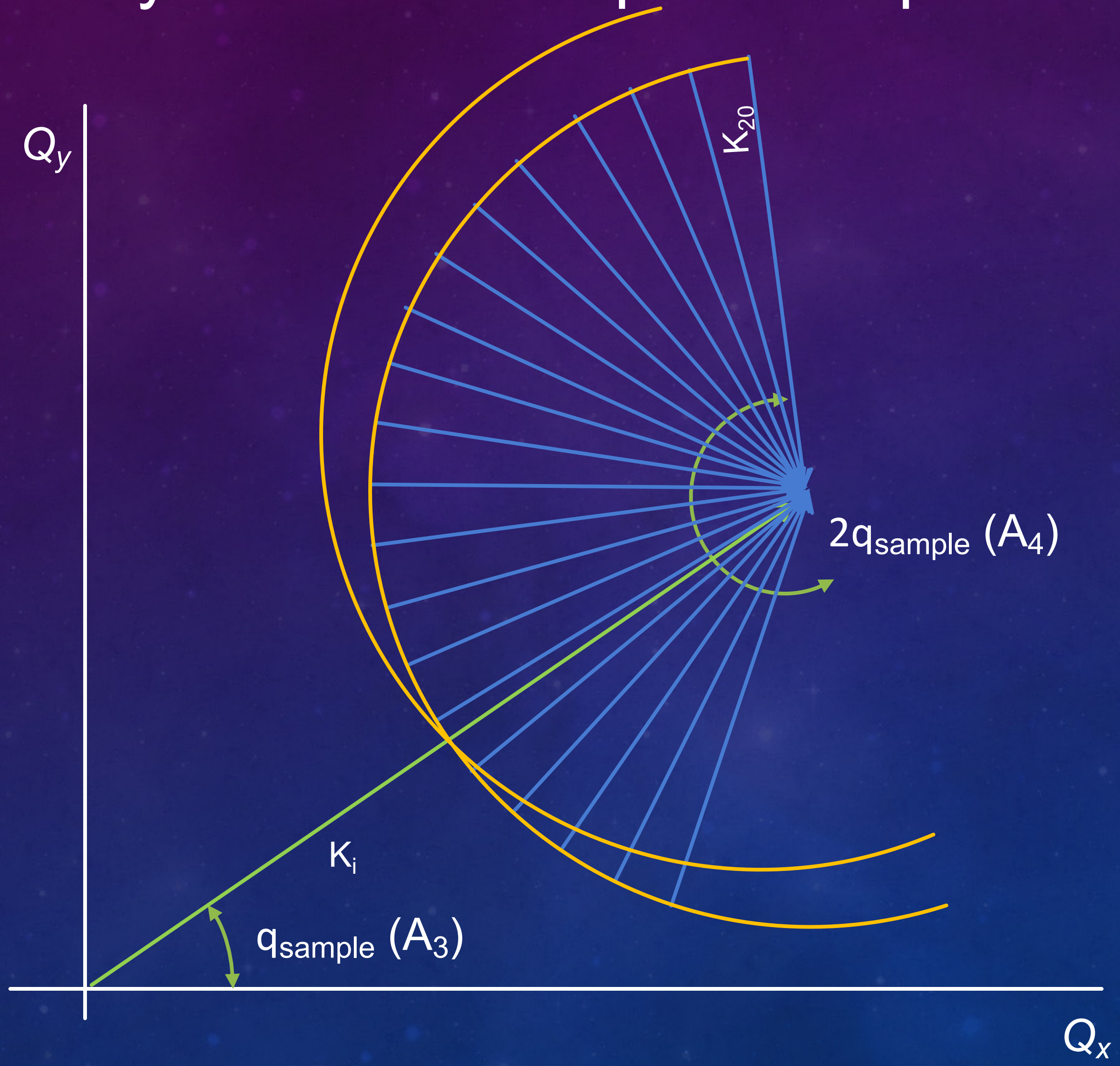

Why the donut shape in reciprocal space?

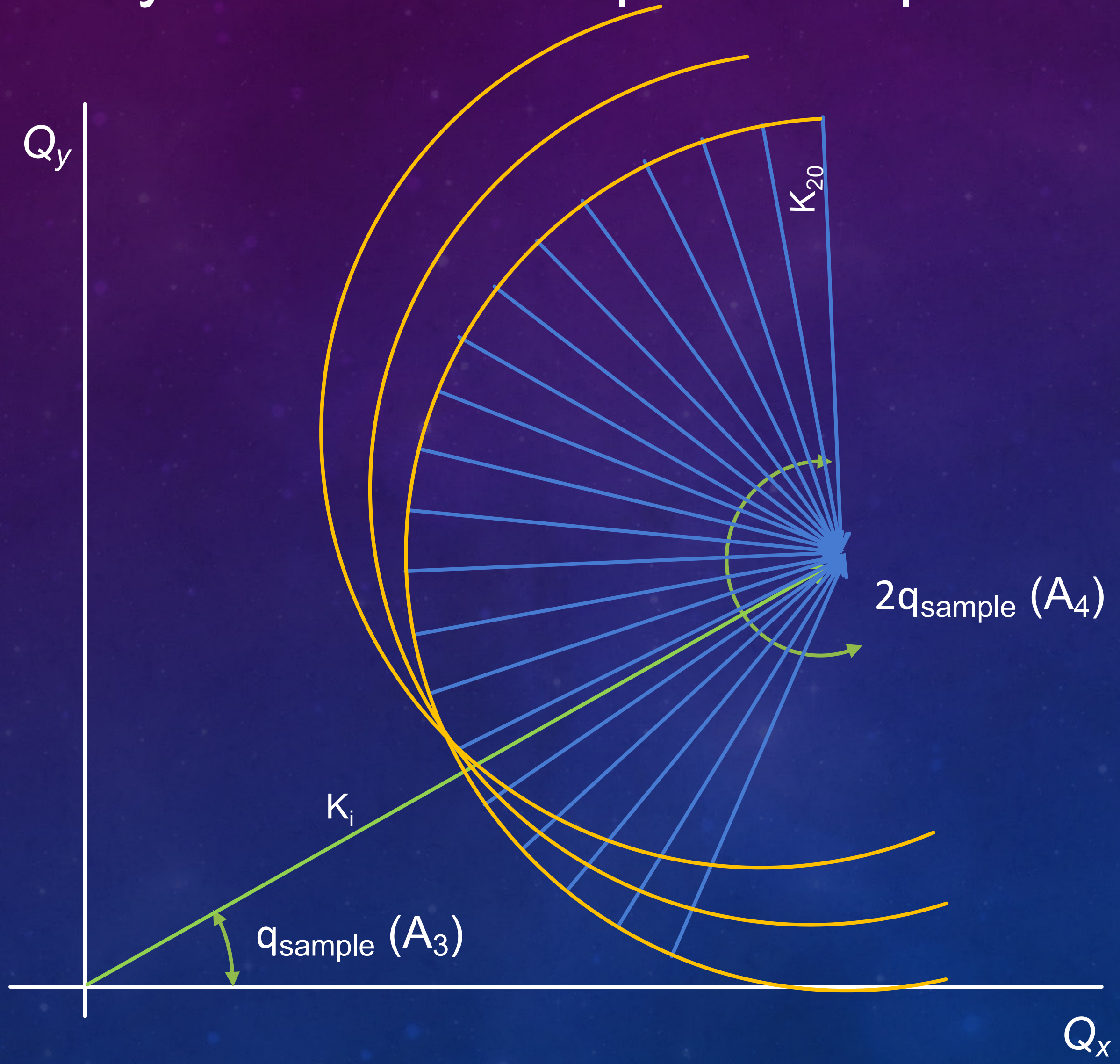

Why the donut shape in reciprocal space?

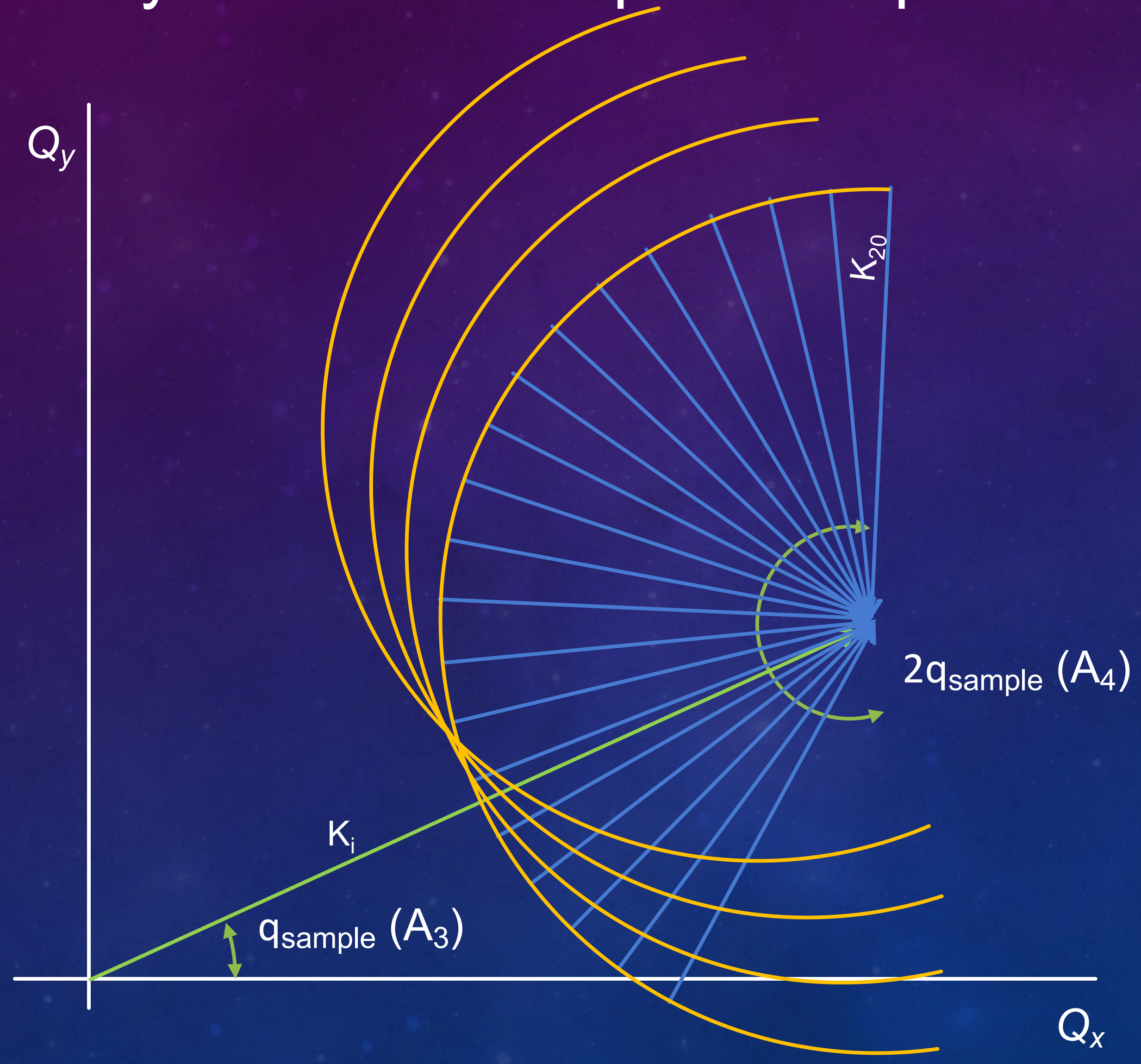

Why the donut shape in reciprocal space?

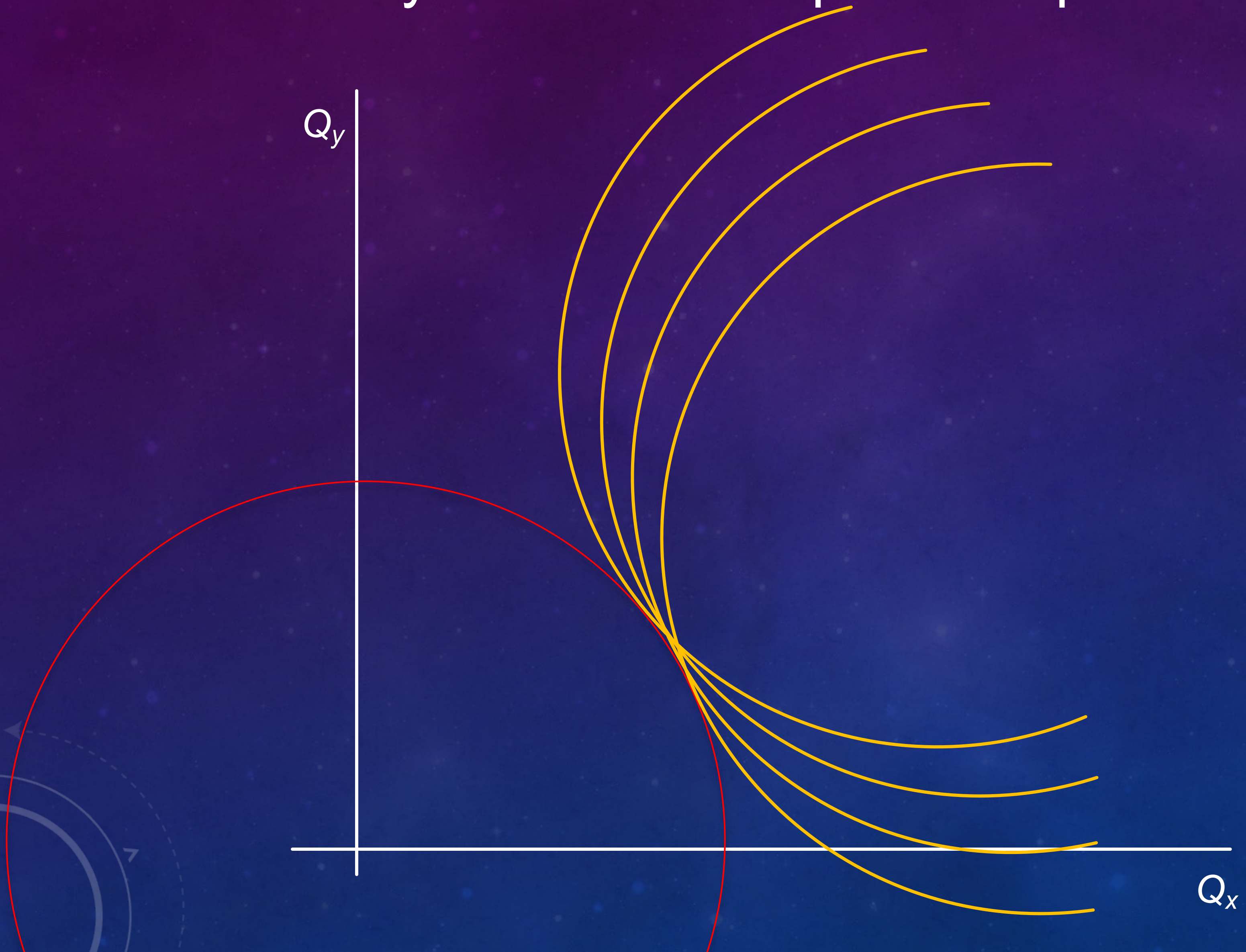

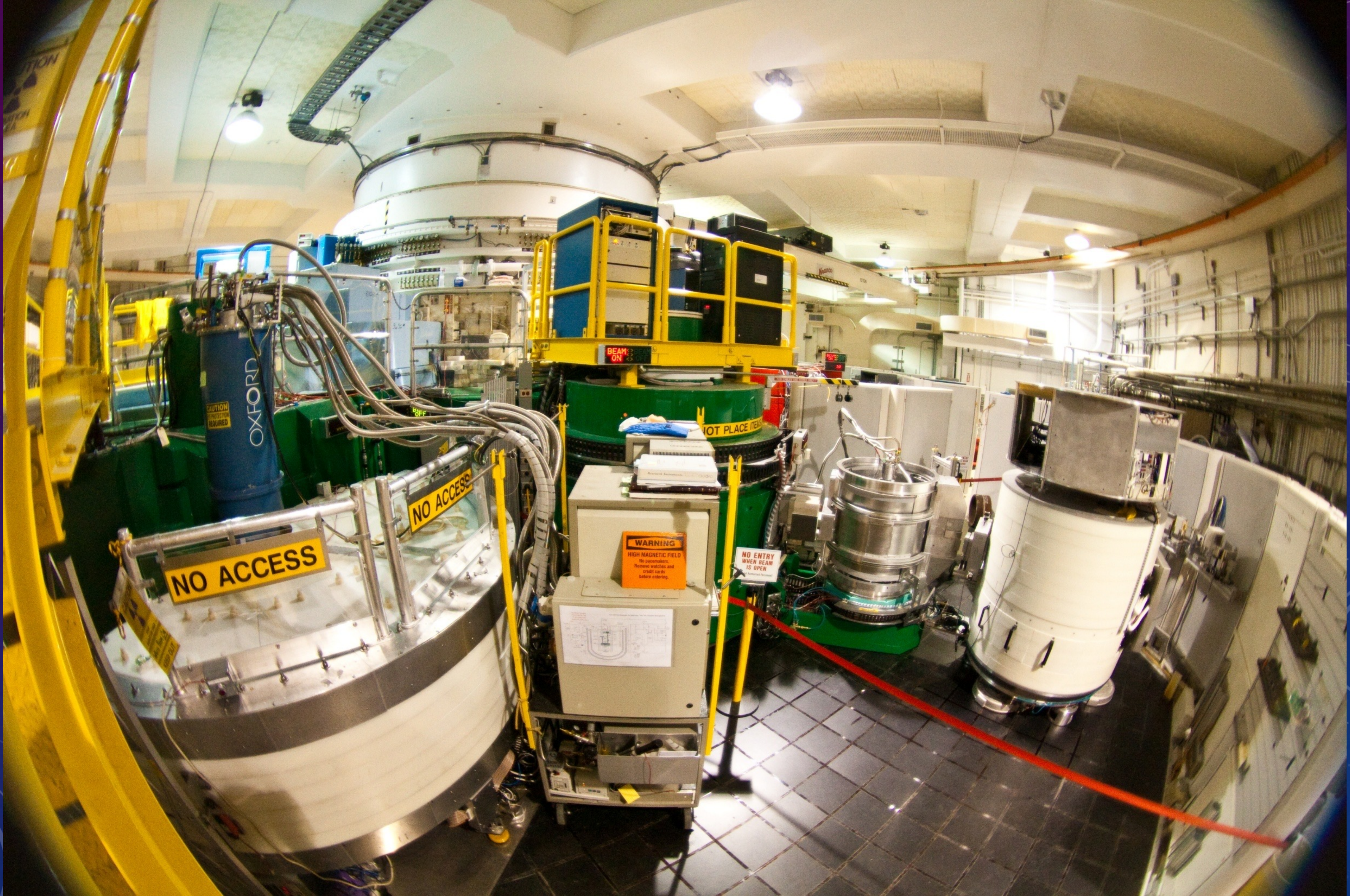
NO ACCESS
NO ACCESS
OXFORD
BEAM ON
WARNING
HIGH MAGNETIC FIELD
No pacemakers.
Remove watches and
credit cards
before entering.
NO ENTRY
WHEN BEAM
IS OPEN

Break….

MACS and the 1-D antiferromagnetic ½ spin chain

1. 1Introduction to the 1-D spin-chain
   I. Quantum vs Classical picture
   II. Spinons and continuum scattering
2. Continuum in 2-D magnets
3. CuPZN Experimental setup

1-D antiferromagnetic S=½ chains:

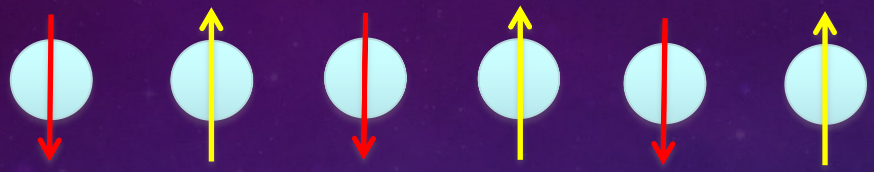

$$\hat{H} = J\sum_{\vec{r}} \vec{S}_{\vec{r}} \cdot \vec{S}_{\vec{r}+1}$$

When S=1/2, there is no long-range Neel state ->H. Bethe, Z Phyis 71, 205 (1931).

Normal spin-wave theory: $E = J|\sin(Q)|$

PHYSICAL REVIEW B VOLUME 5, NUMBER 5 1 MARCH 1972

Spin Dynamics in the One-Dimensional Antiferromagnet $(CD_3)_4NMnCl_3$

M. T. Hutchings* and G. Shirane
Brookhaven National Laboratory,† *Upton, Long Island, New York* 11973

and

R. J. Birgeneau‡
Bell Laboratories, Murray Hill, New Jersey 07974

and

S. L. Holt
Chemistry Department, University of Wyoming, Laramie, Wyoming

(Received 9 July 1971)

Recent studies of the instantaneous magnetic correlations in $(CD_3)_4NMnCl_3$ using quasielastic-neutron-scattering techniques have shown that the $MnCl_3$ chains in this compound exhibit purely one-dimensional paramagnetic behavior down to 1.1 °K. The interactions between Mn^{2+} ions along the chain are such that a molecular field theory would predict an ordering at ~76 °K. It was found that both the spatial and thermal variation of the instantaneous correlations could be quantitatively accounted for using Fisher's theory for the classical Heisenberg linear chain. In this paper we report a detailed study of the time-dependent magnetic correlations in $(CD_3)_4NMnCl_3$ using inelastic–neutron-scattering techniques. It is bound that at low temperatures, for $q \gg \kappa$ and $\omega \neq 0$, the Van Hove scattering function $S(\vec{Q}, \omega)$ may be accurately described by spin-wave theory with a dispersion relation $\hbar\omega = 6.1/\sin \pi q_{c^*}^{z}$ meV over the entire one-dimensional Brillouin zone, even though there is no long-range order. As the temperature is increased from 1.9 to 40 °K these "spin waves" typically weaken in intensity and broaden asymmetrically, with the scattering increasing on the low-energy side. In no case were both well-defined spin waves and a central diffusive component observed simultaneously, although the latter, if weak, could have been masked by the large incoherent scattering.

S=7/2 chains

Classical spin-wave dispersion:

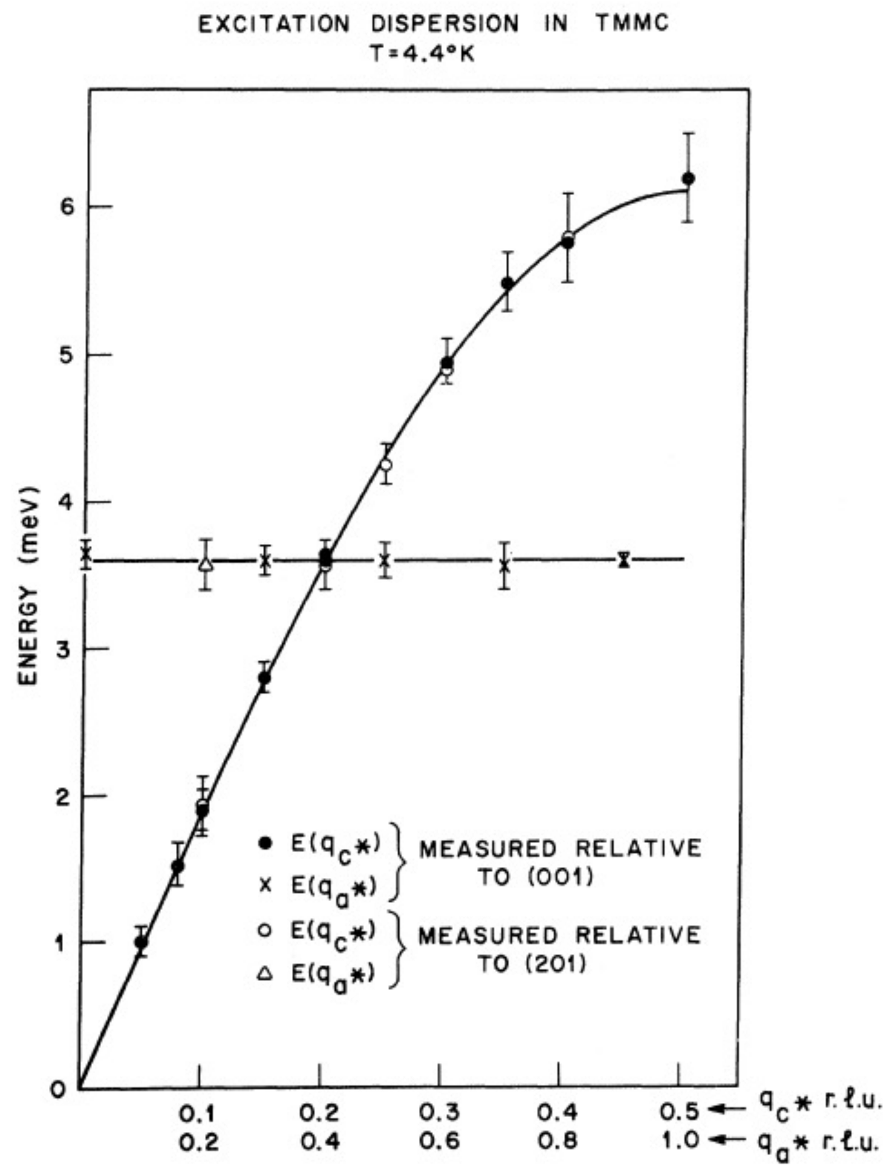

FIG. 9. Dispersion of the excitations in TMMC at 4.4 °K. The experimental points with circles show dispersion in the c^* direction. The other points show the dispersion in the a^* direction at $q_{c^*} = 0.2$ reciprocal-lattice units. The errors represent single standard deviations. The solid-line curve is the best fit to the c^* dispersion. q_{c^*} and q_{a^*} are in reciprocal-lattice units, $2\pi/c$ and $4\pi/\sqrt{3}a$.

Constant-Q scans…sharp resolution limited spin-waves:

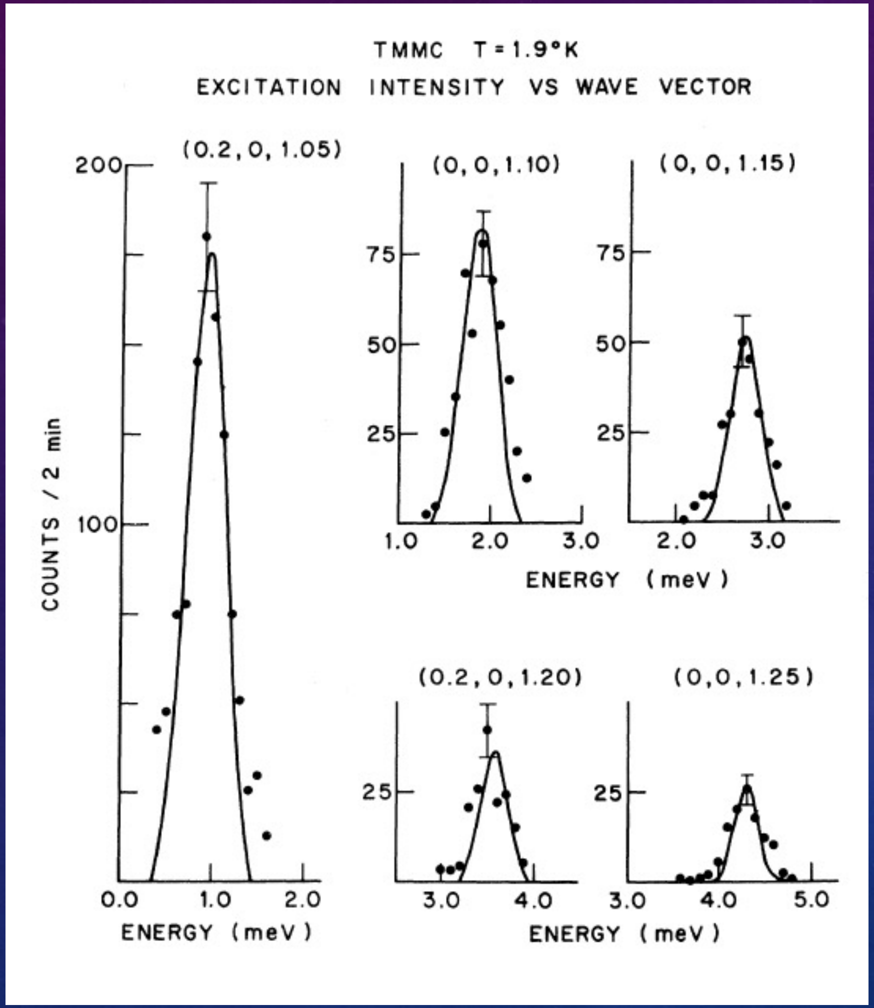

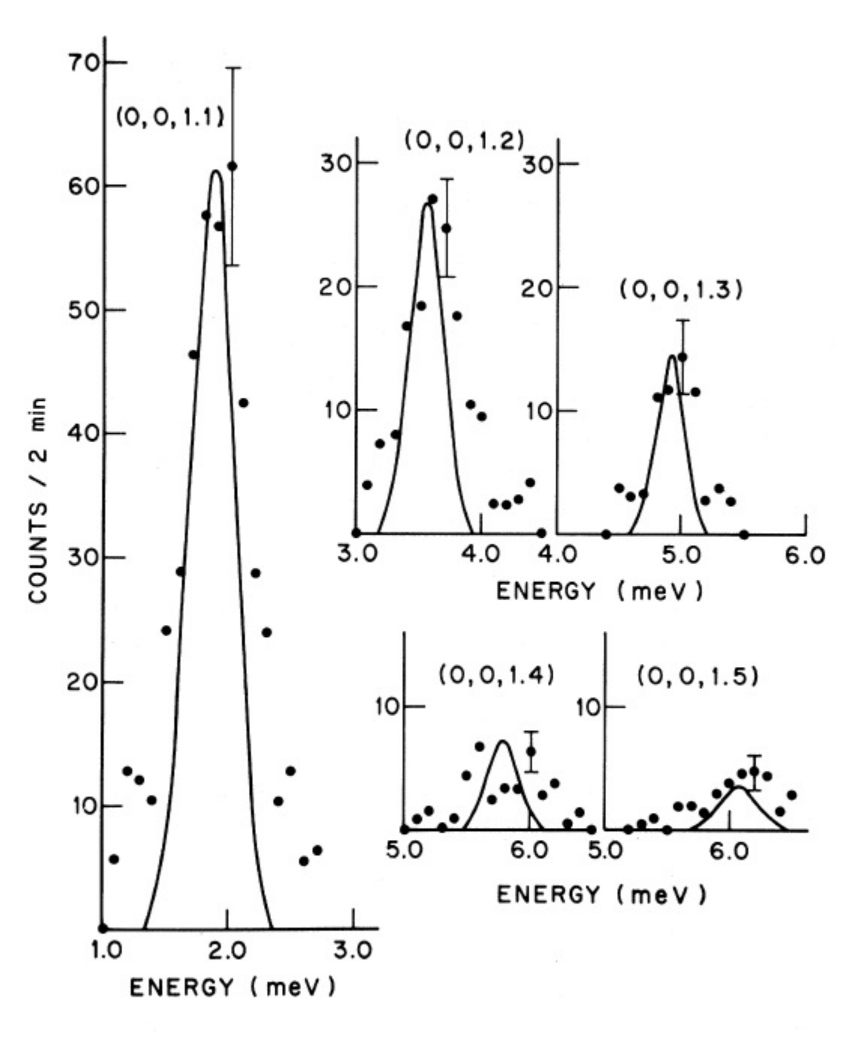

PHYSICAL REVIEW VOLUME 128, NUMBER 5 DECEMBER 1, 1962

Spin-Wave Spectrum of the Antiferromagnetic Linear Chain

JACQUES DES CLOIZEAUX* AND J. J. PEARSON†
University of California, San Diego, La Jolla, California

(Received July 30, 1962)

The methods of Bethe and Hulthén are used to build spin-wave states for the antiferromagnetic linear chain. These states, of spin 1 and translational quantum number k, are eigenstates of the Hamiltonian $H=\Sigma_j \mathbf{S}_j\cdot\mathbf{S}_{j+1}$ with periodic boundary conditions. For an infinite chain, their spectrum is $\epsilon_k=(\pi/2)|\sin k|$, whereas Anderson's spin-wave theory gives $\epsilon_k=|\sin k|$. For finite chains it has been verified by numerical computation that these states are the lowest states of given k, but no rigorous proof has been given for an infinite chain.

DCP relation (S=1/2): $$E=\frac{\pi}{2}J|\sin(Q)|$$

Normal spin-wave theory: $$E=J|\sin(Q)|$$

Physical picture of spinon

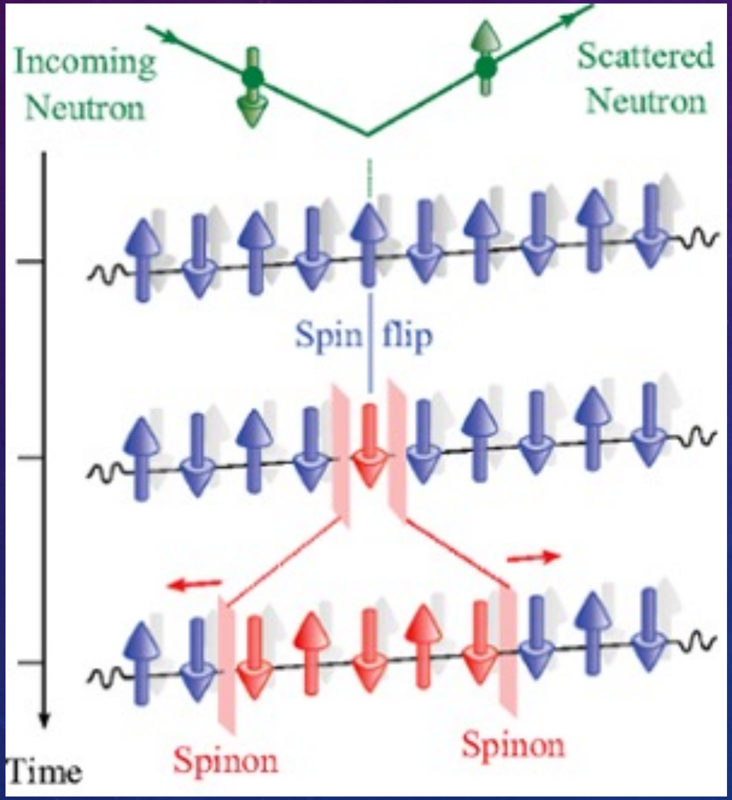

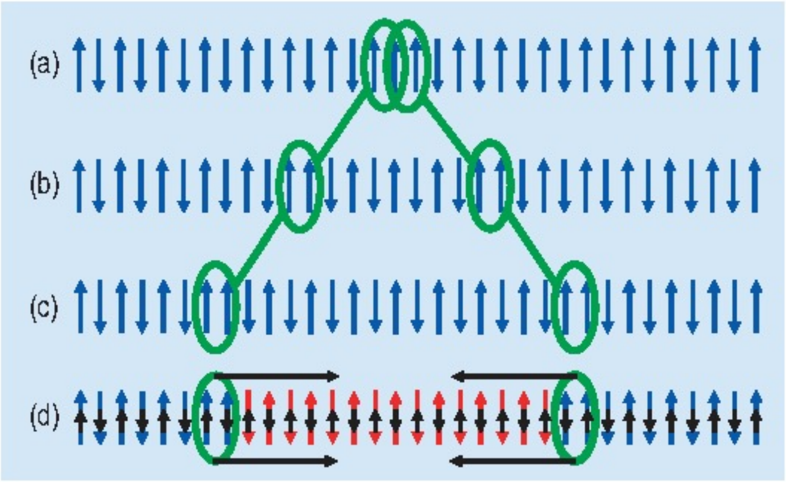

Fig. 1. Qualitative illustration of spinons in a spin-1/2 chain. (a) Shows a spin-flip excitation in an otherwise ordered segment of a spin chain. In the subsequent two frames the spin-flip is spatially separated into domain wall boundaries illustrating spinons that each carry half a spin flip. Separation of the walls costs no energy. (d) shows the situation when a staggered field (small black arrows) breaks the symmetry between even and odd sites of the lattice. Spinons now attract each other (separation costs energy) and can be expected to form bound states. Note that in a real spin-1/2 chain spinons are dynamic quantum degrees of freedom with a finite spatial extent.

Dynamics of an $S=\frac{1}{2}$, One-Dimensional Heisenberg Antiferromagnet

Y. Endoh* and G. Shirane
Brookhaven National Laboratory,† Upton, New York 11973

and

R. J. Birgeneau‡
Bell Laboratories, Murray Hill, New Jersey 07974

and

Peter M. Richards
Sandia Laboratories,† Albuquerque, New Mexico 87115

and

S. L. Holt
University of Wyoming, Laramie, Wyoming 82070
(Received 7 December 1973)

We report a detailed neutron-scattering study of the spin dynamics in $CuCl_2 \cdot 2N(C_5D_5)$, a physical realization of the one-dimensional $S=\frac{1}{2}$ Heisenberg antiferromagnet. At $T=1.3$ K well-defined excitations are observed over the whole zone with energies given by $E(q)=\pi J_{nn}\sin(qc)$, the celebrated des Cloizeaux–Pearson exact solution for the spectrum of first excited states, but with intensities approximately those expected from classical spin-wave theory. At $T=8$ K the excitations are broad and ill defined.

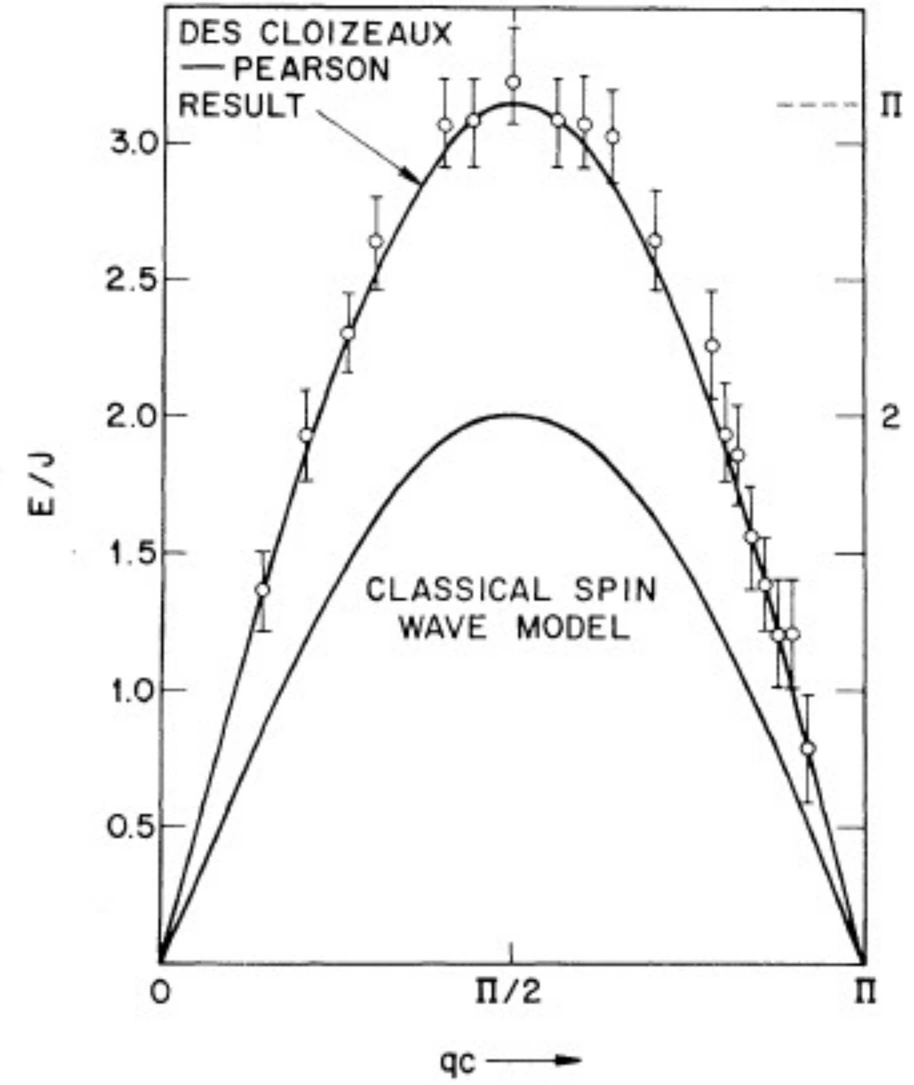

FIG. 3. Dispersion of the excitations in CPC at $T = 1.3$ K with energy in units of $J = 13.4$ K.

Classical (large S):

$$E = J|\sin(Q)|$$

Quantum (small S):

$$E = \frac{\pi}{2} J|\sin(Q)|$$

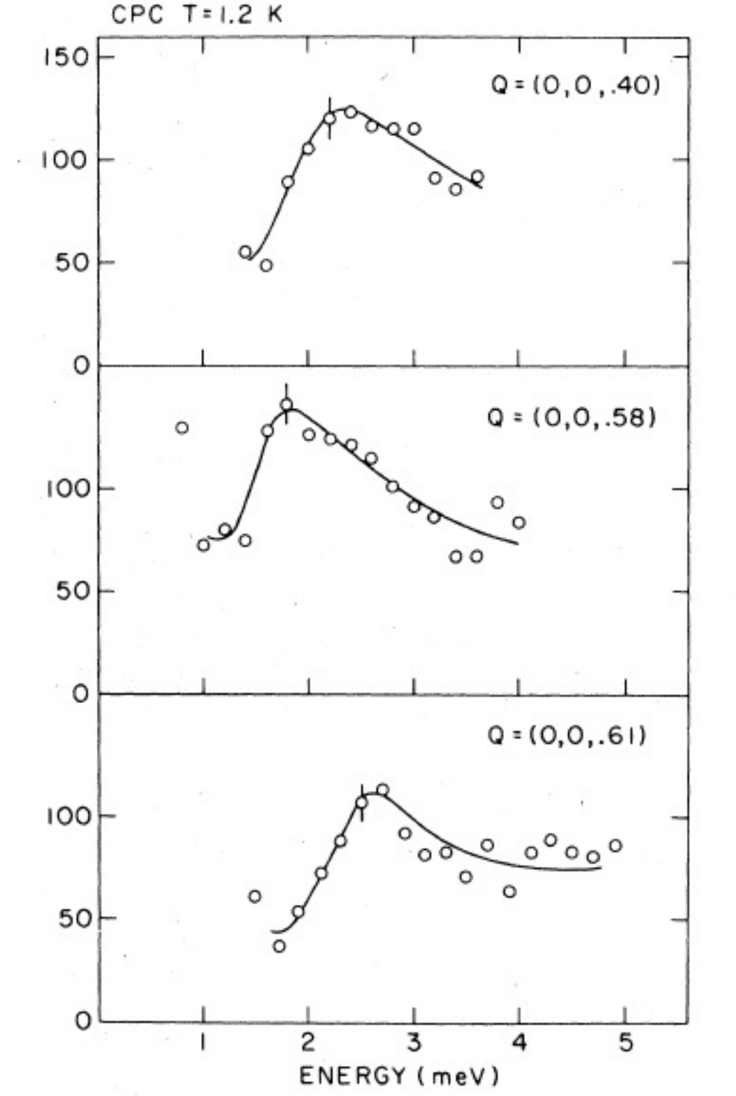

FIG. 5. Inelastic scans at $T = 1.2$ K and zero magnetic field at three points in reciprocal space close to an antiferromagnetic Bragg point (0,0,0.50), showing magnetic excitations. The upper scan shows data from the present work, while the two others are from the previous work.

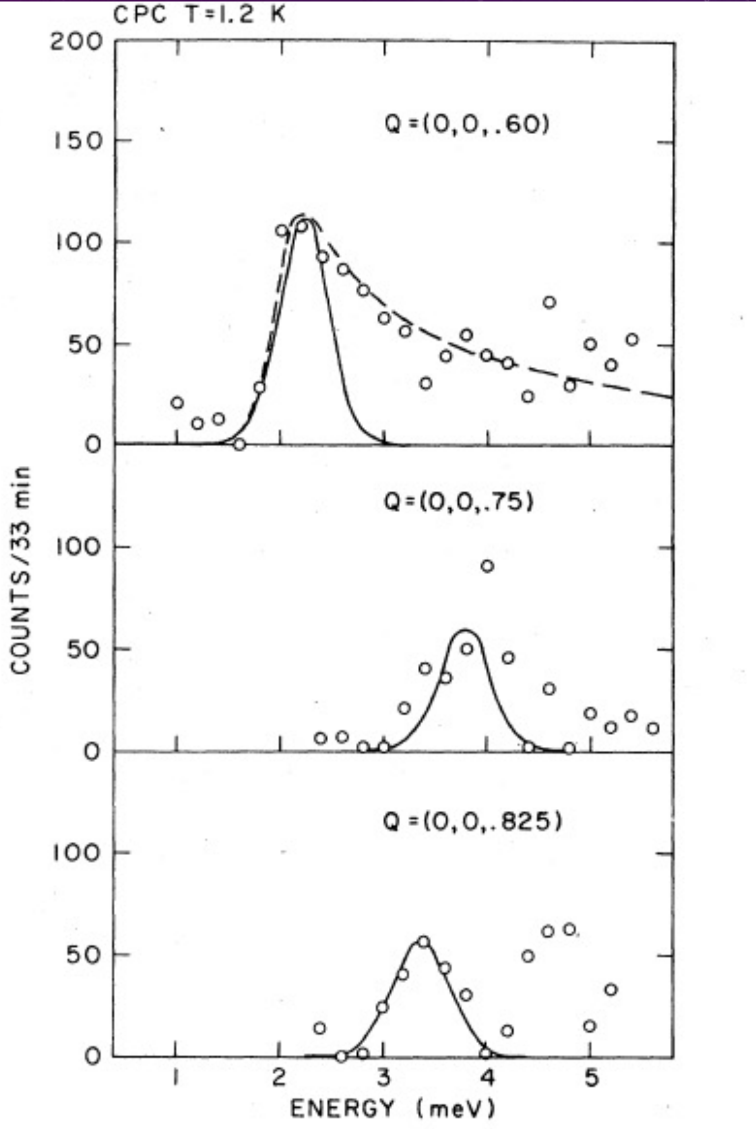

FIG. 7. Experimental points of Fig. 4 after background— and resolution correction. The full curves show the calculated line shapes based on Lorentzian cross sections and a sample mosaic spread of 2.5°. The dashed curve represents the calculated line shape corresponding to the scattering function Eq. (4).

PHYSICAL REVIEW B VOLUME 18, NUMBER 7 1 OCTOBER 1978

Neutron study of the line-shape and field dependence of magnetic excitations in $CuCl_2 \cdot 2N(C_5D_5)$

I. U. Heilmann and G. Shirane
Brookhaven National Laboratory, Upton, New York 11973

Y. Endoh
Department of Physics, Tohoku University, Sendai 980, Japan

R. J. Birgeneau
Department of Physics, Massachusetts Institute of Technology, Cambridge, Massachusetts 02139

S. L. Holt
Department of Chemistry, University of Wyoming, Laramie, Wyoming 82070
(Received 24 April 1978)

We have carried out inelastic neutron scattering on $CuCl_2 \cdot 2N(C_5D_5)$, at $T = 1.2$ K and at magnetic fields up to 70 kOe. The spin dynamics of this typical $s = \frac{1}{2}$ one-dimensional Heisenberg antiferromagnet have previously been investigated at zero magnetic field by Endoh *et al.*, using neutron scattering. They observed a spectrum of magnetic excitations in close agreement with the spectrum of lowest excited states as calculated exactly by des Cloizeaux and Pearson (dCP). The marked asymmetry in the line shape of the neutron response previously observed is carefully reexamined and is shown to be a true effect, in agreement with several theoretical predictions. At high magnetic field, a broadening of the neutron response is observed, especially pronounced at the antiferromagnetic zone boundary, where the peak smears out at 70 kOe. For wave vectors near an antiferromagnetic Bragg point a decrease in the peak energy is observed for increasing field, lending qualitative support to the calculations of Ishimura and Shiba of the field dependence of the dCP states.

S=1/2 chain

Volume 85A, number 6,7 PHYSICS LETTERS 12 October 1981

WHAT IS THE SPIN OF A SPIN WAVE?

L.D. FADDEEV and L.A. TAKHTAJAN
Leningrad Branch of the Steklov Mathematical Institute, Leningrad, USSR

Received 15 July 1981

We argue that the spin of a spin wave in the Heisenberg antiferromagnetic chain of spins $\frac{1}{2}$ is equal to $\frac{1}{2}$ rather than 1 as is generally considered to be true.

Predict a continuum of excitations…would appear as a continuum in neutron scattering.

PHYSICAL REVIEW B VOLUME 44, NUMBER 22 1 DECEMBER 1991-II

Spin dynamics in the quantum antiferromagnetic chain compound $KCuF_3$

S. E. Nagler,* D. A. Tennant, and R. A. Cowley
Clarendon Laboratory, Department of Physics, University of Oxford, Parks Road, Oxford, United Kingdom

T. G. Perring
Rutherford Appleton Laboratory, Chilton, Didcot, Oxon, United Kingdom

S. K. Satija
National Institute of Standards and Technology, Gaithersburg, Maryland 20899

(Received 11 June 1991)

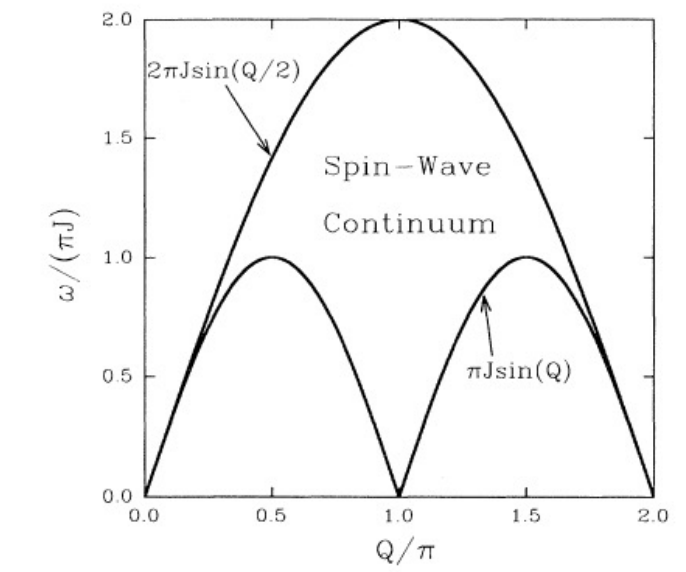

FIG. 1. The spin-wave continuum (SWC) spectrum of the spin-$\frac{1}{2}$ Heisenberg antiferromagnetic chain. The lower bound is the des Cloizeaux-Pearson dispersion relation.

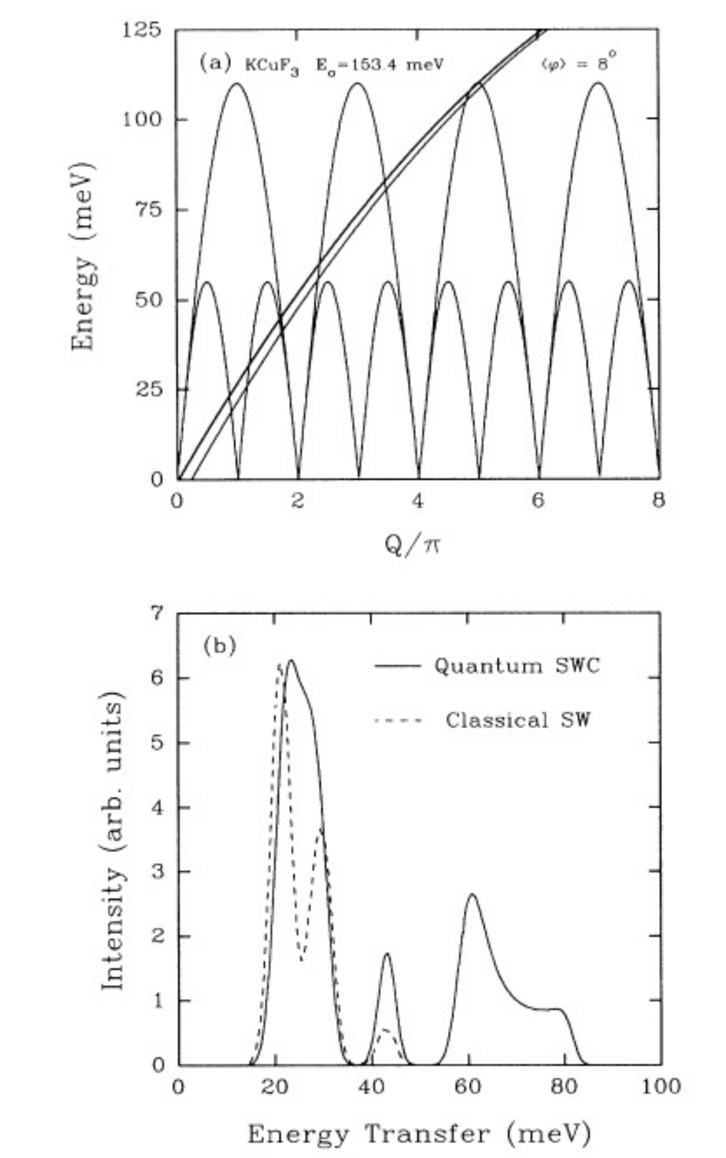

The lower boundary is a spinon pair exitation with one of the pair with momentum 0 and upper level is two spinons each with a momentum of q/2. In the continuum region a pair of interacting spinons can propagate freely along the one-dimensional chain with a total momentum of q. (M. Aria et al. Phys Rev. Lett 77, 3649 (1996)

Time of flight Spectrometers:

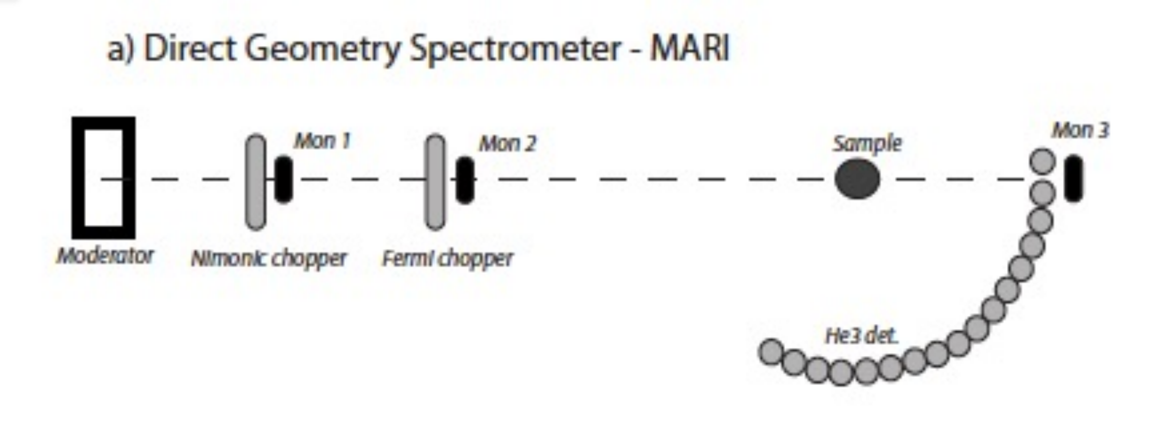

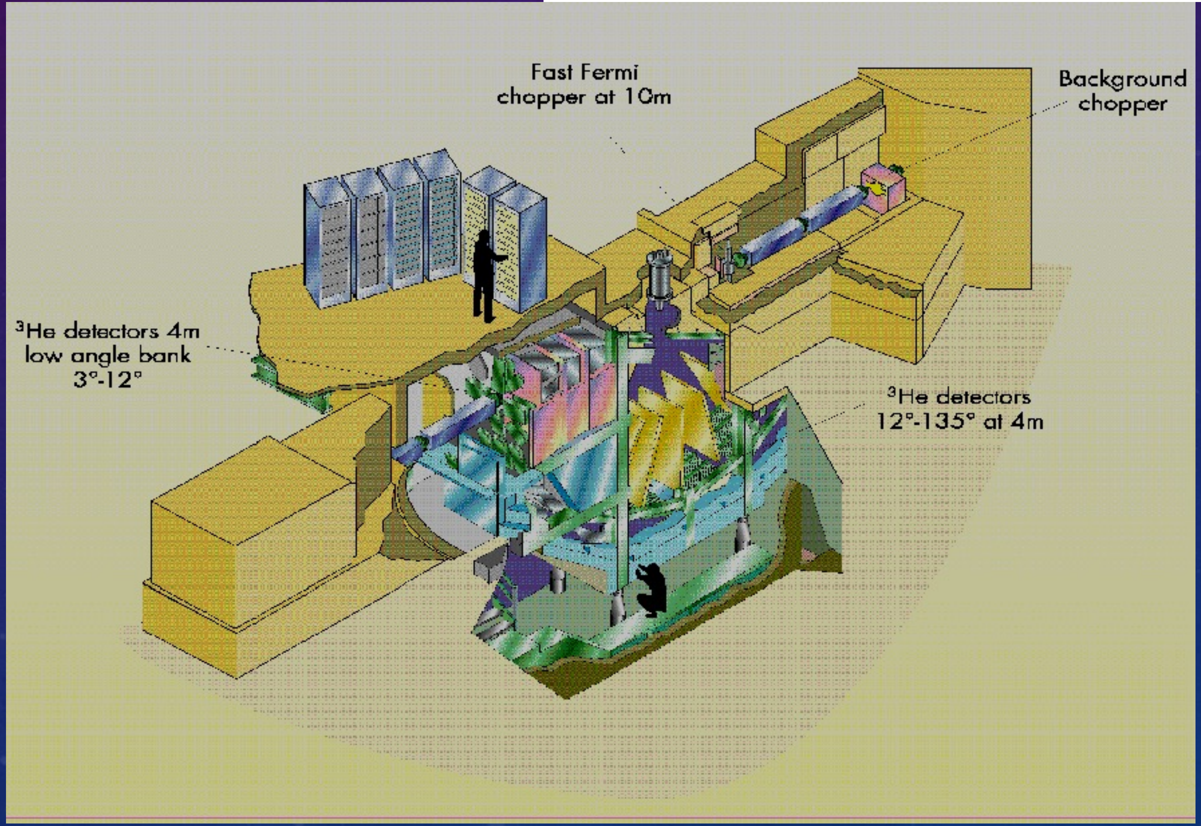

Data shows a continuum of excitations:

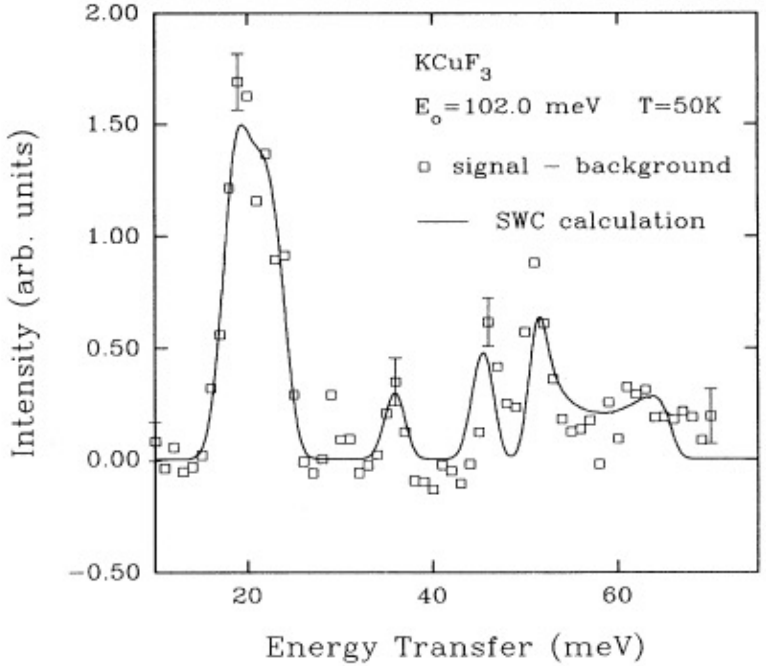

FIG. 10. The scan with $E_0 = 102.0$ meV, $\mathbf{k}_0 \| \mathbf{c}^*$, with the smoothed nonmagnetic background subtracted. The representative 1σ error bars are statistical only, and are not adjusted to account for the background subtraction. The solid line is the fitted quantum $S(Q,\omega)$.

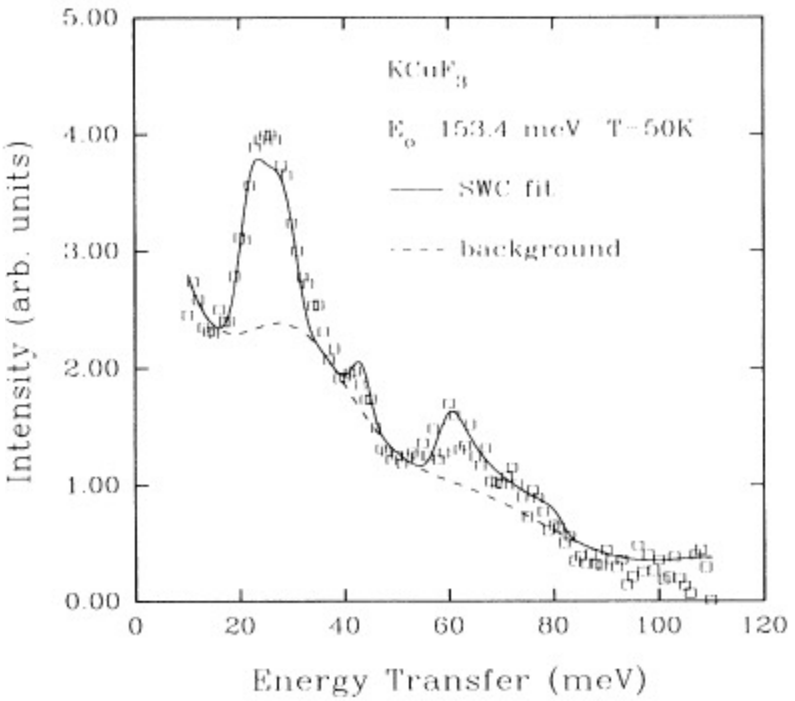

FIG. 5. Scan with $\mathbf{k}_0 \| \mathbf{c}^*$, and $E_0 = 153.4$ meV. The data are rouped into 1-meV bins. The dashed line represents the non-ıagnetic background. The solid line is a model fit as described ı the text.

Physical picture of spinon:

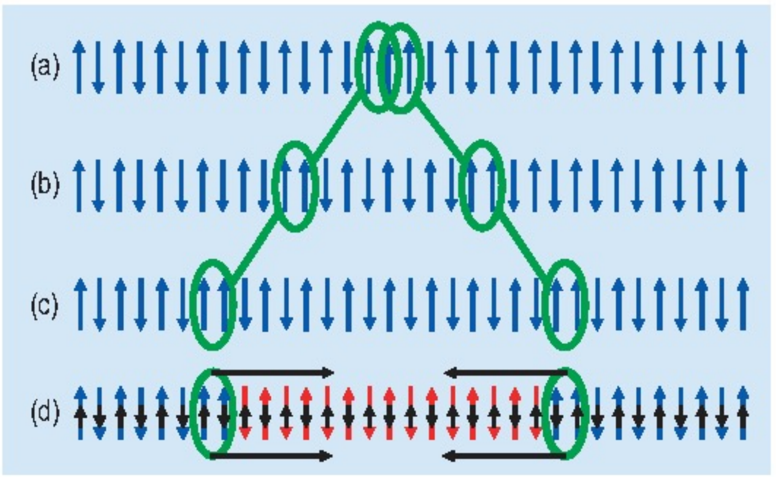

Fig. 1. Qualitative illustration of spinons in a spin-1/2 chain. (a) Shows a spin-flip excitation in an otherwise ordered segment of a spin chain. In the subsequent two frames the spin-flip is spatially separated into domain wall boundaries illustrating spinons that each carry half a spin flip. Separation of the walls costs no energy. (d) shows the situation when a staggered field (small black arrows) breaks the symmetry between even and odd sites of the lattice. Spinons now attract each other (separation costs energy) and can be expected to form bound states. Note that in a real spin-1/2 chain spinons are dynamic quantum degrees of freedom with a finite spatial extent.

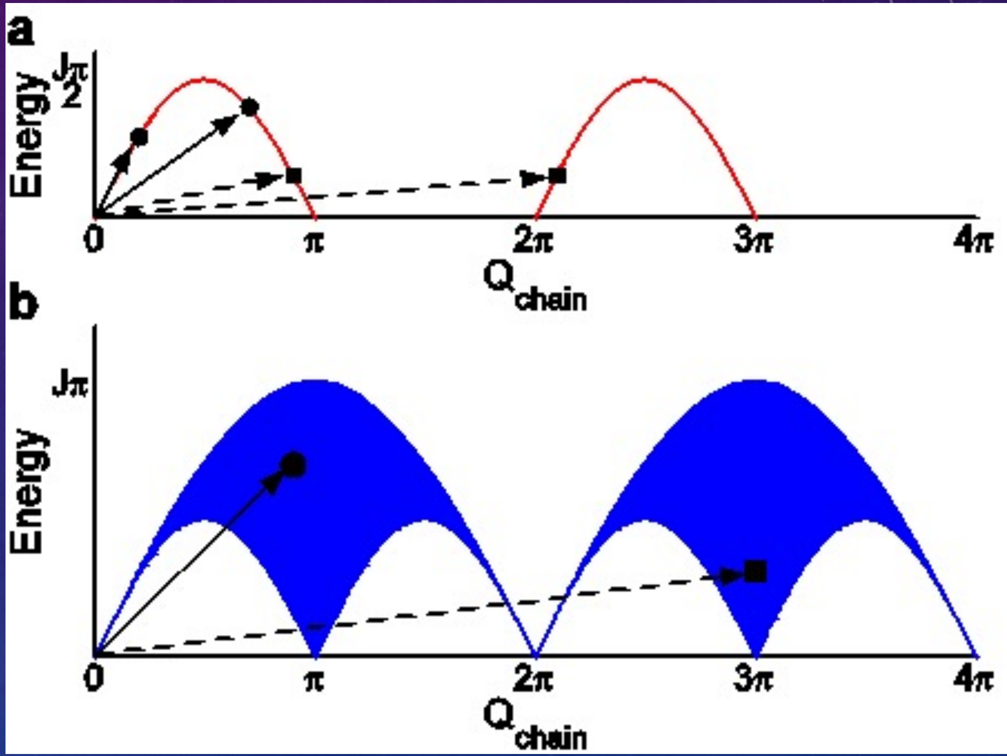

VOLUME 77, NUMBER 17 PHYSICAL REVIEW LETTERS 21 OCTOBER 1996

Quantum Spin Excitations in the Spin-Peierls System $CuGeO_3$

M. Arai,[1,2,*] M. Fujita,[1] M. Motokawa,[3] J. Akimitsu,[4] and S. M. Bennington[5]
[1]*Department of Physics, Kobe University, 1-1 Rokkodai, Nada, Kobe 657, Japan*
[2]*Research Development Corporation of Japan, Honcho, Kawaguchi 332, Japan*
[3]*Institute of Material Research, Tohoku University, Katahira, Sendai 980, Japan*
[4]*Department of Physics, Aoyama-Gakuin University, Chitosedai, Setagaya, Tokyo 157, Japan*
[5]*ISIS Facility, Rutherford Appleton Laboratory, Chilton, Didcot, Oxfordshire, OX11 0QX, United Kingdom*
(Received 3 May 1996)

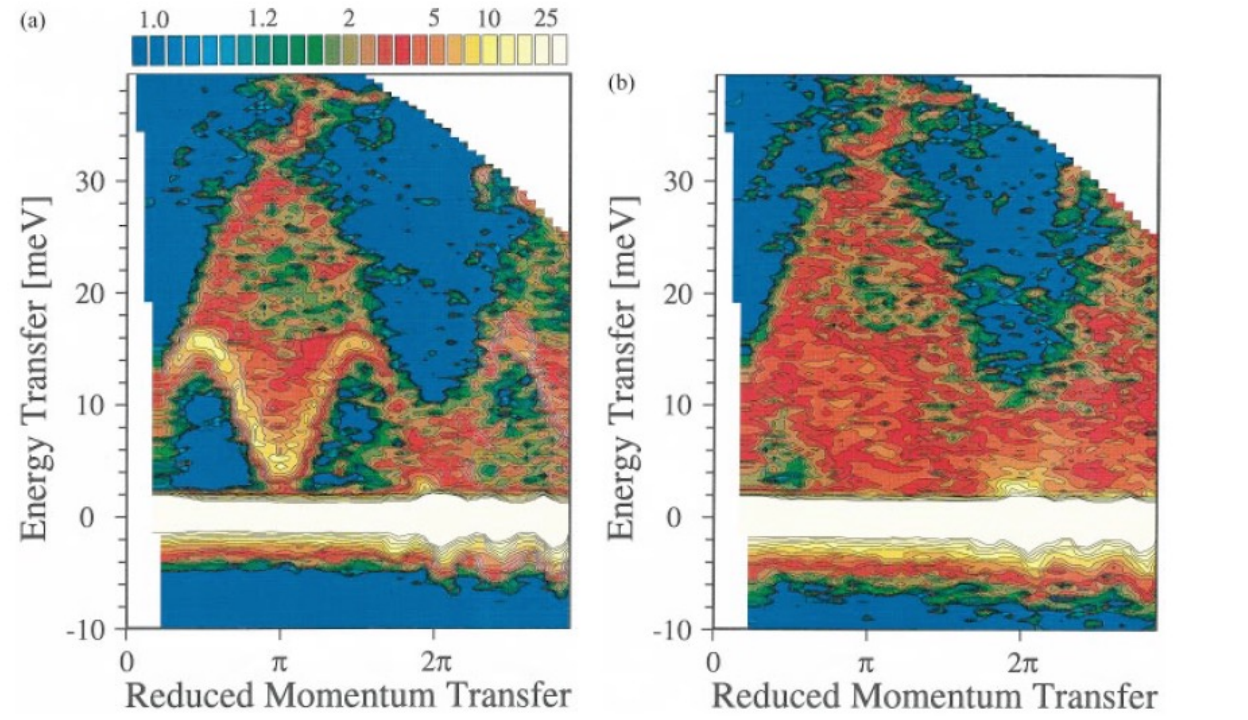

FIG. 1(color). A color contour map of the dynamical structure factor at 10 K (a) and 50 K (b).

First complete map using MARI chopper instrument (ISIS)

CRITICALITY: SCALING THE DYNAMIC SUSCEPTIBILITY

Haldene[1] and Shultz[2] predicted for $\tilde{q} = \pi$ is gapless and the spin correlations decays algebraically with Critical exponent $\eta = 1$

$$\chi''(\tilde{q} = \pi, \omega) = \frac{\pi}{T} Im\left[\rho^2\left(\frac{\hbar\omega}{4\pi k_B T}\right)\right]$$

$$\rho(x) = \frac{\Gamma\left(\frac{1}{4} - ix\right)}{\Gamma\left(\frac{3}{4} - ix\right)}$$

$$S^{\alpha\alpha}(\tilde{q}, \omega) = \frac{1}{\pi}\left(1 - e^{-\frac{\hbar\omega}{k_B T}}\right)^{-1} \chi''(\tilde{q}, \omega)$$

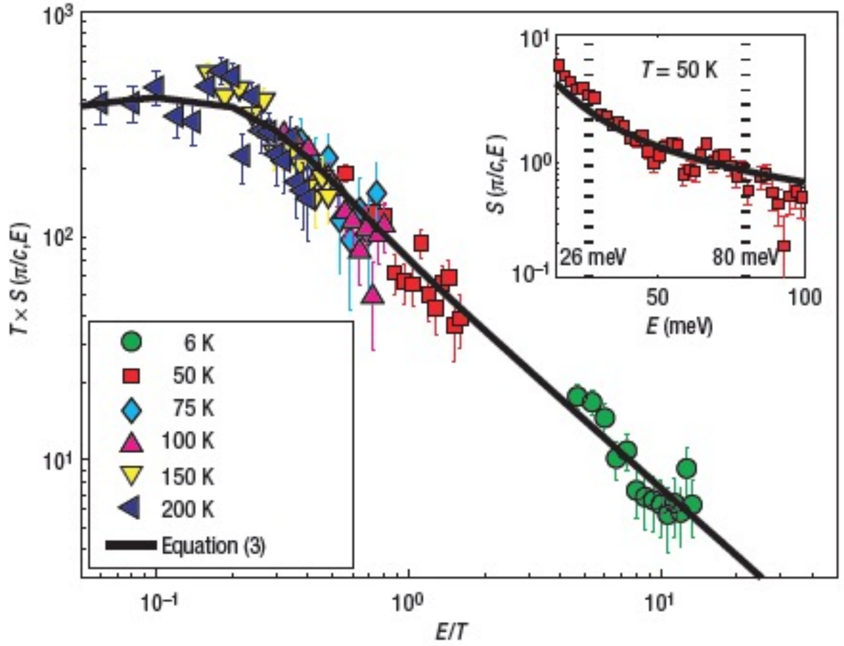

Figure 3 Universal energy/temperature scaling in $KCuF_3$. Inset: The corrected data at $T = 50$ K plotted as a function of energy. The data is integrated over the entire Brillouin zone perpendicular to the chain direction and summed over a narrow range at the AFZC parallel to the chain direction ($0.48 < qc/2\pi < 0.52$). The error bars represent two standard deviations. The solid line through the data is the field-theory expression for an ideal 1D $S = ½$ HAFC given by equation (3), which maps onto the 1D LL. The data follows this line for energies in the range $26 < E < 80$ meV (bounded by the vertical dashed lines) indicating that the 1D LL description is valid for $KCuF_3$ at these energies. Main figure: The data for all the other temperatures (except 300 K) were treated in a similar manner and were also found to follow equation (3) over a defined energy range. The combined data showing 1D LL behaviour is multiplied by temperature and plotted as a function of the universal parameter E/T in the main part of the figure. Again the solid line through the data is equation (3).

Duncan Haldene Nobel prize 2016

Nature Materias 4, 329,(2005)

Spin excitations in S=1/2 one dimensional chains:

1) Large S chains have an energy dispersion relation…

$$E = J|\sin(Q)|$$

2) Low S chains have an energy dispersion relation…

$$E = \frac{\pi}{2} J|\sin(Q)|$$

and continuum of excitations.

MACS is ideally suited for measuring excitations in low dimension systems….CuPzN

CuPzN, $Cu(C_4H_4N_2)(NO_3)_2$

Space Group: *Pmna*

Lattice parameters:

a=6.712 b= 5.112 c=11.732

alpha=beta=gamma=90

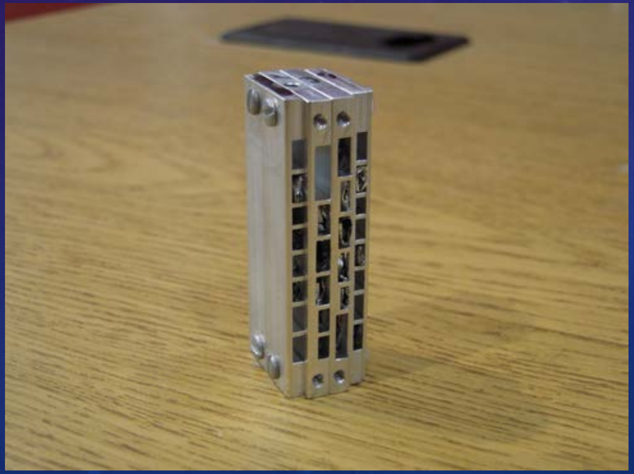

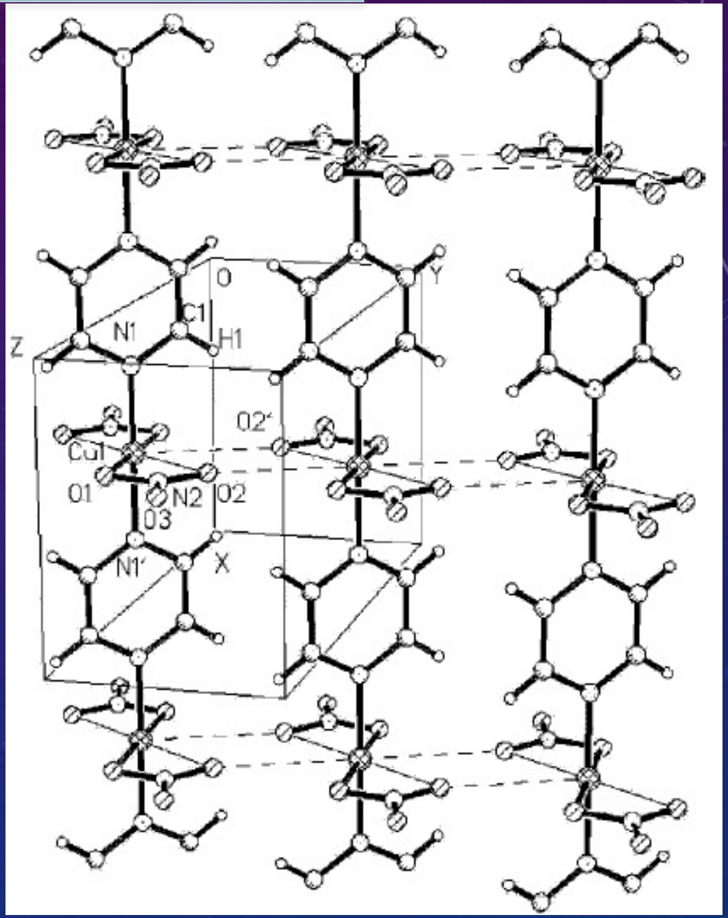

Figure : *Crystal structure of CuPzN showing the Cu2+ ions (hatched spheres) are linked through pyrazine rings to form one-dimensional chains. The chain axis (a) is vertical on the page, with the b axis nearly horizontal.*

EXPERIMENTAL PLAN

- Is it a S=½ spin chain?
- Classical or quantum model?
- Continuum?
- What is the behavior at different T?

MACS SETTINGS

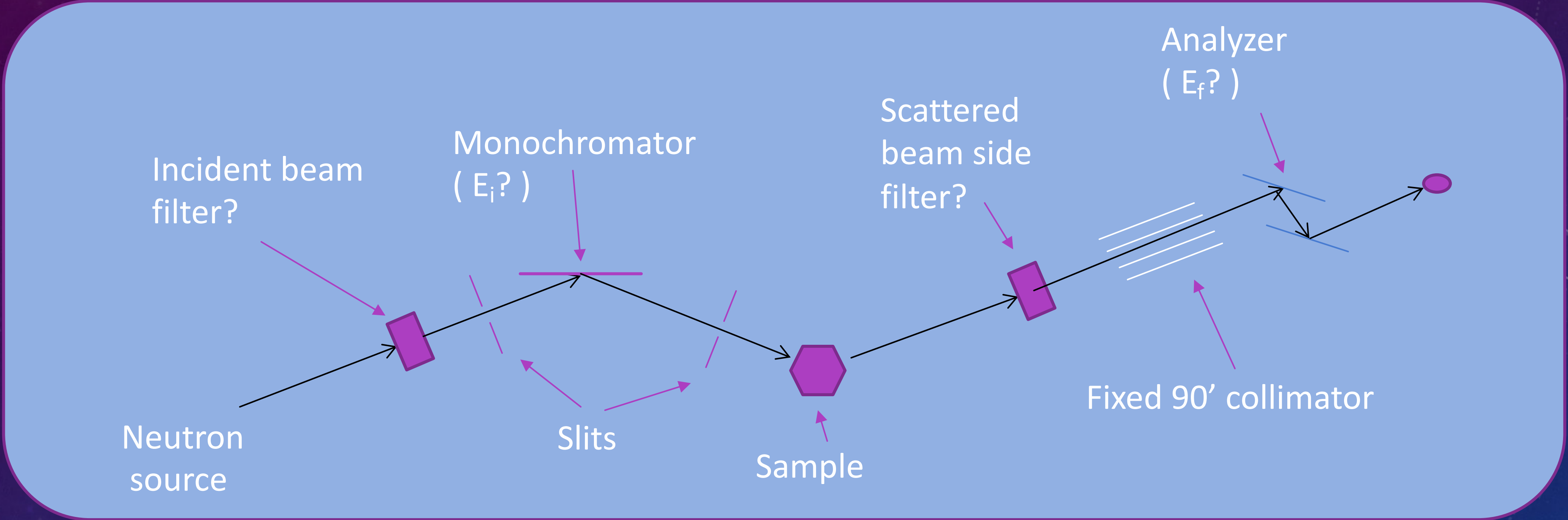

- Let’s choose first Ei and Ef.
- Ei and Ef depends on the energy range and resolution.
- We would like to have good Energy resolution
- Once we know Ei and Ef, we will choose the filters.

MACS NEUTRON FLUX AND ENERGY RESOLUTION.

MACS at NG0 Neutron flux

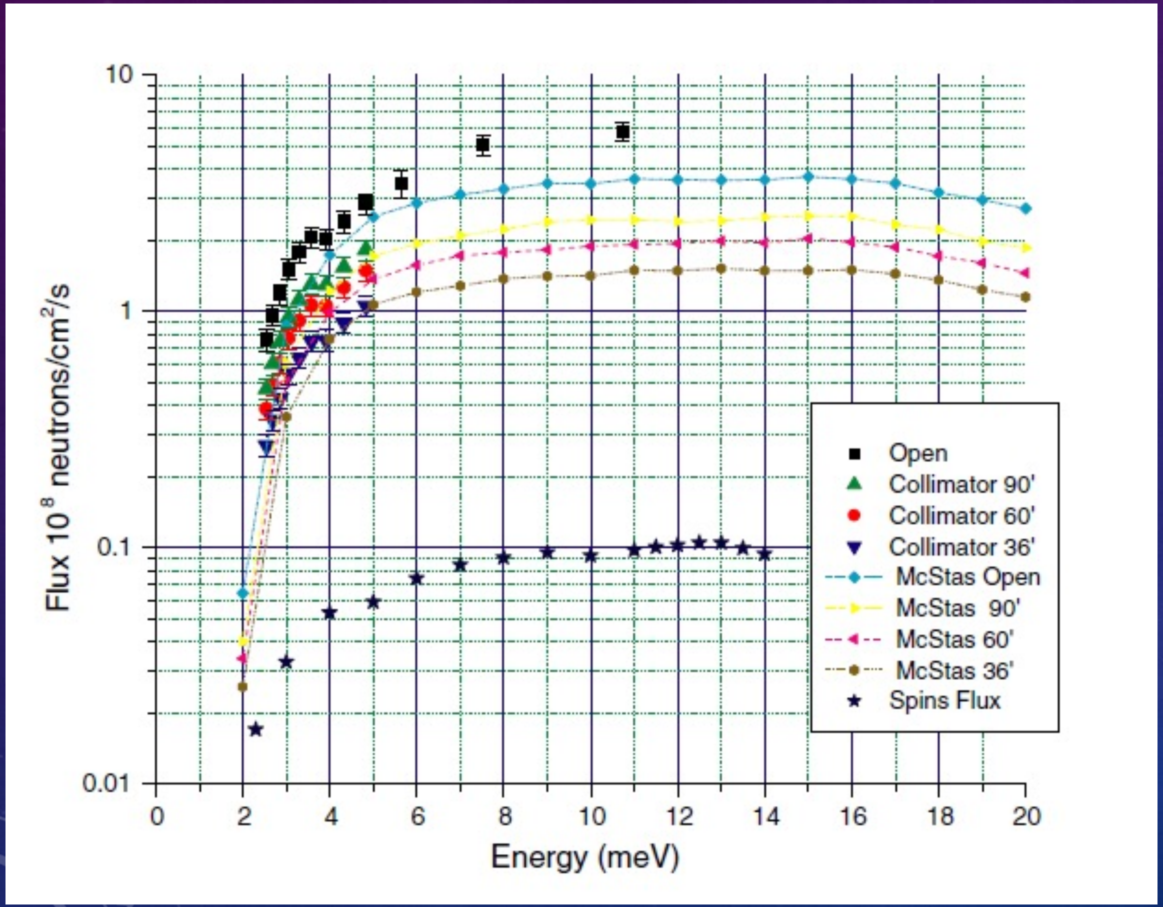

MACS Resolution measured with a V standard.

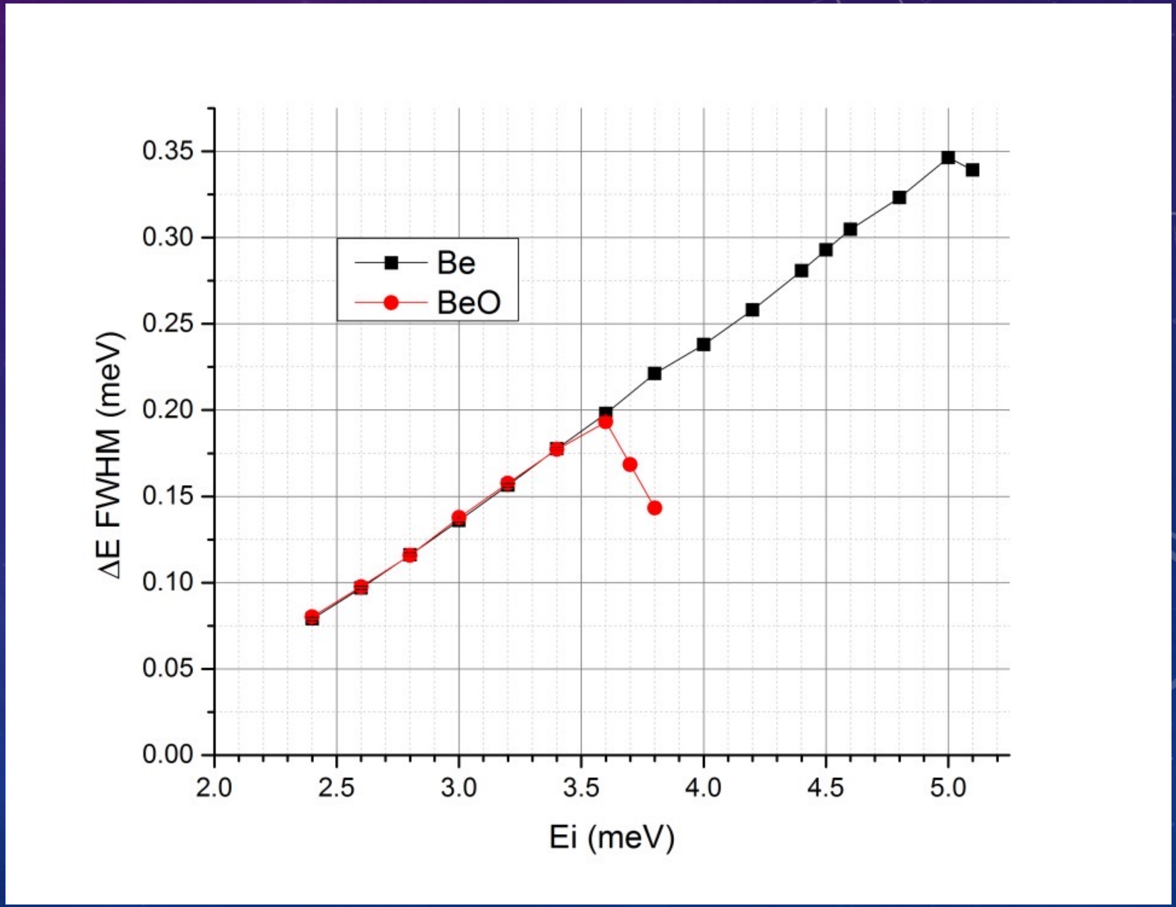

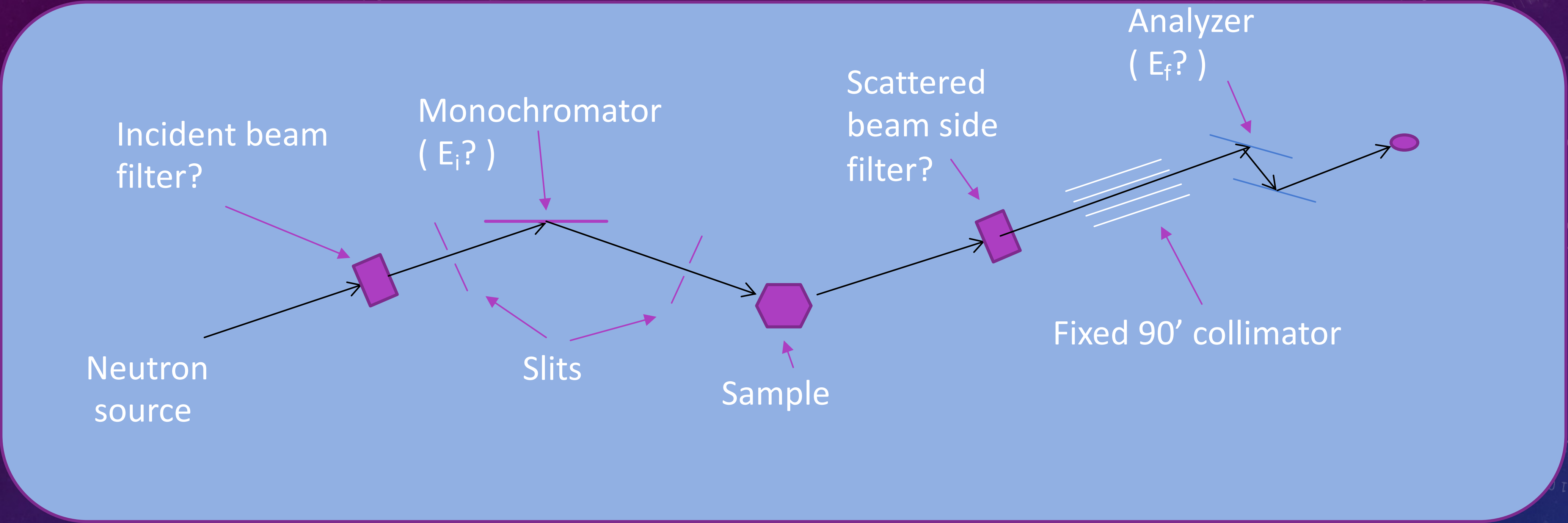

- Best Energy resolution at Ef=2.35
- From heat capacity measurements J=0.9 meV.
- ΔE?
- Now… filters?
- Incident beam fiters : Be or HOPG
- Scattered beam filters: Be, BeO or HOPG

HOPG FILTER

- Good to eliminate high order contamination.
- Good windows: 8.1meV, 13.5 meV and 14.7 meV

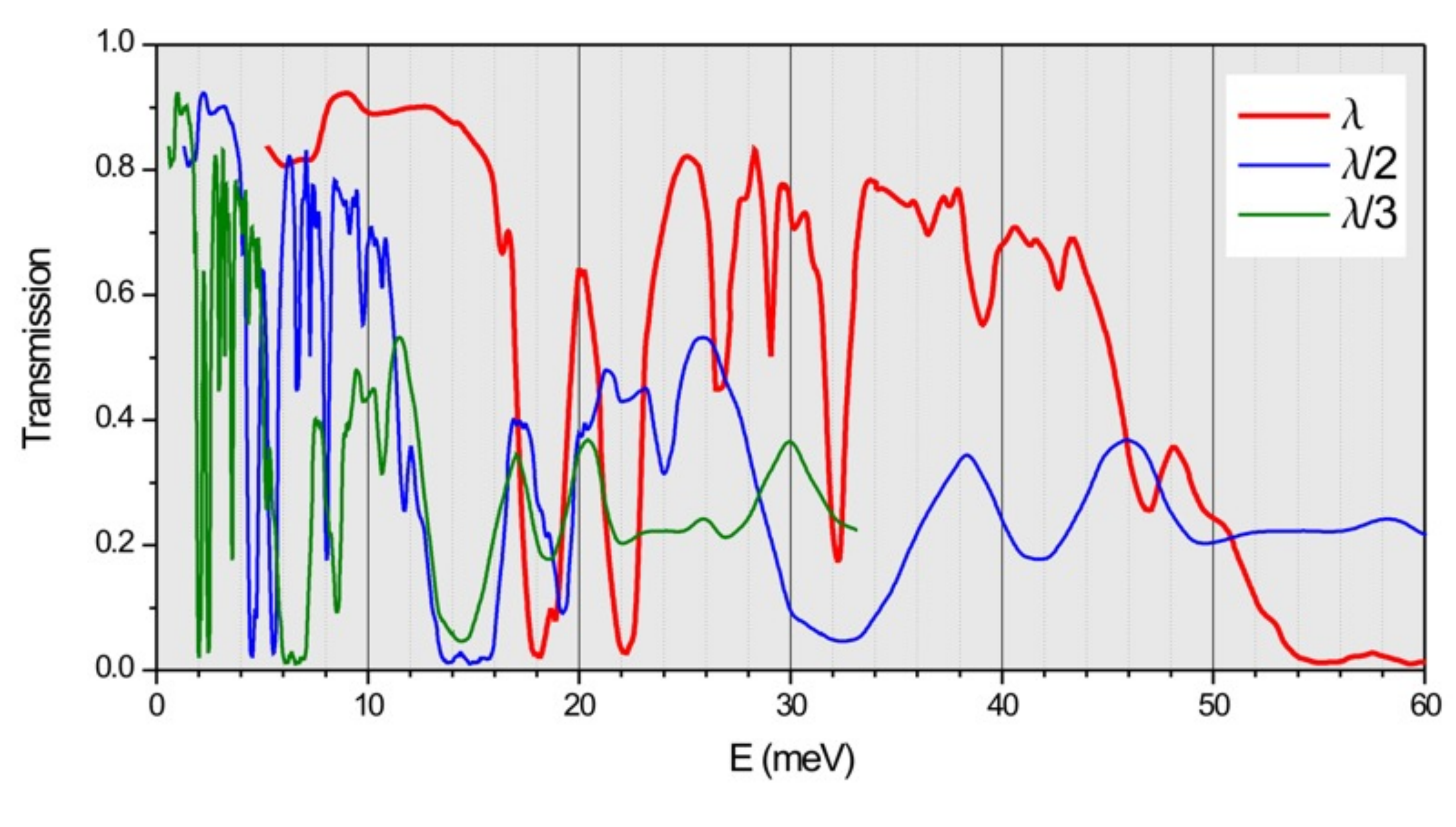

BE FILTER.

- Cuttoff at 5 meV (.404 nm)
- ~75% transmission below 5 meV
- ~20% transmission between 5 - 7 meV

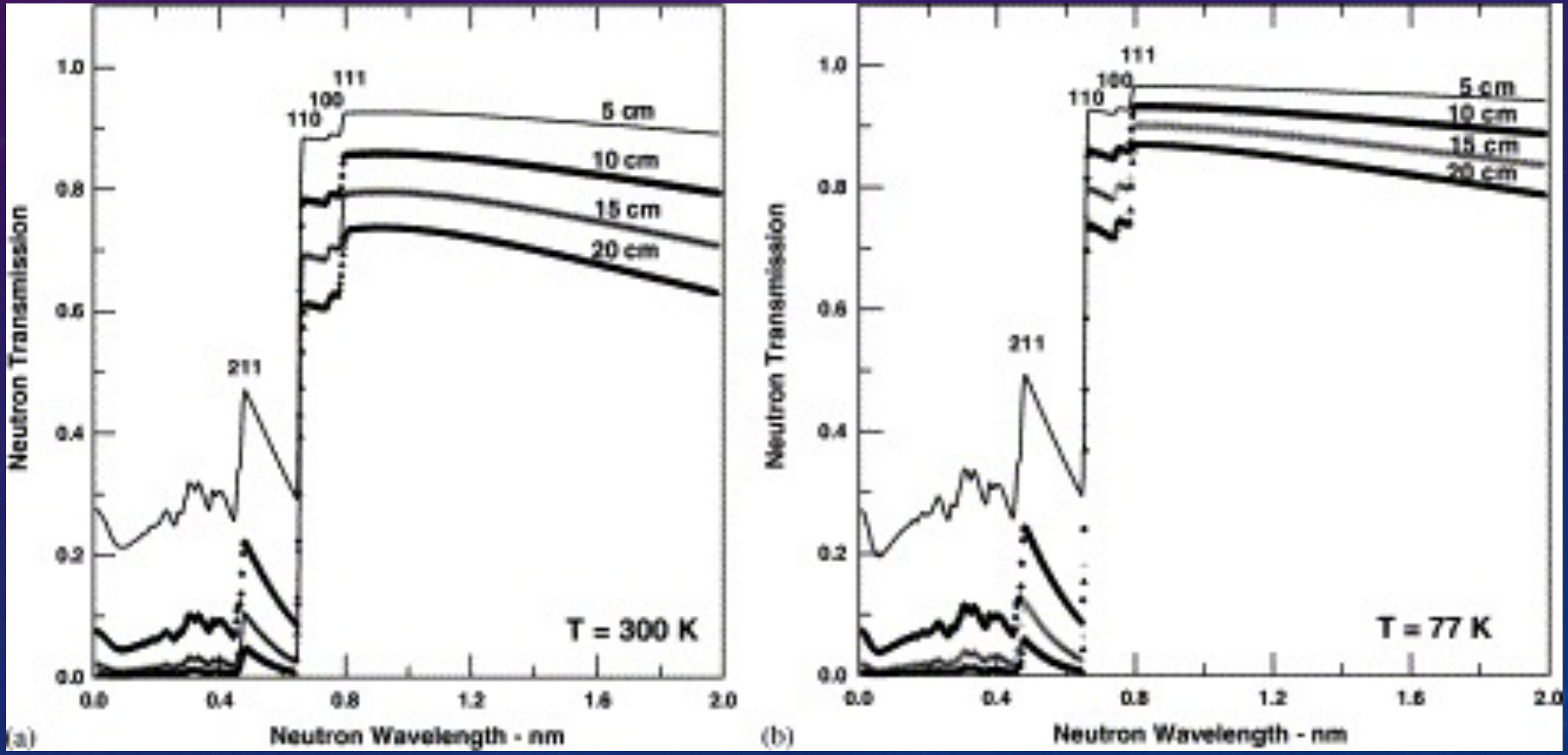

BeO Filter

- Cuttoff at 3.7 meV
- Clean cutoff than Be.
- ~ 60% Transmission below 3.7meV

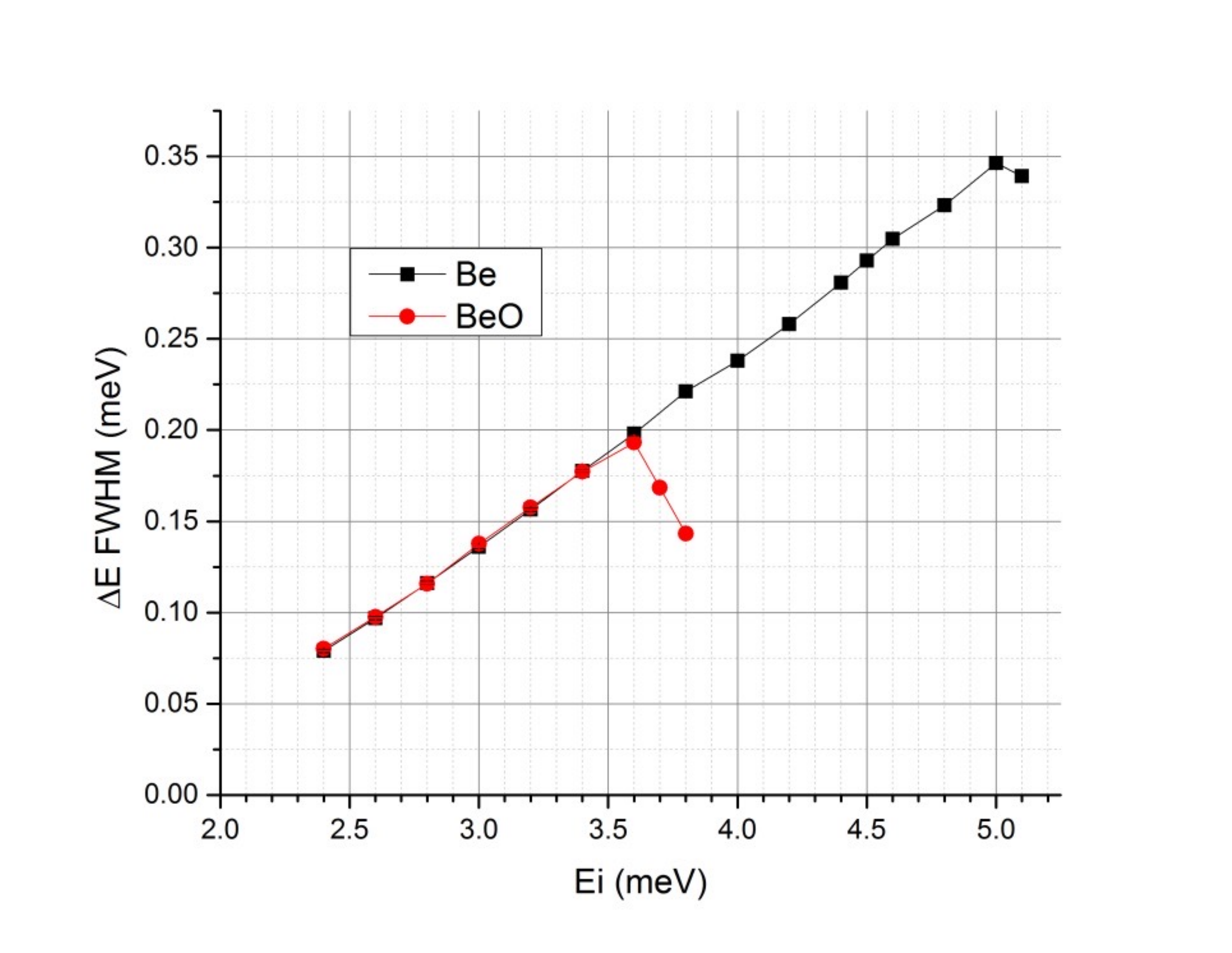

MACS SETTINGS

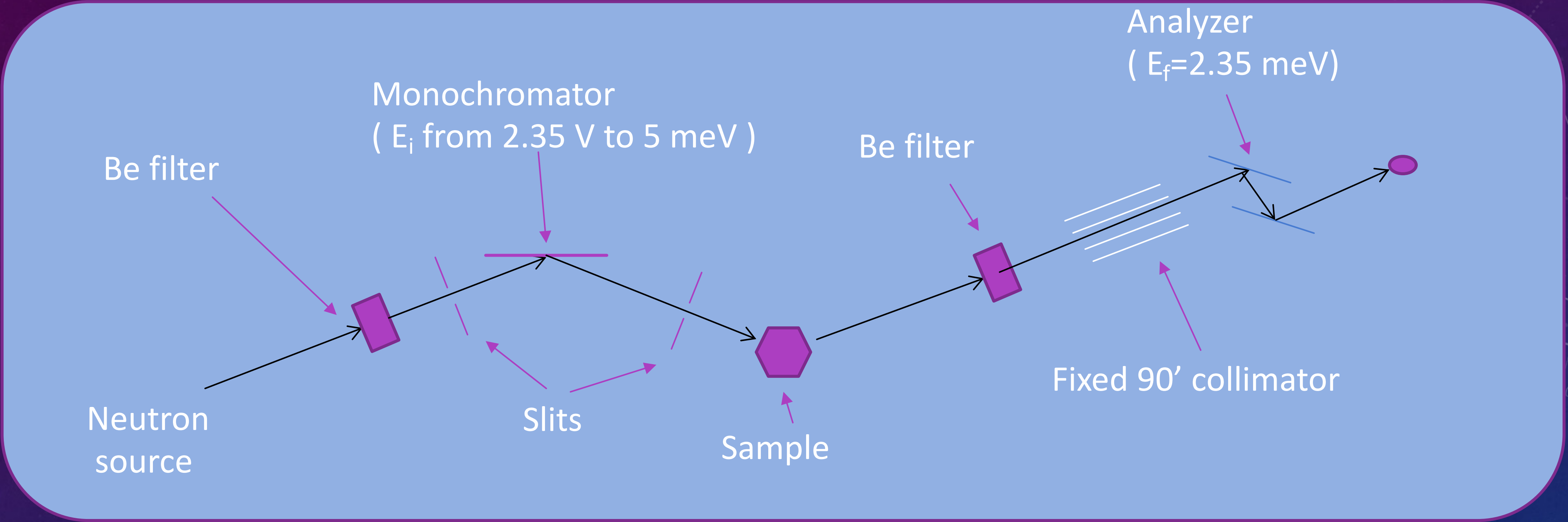

- Best Energy resolution at Ef=2.35
- ΔE about ___ meV → Ei= ___ to __ meV
- Incident beam fiters : ____
- Scattered beam filters: ____

CuPzN dispersion HKL

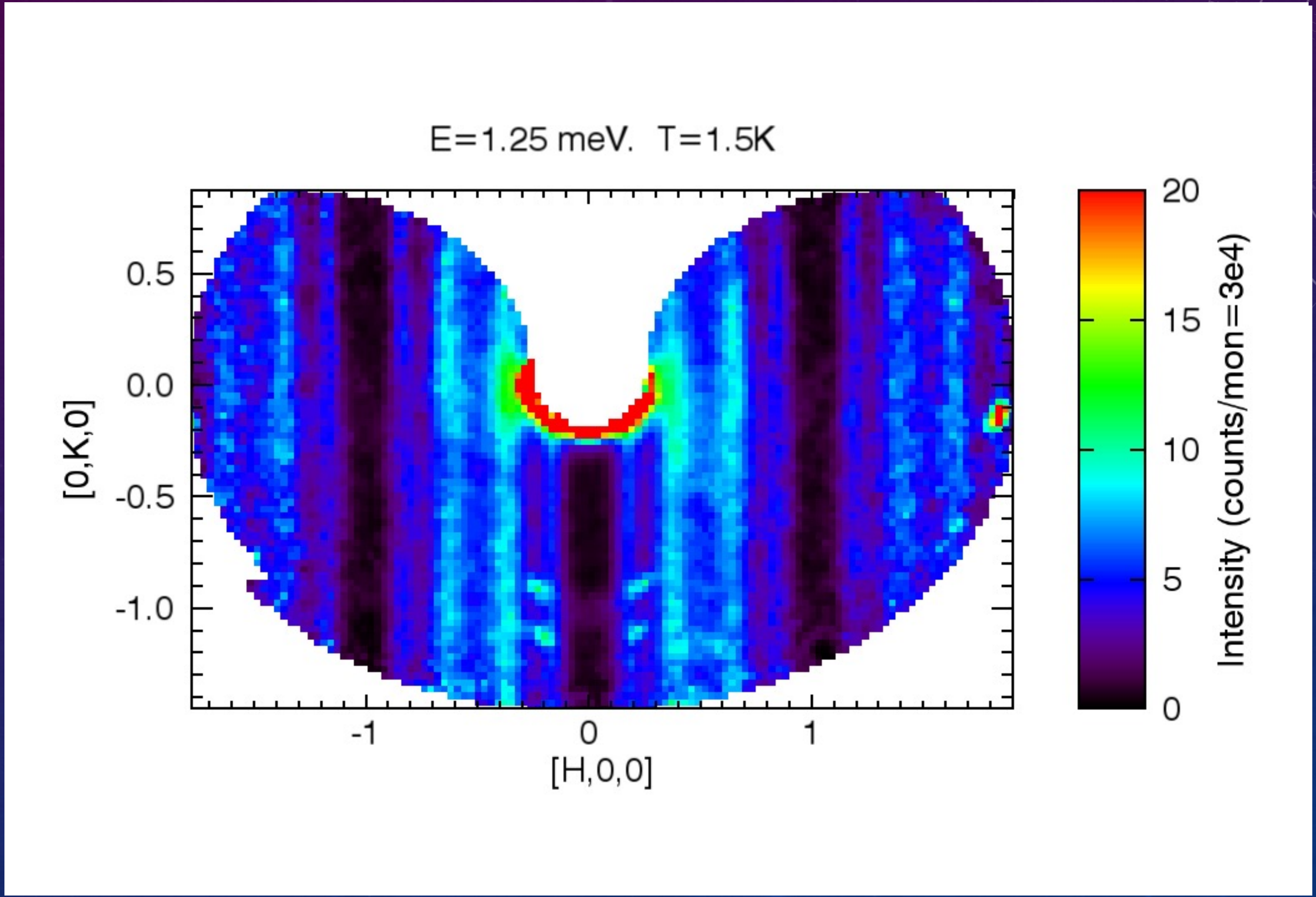

Dispersion along
(h 0 0) direction

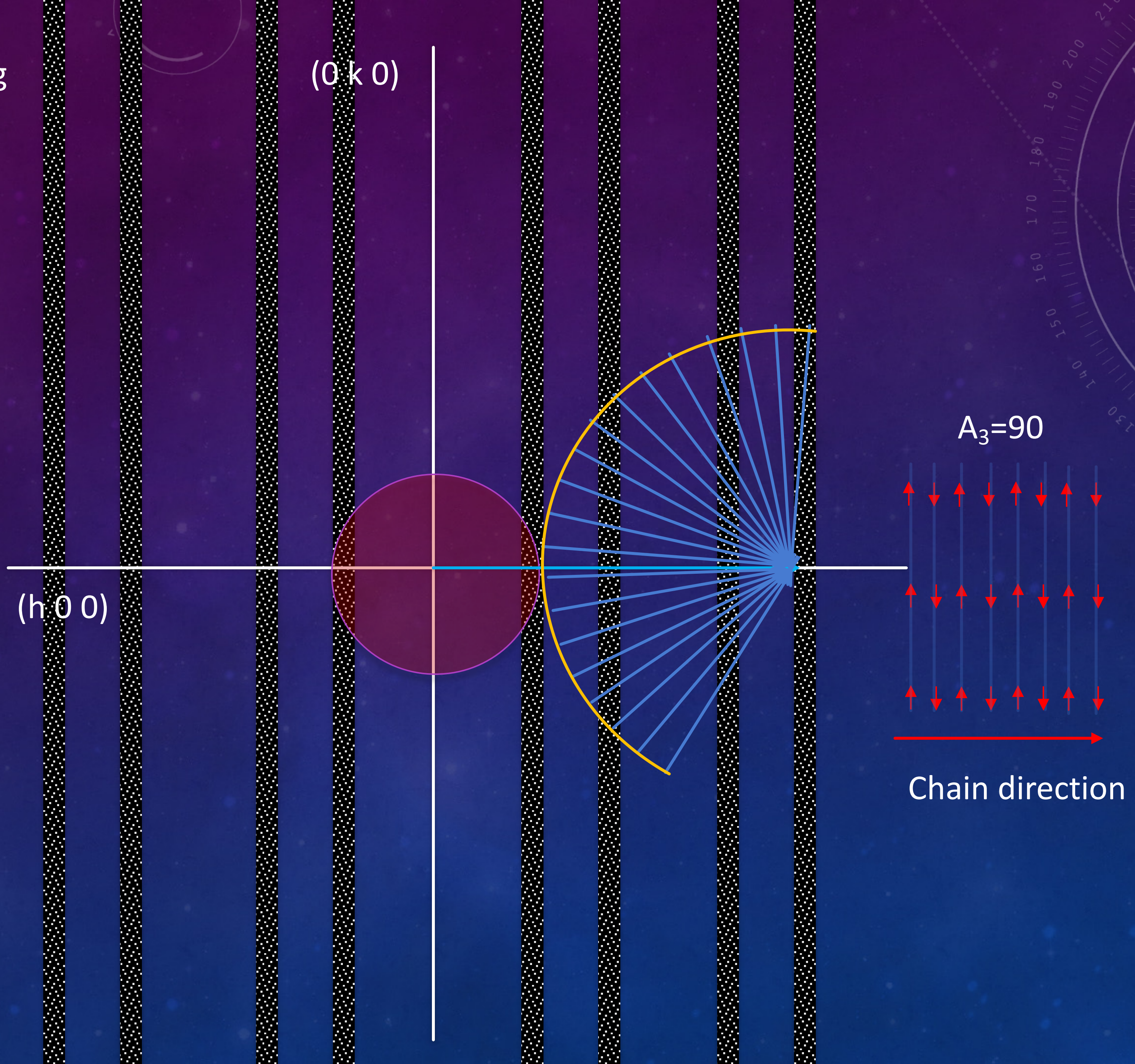

Dispersion along (h 0 0) direction

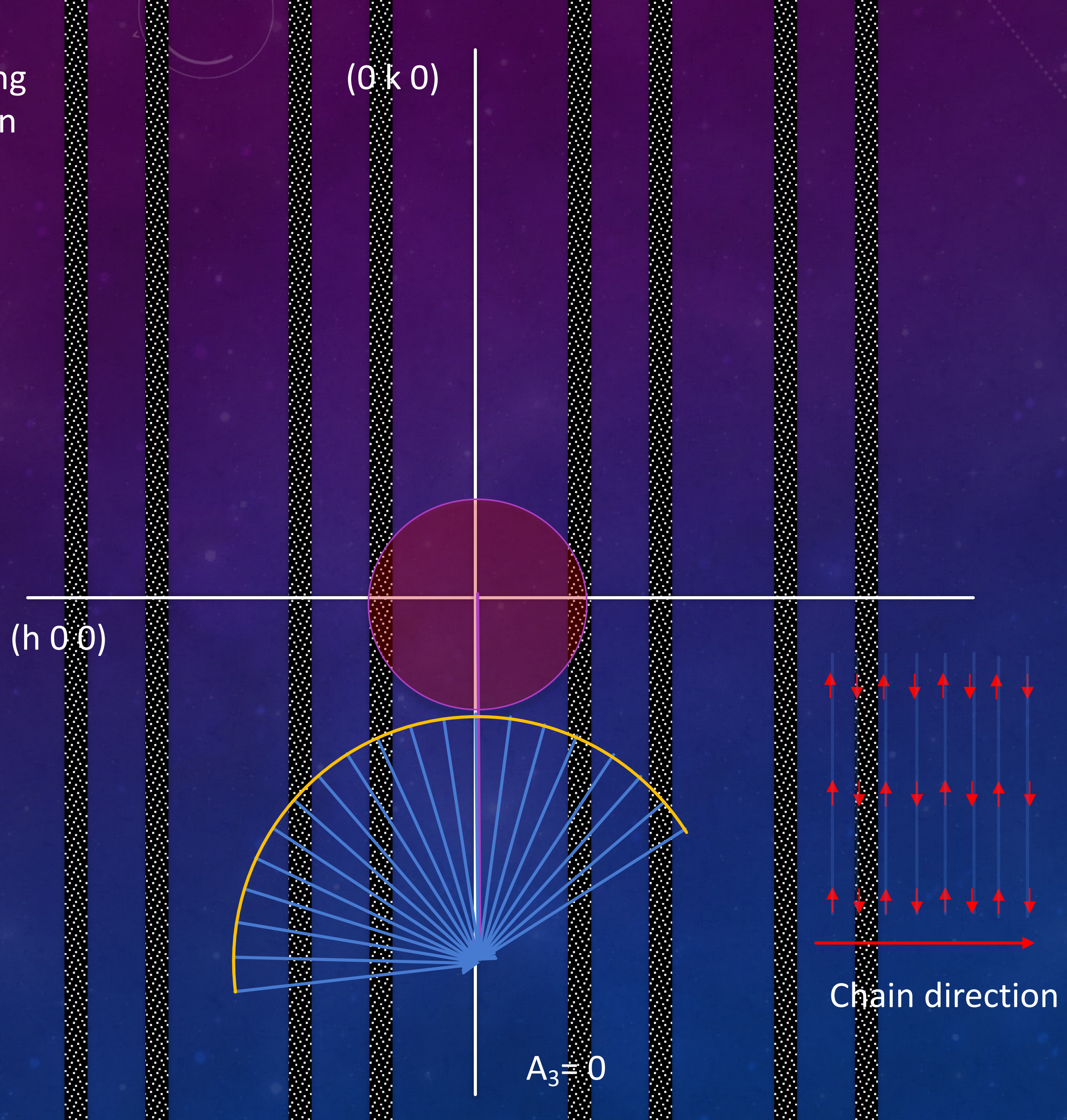

(h 0 0)

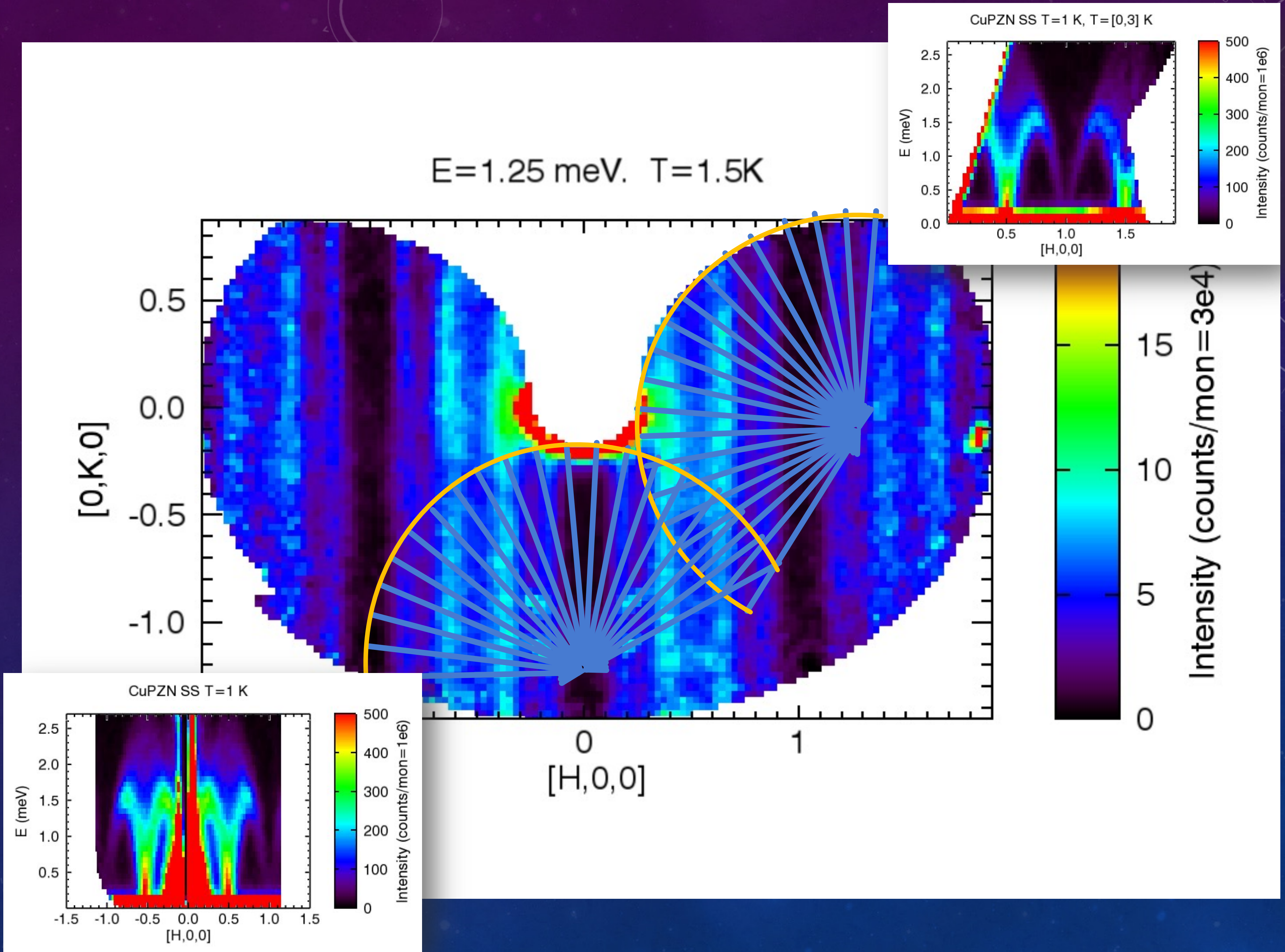
E=1.25 meV. T=1.5K
[0,K,0]
0.5
0.0
-0.5
-1.0
0
1
[H,0,0]
Intensity (counts/mon=3e4)
15
10
5
0
CuPZN SS T=1 K, T=[0,3] K
E (meV)
2.5
2.0
1.5
1.0
0.5
0.0
0.5
1.0
1.5
[H,0,0]
500
400
300
200
100
0
Intensity (counts/mon=1e6)
CuPZN SS T=1 K
E (meV)
2.5
2.0
1.5
1.0
0.5
-1.5
-1.0
-0.5
0.0
0.5
1.0
1.5
[H,0,0]
500
400
300
200
100
0
Intensity (counts/mon=1e6)

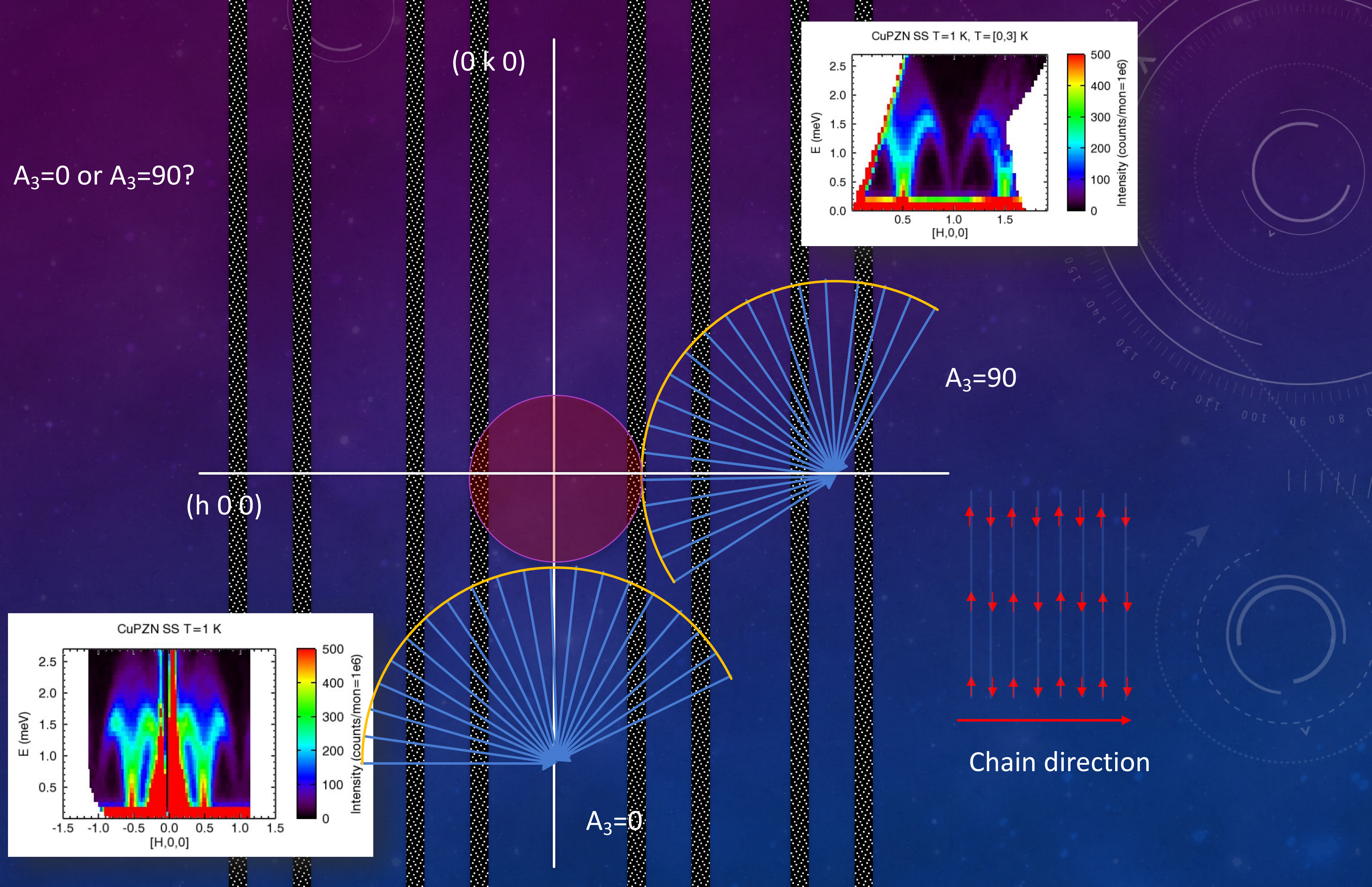
A3=0 or A3=90?
(0 k 0)
(h 0 0)
A3=90
A3=0
Chain direction
CuPZN SS T=1 K, T=[0,3] K
E (meV)
[H,0,0]
Intensity (counts/mon=1e6)
CuPZN SS T=1 K
E (meV)
[H,0,0]
Intensity (counts/mon=1e6)

CAUTION SPOILER!! DINAMIC SUCEPTIBILITY

Haldene[1] and Shulz[2] predicted for a 1D antiferromagnetic spin chains is gapless at $\tilde{q} = \pi$ and the spin correlations decays algebraically with $\eta = 1$.

The scaling factor do not depend on the coupling constant (The susceptibility is a function of E and T)

CuPzN behaves as a 1D spin chain. It its expected to behave as a 1D spin chain above 200K, where the thermal fluctuations dominate over the quantum fluctuations.

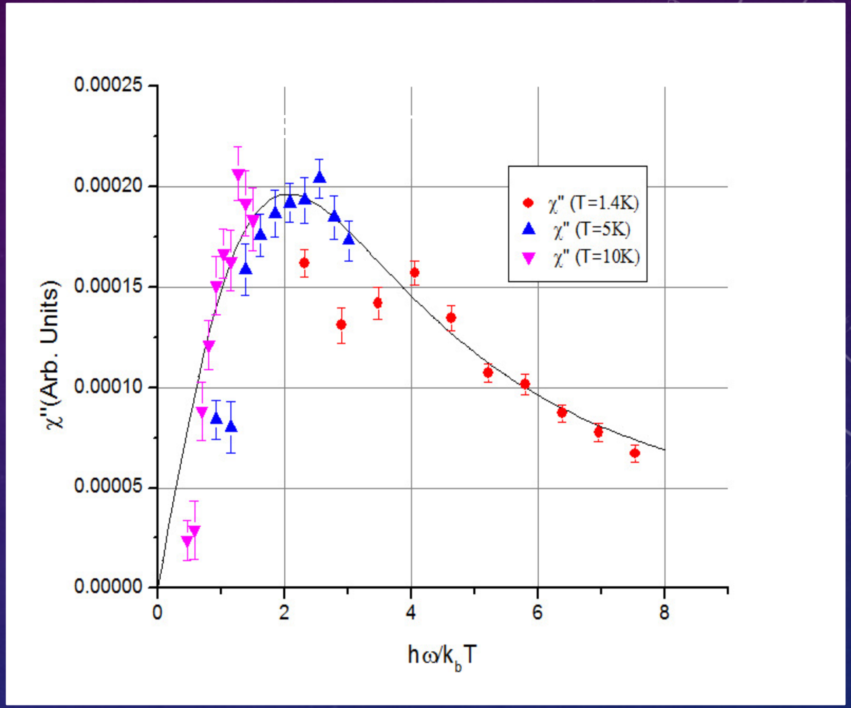

$$\chi''(\tilde{q} = \pi, \omega) = \frac{\pi}{T} Im\left[\rho^2\left(\frac{\hbar\omega}{4\pi k_B T}\right)\right]$$

$$\rho(x) = \frac{\Gamma\left(\frac{1}{4} - ix\right)}{\Gamma\left(\frac{3}{4} - ix\right)}$$

$$S^{\alpha\alpha}(\tilde{q}, \omega) = \frac{1}{\pi}\left(1 - e^{-\frac{\hbar\omega}{k_B T}}\right)^{-1} \chi"(\tilde{q}, \omega)$$

[1] Haldene, FDM. Phys Rev Let. 50,1153 (1983)
[2] Shulz, HJ. Phys Rev B. 34, 6372 (1986)

EXPERIMENT

We are going to measure the spin waves energy dispersion curves .

Steps:

- Mount the sample into the cryostat.
- Align the sample. (flat monochromator)
- Point the spin chain along k_i.
- Set Ei, Ef filters and slits.
- Scan A4 ($2\theta_{sample}$) at different energy transfers.

MACS SETTINGS

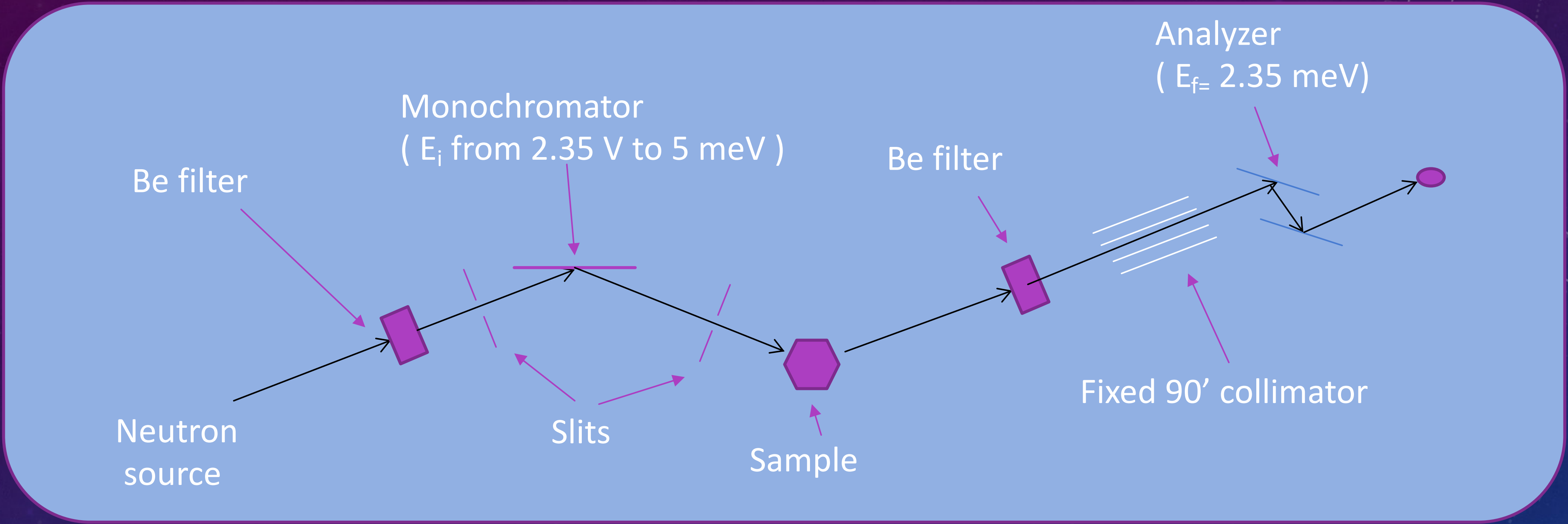

- Best Energy resolution at Ef=2.35
- ΔE about 2.65 meV → Ei= 2.35 to 5meV
- Incident beam fiters : Be
- Scattered beam filters: Be

Setting the Energy and A4 scans:

- 20 detectors (20 A4)
- Spacing between detectors: 8°
- What A4 steps are we going to choose?
    - The dispersion is broad. We can choose 3.5 degrees steps to do not overlap detectors between points.
- What Ei steps are we going to choose?
    - Energy resolution, time constrains, Experimental plan, etc.
    - For this experiment we will use 0.075 meV. Energy resolution at Ei=Ef=2.35meV is about 0.08 meV.

SAMPLE ENVIROMENT EQUIPMENT AT THE NCNR

EQUIPMENT | NIST

https://www.nist.gov/ncnr/sample-environment/equipment

The equipment is separated into general categories by function. To find more information select one of the categories below and then select the specific piece of equipment you are interested in.

*** Range covered by one type of equipment is not necessarily covered by one single piece of equipment.**

Type	Temperature Range *	Other *
Closed Cycle Refrigerators	4 - 800K	Gas Handling High Voltage (0 - 6KV)
Liquid Helium Cryostats	1.4 - 300K	High Pressure Gas Handling
Superconducting Magnets	0.05 - 300K	Vertical Magnetic Field (0 - 15T) Horizontal Magnetic Field (0 - 9T)
Below 1K Inserts	0.05 - 300K	
Furnaces	200 - 1600C	
High Pressure	4 - 300K	Pressure (0 - 2.5 GPa)
Gas Loading	300K	Inert Gases

- For Small Angle Neutron Scattering (SANS) experiments see the SANS sample environment page.
- Below is a table which can help you determine which equipment is the best for your experiment. Please discuss with sample environment team members if you have any questions.

SAMPLE ENVIROMENT ILL CRYOSTAT (ORANGE CRYOSTAT)

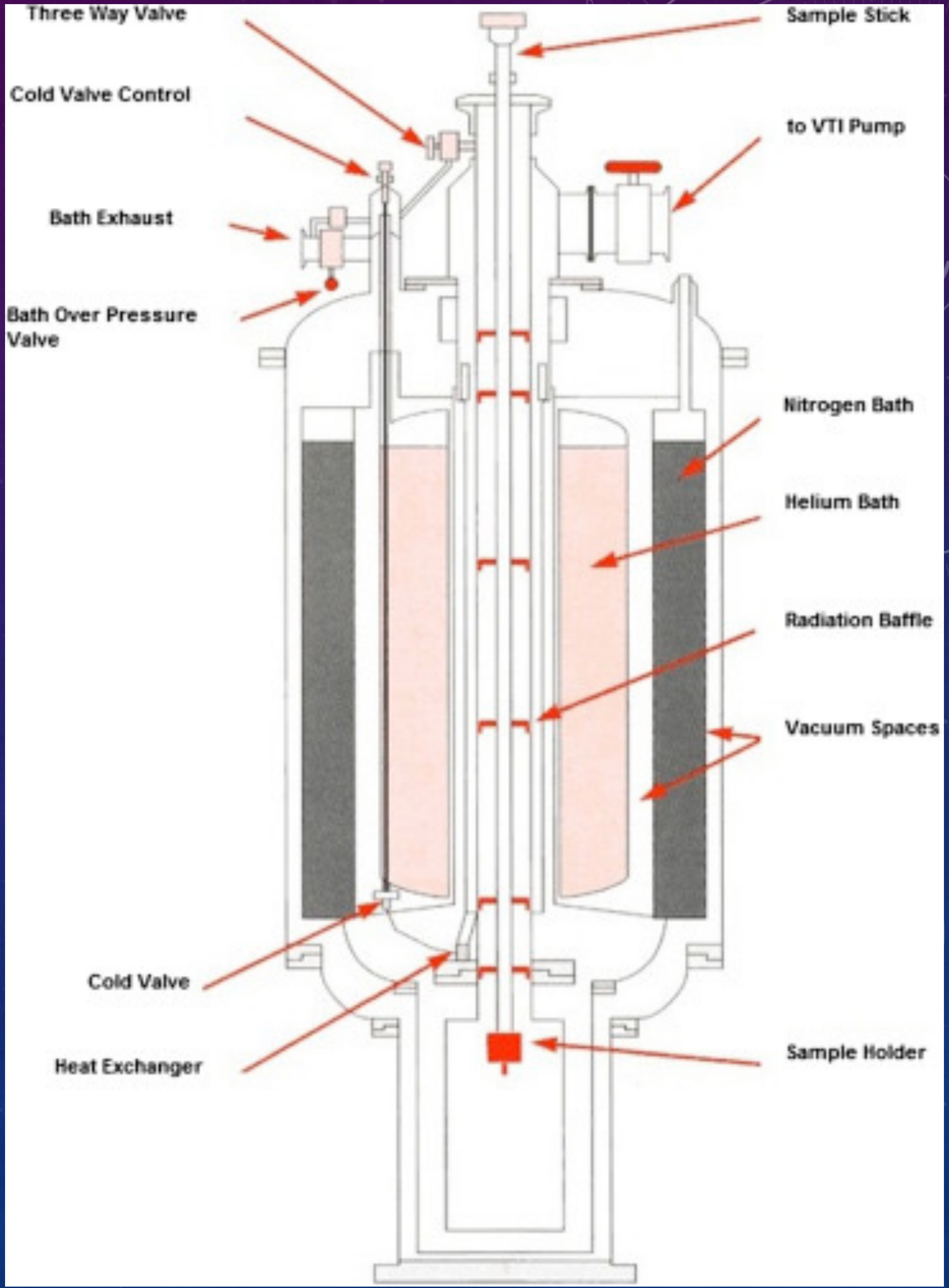

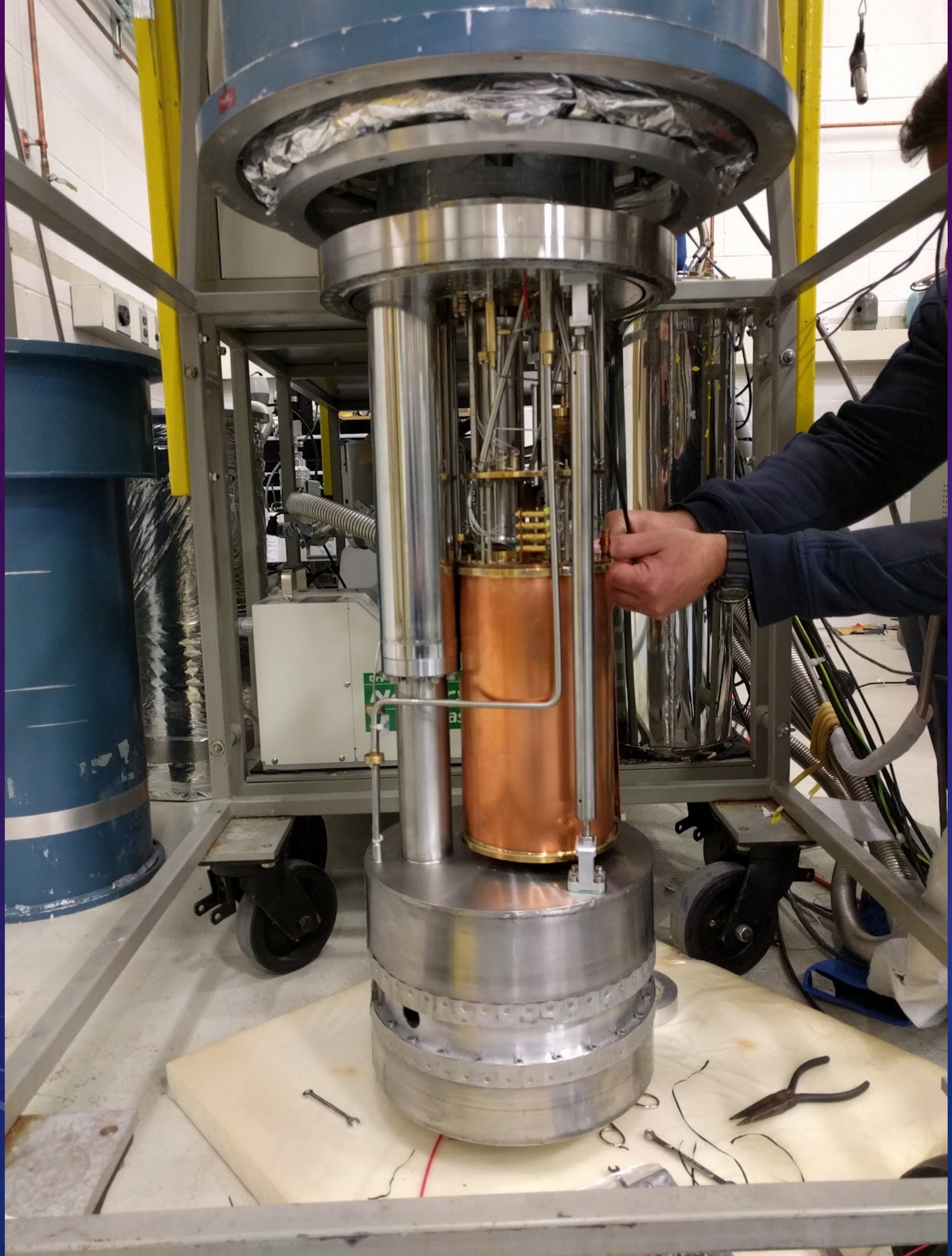

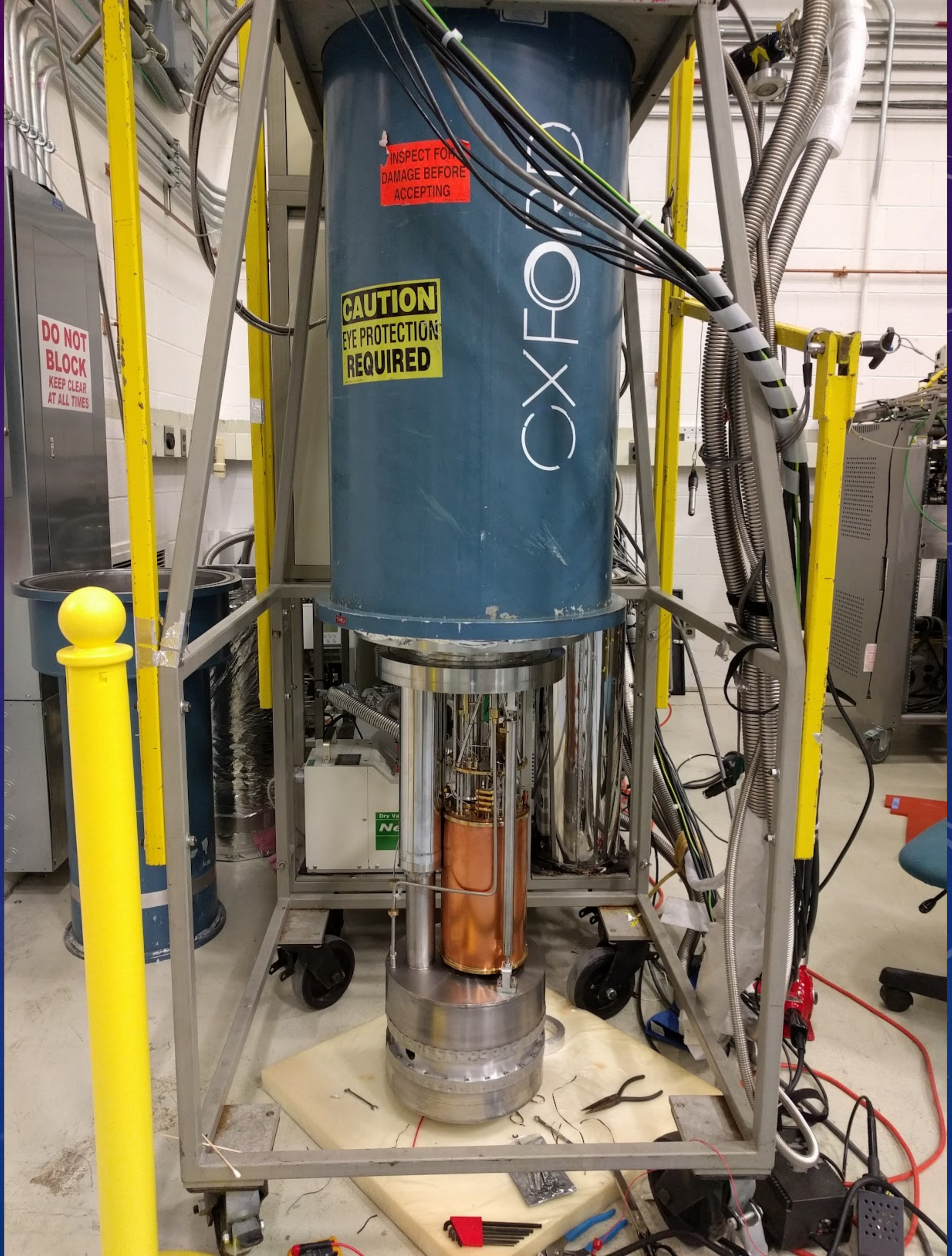
INSPECT FOR DAMAGE BEFORE ACCEPTING
CAUTION
EYE PROTECTION REQUIRED
OXFORD
DO NOT BLOCK
KEEP CLEAR AT ALL TIMES